PHENOTYPE ANALYSIS OF DERMAL-EPIDERMAL ORGANOTYPICS MADE WITH HaCaT CELL LINE SEEDING ON TOP OF THREE HUMAN FIBROBLAST POPULATED MATRICES (POLYETHYLENE TEREPHTHALATE, FIBRIN OR COLLAGEN I+III)

Trabajo de Grado para optar por el título de Magister Ciencias Básicas Biomédicas con énfasis en Ingeniería de Tejidos y Medicina Regenerativa

Candidato al Título
David José Pérez Cardona

Tutor del Trabajo
Dsc. Luz Marina Restrepo Múnera

Comité Tutorial
Dsc. Luz Marina Restrepo Múnera
Dsc. Natalia Yiset Becerra Colorado
Dsc. Iván Darío Gómez Castaño
Dsc. Andrés Augusto Arias Sierra

Corporación de Ciencias Básicas Biomédicas
Universidad de Antioquia
2017

PHENOTYPE ANALYSIS OF DERMAL-EPIDERMAL ORGANOTYPICS MADE WITH HaCaT CELL LINE SEEDING ON TOP OF THREE HUMAN FIBROBLAST POPULATED MATRICES (POLYETHYLENE TEREPHTHALATE, FIBRIN OR COLLAGEN I+III)

David José Pérez Cardona[1]

[1]Tissue Engineering and Cell Therapy Group (GITTC), Medical Research Institute, School of Medicine, University of Antioquia, Colombia, grupoingenieriadetejidos@udea.edu.co

Abstract: Objective: The aim of this study was to phenotype determination of dermal-epidermal organotypics (DEpOs) made with a hypotetraploid human keratinocyte cell line known as HaCaT. Three matrices were used, polyethylene terephthalate, human fibrin or type I and type III rat collagen mixture. Methods: Population doubling time and the mitogenic effect of several media were assessed by formazan production assay. Microanatomical features were evaluated by bright-field/phase-contrast microscopy and hematoxylin and eosin (H&E) staining. Keratinization development markers (i.e. Ki67, K14, K10, filaggrin and loricrin) were determined by indirect immunohistochemistry. Free fatty acids (FFAs) fraction was estimated by gas chromatography with fire ionization detector (GC-FID). Barrier function was estimated by transepithelial electrical resistance (TEER) as well as permeability to Lucifer yellow (LY) measuring. DNA content of HaCaT was determined by propidium iodide (PI) staining and flow cytometry. Findings: Used HaCaT need 16.92±2.03 hours to divide in used medium. Irrespective to matrix type, histology and immunohistochemistry DEpOs showed a poor stratified epidermis (3-5 layers). Flattened cell shape in all layers, no enucleation and a poor spatiotemporal expression of differentiation markers was obtained. All observed features were in accordance with parakeratotic keratinization. Poor FFA detected profile and low TEER values showed absence of a significantly barrier function which correlates with parakeratosis and results of permeability assay. HaCaT DNA content analysis by flow cytometry revealed the presence of at least two different populations. High genetic alterations events might provoke a decreased sensitivity of this cell line to differentiation factors (e.g. air-liquid raising, insulin, adenine, etc.), as was reported previously.

Keywords: HaCaT, fibroblast, polyethylene terephthalate, fibrin, collagen.

1. INTRODUCTION

Primary keratinocytes culture is a common way to study the epidermal morphogenesis and physiology. Since Rheinwald and Green description, in 1975, to present, thousands of protocols have been described to isolate, propagate and differentiate epidermis artificially from primary keratinocytes (Pruniéras, Régnier, Woodley; 1983) (Boelsma *et al*.; 2000) (Poumay *et al.*; 2004) (Böttcher-Haberzeth, Biedermann, Reichmann; 2010) (Debels *et al.*; 2015). Human reconstructed epidermis from normal human keratinocytes (NHK), produced through organotypic coculture, has been one of the most used strategy (Stark *et al*.; 1999) (Gangatirkar *et al.;* 2007) (Nyame *et al*.; 2015). This tissue-like culture system emulates the physiologic dermal-epidermal cross talking by coculture of keratinocytes over a given matrix populated with fibroblasts (Boehnkea *et al*.; 2007). Those skin resident cells secrete growth factors in a double paracrine fashion that mediates the keratinocyte conversion to corneocyte. So, organotypics are a useful tool to study the molecular mechanisms that regulates epidermis development (Wojtowicz *et al*.; 2014). In regenerative medicine, they have been used to improve the

natural wound healing process after skin loss. For example, in burns, venous leg ulcers, limb amputations and after a reconstructive surgery (Bello, Falabella, Eaglstein; 2001) (Geer, Swartz, Andreadis; 2004) (MacNeil; 2007) (Zhong, Zhang, Lim; 2010) (Bin *et al.*; 2016). Artificial reconstructed epidermis also has been used in so many *in vitro* tests models related with transdisciplinary scientific knowledge as toxicology (Netzlaff *et al*.; 2005) (van der Veen *et al*.; 2015), pharmacology (Damour, Augustin, Black; 1998) (De Wever, Kurdykowski, Descargues; 2015) and cosmetology (Auger *et al.*; 2004) (Poumay, Coquette; 2007) (Küchler, Strüver, Friess; 2013). Artificial skin built with primary cells could be a target of pre-market or preclinical tests implying, for instance, outstanding decreases on experimental animal use. In spite of their potential uses, primary keratinocytes have serious limitations, namely: non-reproducible results associated to biological variability between donors (Kaji *et al.*; 2009) (Sriram, Bigliardi, Bigliardi-Qi; 2015), a short culture lifetime (i.e. Hayflyck limit) (Hayflyck; 1965) and variations between passages (Kretlow *et al.*; 2008) (Lennon, Schluchter, Caplan; 2012). Quoted problems are not encountered to the same extent with immortalized cell lines (Schürer *et al.*; 1993) (Schoop, Mirancea, Fusenig; 1999).

Techniques as enzymatic digestion (Wang *et al*.; 2004) and biopsy explant culture (Vangipuram *et al.*; 2013), to isolate primary human dermal fibroblasts, are relatively easy. Once primary fibroblasts are obtained, its culture and cryopreservation is relatively stable from most point of view: lifespan (Kan, Yamane; 1982) (Balin *et al.*; 2002), cell phenotype (Isnard *et al.*; 2002) (Boraldi *et al*.; 2010) and genome stability in terms of DNA content (Schneider, Shorr; 1975). We use all afore cited techniques with considerable efficiency in our laboratory to obtain primary fibroblast cultures in most of the processed skin biopsies (Morales *et al.*; 2016). On the other hand, procurement process, maintenance and differentiation of primary keratinocytes has so many difficulties. Specifically, viable epidermal adult stem cells (EpiASCs) have stringent culture requirements (i.e. supplementary growth factors are mandatory) (Mahabal *et al*.; 2016). EpiASCs have also a limitation imposed by its intrinsic physiology: once are committed to cornification, die rapidly. This complicate its use in long-term investigations (Borowiec *et al*.; 2013). Additionally, EpiASCs expansion and technical isolation requirements are complicated and expensive compared with standard cell lines cultures:

1) Widespread source of primary EpiASCs is circumcised newborn foreskin. This tissue has a high mitosis rate of epidermal cells. Circumcision also is “highly” frequent in some towns (Flaxman; 1974). Nevertheless, in Colombia, such surgical process is relatively not common, i.e. less than 20% prevalence (IATT; 2007). Thus, the procurement of newborn foreskin is not easy in our context.

2) Once harvested, EpiASCs expansion implicates a lot of delicate steps and so many time for its maintenance. For example, requires the use of a lethally irradiated or mitomycin C treated 3T3 murine fibroblasts cell line as feeder layer (Rheinwald, Green; 1975).

3) Specialized media are necessary to guaranteed and improve the keratinocyte growth (e.g. KGM, EpiLife, K-SFM, etc.). Those media are more expensive than standard. Our experience in adult skin explant culture (i.e. from blepharoplasty, mammary reduction or retroauricular biopsies) do not guaranteed EpiASCs isolation.

4) Compared to cell lines, e*x vivo* cultured EpiASCs have a finite lifespan (i.e. 3 to 7 cell generations). Differentiation potential also decrease with time, limiting its *in vitro* applications (Choi, Lee; 2015).

In sharp contrast, epidermal cell lines are easy and cheap to maintain *in vitro*. Do not need cell feeder layer or specialized media to grow and its lifespan and differentiation potential are stable in time. An excellent example is the human keratinocytes cell line HaCaT. Its designation was based on its origin and the starting culture conditions: **H**uman **a**dult skin keratinocytes propagated under low **Ca**$^{2+}$ conditions and elevated **T**emperature (Ha: human adult, Ca: calcium, T: temperature or Human adult low Calcium Temperature (HaCaT) keratinocytes). HaCaT was the first spontaneously transformed human epithelial cell line from normal adult abdominal skin. Was obtained by Boukamp *et al.* in 1988.

The aim of this study was to generate a dermal-epidermal organotypic (DEpO) culture phenotypically similar to native skin. DEpOs were made with HaCaT human keratinocyte cell line cultured on three different matrices populated with primary human fibroblasts: polyethylene terephthalate (PET), human fibrin or type I and III (CI+III) rat tail collagen. PET was chosen because it is a transparent polyester family member, which allows an ideal microscopically tracing during all incubation time. Used criteria to select biopolymers was its pivotal role in skin biology. A dermal structural component termed collagen (i.e. Type I and III) and other involved in early wound healing phases, the fibrin. Dermal matrix variation purpose was to choose the most efficient model in terms of required time and final epidermis quality. To develop the commented objective, a methodological design was proposed in accordance with specific intentions. HaCaT proliferative potential and its DNA content were assessed to characterize if cells could show a homogeneous behavior under the tested conditions. A comprehensive characterization of DEpOs is presented. Microanatomy features were evaluated by hematoxylin and eosin (H&E) to describe the stratification level and whether differentiation pattern of HaCaT cells was normal (i.e. orthokeratotic) or abnormal (i.e. parakeratotic). Representative earliest (i.e. Ki-67, keratin 14 and 10) and latest (i.e. filaggrin and loricrin) differentiation markers were assessed by indirect immunohistochemistry to depict the molecular events associated to keratinocyte differentiation quality. Barrier function was measured indirectly as follow. Free fatty acid (FFA) fraction was weighed through gas chromatography with fire ionization detector (GC-FID). Impedance properties determination was carried out by the assessing of trans-epithelial electrical resistance (TEER) in Ohms using the ERS-2 system from Millipore. Paracellular transport was disclosed by permeability resistance to Lucifer yellow integrity marker. Three mentioned measurements describe in an indirect form how functional were DEpOs. Briefly, obtained tissues had no ideal skin engineered features as reported by other researchers. Nevertheless, as far as we know, built DEpOs represent the first approximation in Colombia to generate an *in vitro* epidermal model with HaCaT cell line seeded over the three mentioned fibroblasts-populated matrices. Presented results will allow us to improve technical proceedings to generate better skin equivalents in a near future. This type of engineered epidermis can be further used in epidermal infection models (e.g. *Leishmania*, HPV, *Histoplasma capsulatum*, etc.), topic pharmacopeia, irritation/corrosion tests and in basic dermatology research (e.g. skin histogenesis). Some chemical and biochemical features of used polymers are described and debated at final of this work but are not mentioned in introduction. As an introductory step, the principal cellular features of HaCaT cell line are described at once.

1.1. Immortality and Proliferative Capacity

HaCaT cell line can be considered immortal. Its proliferation, clonogenicity, and serum-independent growth potential has been evidenced during >300 passages (Boukamp *et al*.; 1997). Causal genetic affair that led to its transformation remains unclear. The sequencing of p53 gene, TP53, shows pyrimidine dimer formation (ultraviolet-type mutations) induced by C-T and CC-TT transitions localized at codons

178 (His→Asn) and 281 (Asp→Asn) (Ziegler *et al*.; 1993). p53 is a DNA-repair tumor suppressor gene named "guardian of the genome" by David Philip Lane in 1992. Briefly, p53 monitors the genome DNA integrity, mainly double strand DNA breaks, at G1 cell cycle checkpoint phase and mediate its repair, if it is possible. Then, cell division proceeds through ATM/ATR (ataxia-telangiectasia mutated/ataxia telangiectasia and Rad3-related) → CHK1/CHK2 (Checkpoint kinase 1 and 2) pathway. If DNA repairing is not possible, cell cycle conduces the cell to mitosis arrest and regulated cell death (i.e. ADP-ribosylation factor (ARF) pathway) (Lane; 1992) (Bieging, Mello, Attardi; 2014) (Speidel; 2015). When keratinocyte undergoes a malignant p53 pathway alteration, it promotes a tumor process known as squamous cell carcinoma (SCC) (Ziegler *et al*.; 1994) (Ghaderi, Haghighi; 2007) (Ratushny *et al.*; 2012). Lehmann *et al.* suggested in 1993 that those mutations were the immortality triggers or had an important role, but that they not were the unique cause. In fact, an exhaustive revision in 1998 by Fusenig and Boukamp discusses that p53 mutations acts as conditioning factor or at least as initial stage. Further genetic events occur, as to loss of senescence genes located on human short arm of chromosome 3. Finally, HaCaT shows an increased telomerase activity compared with normal keratinocytes (Härle-Bachor, Boukamp; 1996) (Senthilkumar, Robertson, Ludewig; 2012). Telomerase is a ribonucleoprotein type enzyme with reverse transcriptase activity very active in gametes, stem and tumor cells. This enzyme maintains telomeres (i.e. end of chromosomes) length by *de novo* synthesis of tandem guanine (G)-rich repeats (e.g. TTAGGG in humans) (Gomez *et al*.; 2012).

Since HaCaT was established, its long-term growth in primary culture (without passaging) was optimal in low Ca^{2+} medium (0.2 mM) and high temperature (e.g., 38.5 °C), probably due to a marked reduction in its terminal development (Boukamp *et al.*; 1988). At early stage, cells were still very sensitive to modifications of the original culture conditions (i.e. 0.2 mM Ca^{2+}, 38.5 °C). Around the tenth passage, when hypotetraploidy appears, cells developed complete independence of both Ca^{2+} concentration ($[Ca^{2+}]$) and temperature. Recent investigations had been showing that low temperature reduces the proliferative potential (Borowiec *et al*; 2013). High calcium concentrations decrease the HaCaT cell cycle time, enhancing the growth by a factor of ~4, and do not induce cell cycle arrest at G1/G0 like in normal keratinocytes (Walker *et al*.; 2006) (Micallef *et al.*; 2009). Further studies demonstrate that changes from low (0.09 mM) to high (1.2 mM) $[Ca^{2+}]$ induces the translation of the major keratinization markers, K1, K10 and involucrin, after 13 days of culture (Wilson; 2014). This calcium level exchange emulates, even though a delay, the normal keratinocyte commitment (Micallef *et al.*; 2009).

HaCaT synthetizes some functional markers. Protein kinase C (i.e. cPKC α/β, nPKC δ/ε/η/θ/ and aPKCζ) switches on/off according external conditions (e.g. $[Ca^{2+}]$, cell density). Some isoforms promote proliferation (PKCε) or differentiation (PKC δ/η isoforms) as in normal epidermis (Papp *et al*.; 2003). Insulin-like growth factor binding protein 3 (IGFBP-3) is also expressed by HaCaT. Both IGF-I and -II exerts a potent mitogenic effect over HaCaT after its union to IGFBR-3. Additionally, IGF-II stimulus is accompanied by MAPK pathway and HIF-1α (hypoxia-inducible factor 1 alpha) activation, leading to massively VEGF (vascular endothelial growth factor) secretion, as in psoriasis (Kwon *et al*.; 2004). HaCaT also responds to mechanical stress by releasing ATP. P2Y-ATP complex induce an intracellular Ca^{2+} wave mediated by TRPC6 (transient receptor potential cation channel, subfamily C, member 6), that leads to a sudden increasing of proliferation (Takada, Furuya, Sokabe; 2014). In fact, mechanical stress can improve the orthokeratinization of artificial epidermis built with HaCaT (Jung, Jung, Shin; 2016).

NHK needs the presence of Epidermal Growth Factor (EGF) to grow at clonal densities. NHK achieves the "autonomous growth" at high confluency because massive *de novo* synthesis of EGF and transforming growth factor alpha (TGF-α), which exert an autocrine mitogenic effect through its surface

human EGF receptor (EGFR) (Rekus; 2000). Instead, HaCaT is independent of the above mechanism even at clonal densities. Finally, our laboratory experience also shows an excellent HaCaT proliferative behavior in most media at low/high calcium concentrations (e.g. DMEM, MEM, HAM-F12, DMEM:HAM-F12, EpiLife, Keratinocyte Growth Medium). Once HaCaT cell line was stablished, a lot of protocols were developed to grow and compromise it in keratinization process (Deyrieux, Wilson; 2007).

1.2. Genetic Features

HaCaT cell line was obtained by primary keratinocytes exposition to afore commented conditions (i.e. 0.2 mM Ca^{2+}, 38.5 °C), which induced aneuploidy. Karyotype is hypodiploid with specific stable marker chromosomes (Fig. 1). In original description, most cells were hypodiploid. An average of 44 chromosomes resulting from full or partial monosomies (e.g. isochromosomes) were found. All metaphases had the XO sex chromosome constitution (i.e. lacking the Y chromosome). Cells were partially monosomic for the short arm of chromosomes 3 and 9. Whole chromosome 4 was lost. Three individual marker chromosomes (M1, t(3q4q); M2, i(9q); and M4, t(4p18q)) were present in 100% metaphases until passage 17. Commented facts, clearly indicates a stem-line monoclonal origin of HaCaT cell line (Boukamp *et al.*; 1988).

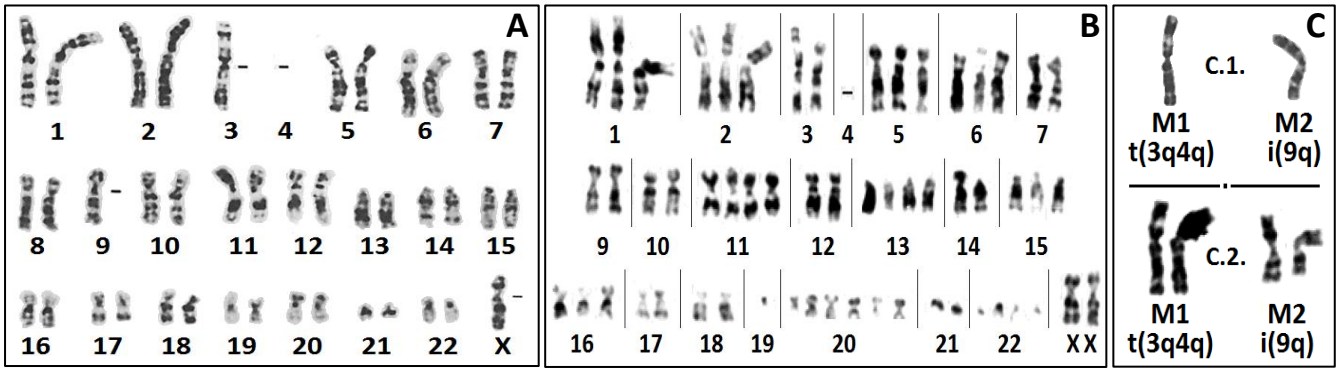

Figure 1. Karyotype of HaCaT cell line. **A.** Karyotype reported by Boukamp *et al.* in 1988 (hypodiploid); passage 2. **B.** HaCaT continues its polyploidization process until stabilizes as hypotetraploid cell line (passage 50) (Boukamp *et al*. in 1997). **C.** The marker chromosomes M1 and M2 are present in all metaphases, from aneuploidy event (> passage 2 hypodiploid; C.1.) until further passages (> 50; hypotetraploid, C.2.). Images taken and modified from its original.

HaCaT
continues its polyploidization after fourth passage and stabilizes at tenth passage. Then hypotetraploidy dominates, keeping it up until higher passages (>200). In 1997 Boukamp *et al.* observed a high frequency of structural chromosomal aberrations up to passage 225, with a particular increase during passages 30 and 50.

1.3. Differentiation Capacity

HaCaT have not tumorigenic properties even when is injected subcutaneously in nude mice (Boukamp *et al.*; 1997). As a matter of fact, collagen co-cultures of fibroblasts spheroids and HaCaT, stops the nemosis experimented by this sphere-like structures in cancer-associated fibroblasts progression (Räsänen *et al*.; 2008). Inversely, nemotic fibroblasts induce proliferation and motility of HaCaT (Räsänen, Vaheri; 2010). Those facts suggest a regulatory hyperplasic cross-talking as in normal skin. Low temperature reduces the proliferative potential but increases HaCaT differentiation capacity (Borowiec *et al.*; 2013). Even after numerous passages, HaCaT cells retain a remarkable capacity for

normal cornification offering a suitable and stable model for keratinization studies. Nevertheless, some studies made evident that this capacity is reduced at late passages (Boukamp *et al.*; 1997).

Both HaCaT and normal keratinocytes transplants maintained its hyperproliferative keratin proteins, basic 58-KDa (K6) and acidic 49-kD (K16), but minor quantities of K4, K13 and K19. Transplants in nude mice as well as collagen based organotypics, shows strong suprabasal reactivity for K1 and K10, and a late appearance of K2e (Ryle *et al*.; 1989) (Breitkreutz *et al*.; 1998). K1 and K10 are synthetized at sub-confluence densities (Ryle *et al*.; 1989) even in submersion into standard medium, without growth factors (Rekus; 2000). Together with the basal keratin K5/K14 pair, K6, K16 and K17, are regularly produced in *in vitro* culture either flask or organotypic. In epidermis those keratins are only present in a hyperplastic state (Boelsma, Verhoeven, Ponec; 1999). Keratin 13 is abundant in foreskin and its derived keratinocytes cultures, but is absent in adult epidermis. K13 presence is prominent in HaCaT cultures (Boukamp *et al.*; 1988). In brief, HaCaT constitutively expresses keratins K5, K6, K14, K16 and K17, as normal cultured keratinocytes. Additionally, K7, K8, K18 and K19, commonly present in simple epithelia, are synthesized by sparse HaCaT cultures (Katagata, Aoki, Kondo; 1999). K4, K13 and K15 appears at 100% confluence of HaCaT cultures, suggesting abnormal stratification onset (Ryle *et al*.; 1989).

As normal keratinocytes, HaCaT undergoes a decrease in the PLC activity when, irreversibly, it leaves out of cell cycle and become committed (Haase *et al*.; 1997). Small hot shock protein 27 (sHsp27) also is accumulated in the later stages of HaCaT differentiation, like NHK (Arrigo, Ducasse; 2002). In stratification process, HaCaT can lay down basement membrane composed by integrins (e.g. $\alpha_{2/3}\beta_1$, $\alpha_6\beta_4$), laminins-1/-5, collagen-IV and collagen VII as well as increased cornification markers such as filaggrin (filament aggregating protein) and loricrin (lat. *lorica*, protective shell or cover) (Breitkreutz *et al*.; 1998).

Two pioneering papers anticipated organotypics with HaCaT seeding on top of type I collagen lattices and in human de-epidermized dermis (DED), populated with primary fibroblasts (Fig. 2) (Breitkreutz *et al*.; 1998) (Schoop, Mirancea, Fusenig; 1999). As in nude mouse model, gotten epidermis did shows a clearly delay in horny layer formation after 1 week of culture (Breitkreutz *et al*.; 1998). Keratins 10 and 16, as well as involucrin and transglutaminase I (TG-I) were present suprabasally. Importantly, epidermal thickness undergone a high dependence with the number of cultured fibroblasts in the collagen gels (Schoop, Mirancea, Fusenig; 1999). Nevertheless, the nuclei were evident, the dysplastic morphology was “improved” after up to 3 weeks of culture showing a better squamous epithelium accompanied by filaggrin, keratin 2e, and loricrin expression (Fig. 2B). Small proline rich proteins (SPRRs) also were detected in HaCaT organotypics (Boelsma, Verhoeven, Ponec; 1999). In contrast, some studies in submerged monolayers advocates that involucrin production level in HaCaT cells, cultured at low calcium concentration, is actually higher than its levels in intermediate or high calcium conditions (Walker *et al*.; 2006). Like showed by cited papers, when HaCaT-collagen populated lattices are grafted in surface of mice, lay downs a complete basement membrane with its classical markers, e.g. laminin 1/5/10, nidogen, BPA, collagen IV/VII, and structures like hemidesmosomes and anchoring fibrils.

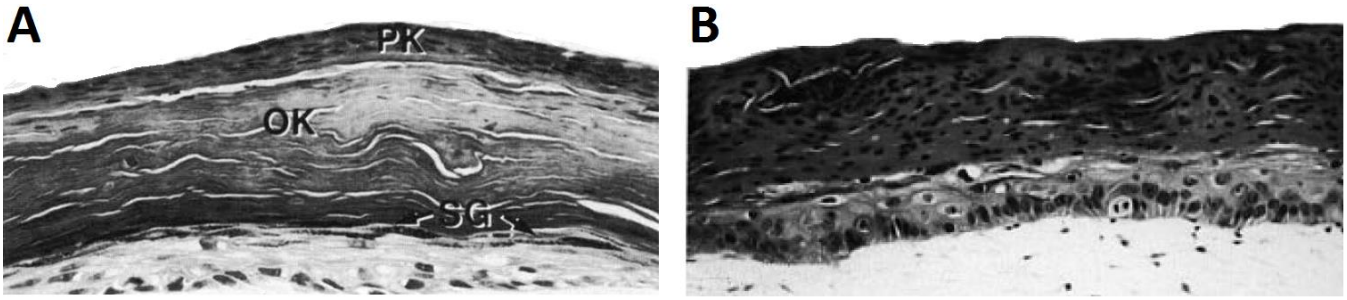

Figure 2. Parakeratotic differentiation of HaCaT in two experimental models. **A**. Cultures on type I collagen gels were grafted onto the deep connective tissue of the muscle fascia (surface transplantation) of nude mice (Breitkreutz *et al.*; 1999). Observed orthokeratosis (OK) was achieved after six weeks of culture. **B**. HaCaT cultured on type I collagen gels from rat tail tendons. A cuboidal parakeratotic (PK) microanatomy is observed throughout the tissue after 3 weeks of culture (Schoop, Mirancea, Fusenig; 1999). SG, stratum granular. Images taken and modified from its original source.

Two common techniques to estimate cell proliferation are TdT-mediated dUTP nick end labeling assay and Ki67 immunohistochemistry (Scholzen, Gerdes; 2000). Despite mentioned above, those techniques demonstrate that HaCaT retains its hyperproliferative behavior through all epithelium thickness, even when most of proliferative cells did restricts to the basal layer (Breitkreutz *et al*.; 1998). The presence of hyperproliferative keratins markers such as K4, K13 and K19 also are in accordance with a high proliferation rate. Similar features have been found in normal keratinocytes from tissues with high proliferation rates, namely, early fetal epidermis (<15 weeks), nonkeratinizing squamous epithelia (e.g. oral mucosa, esophagus, exocervix, etc.) and in abnormal parakeratotic epithelia (Boelsma, Verhoeven, Ponec; 1999). In surface transplants, HaCaT proliferative activity become restricted to the basal layer belatedly. After 2-3 weeks of tissue transplantation, a complete cornification is achieved with a delay too (>3 weeks), compared with normal transplanted keratinocytes (Fig. 2A) (Schoop, Mirancea, Fusenig; 1999). HaCaT loss of sensitivity to paracrine factors might explain commented behavior either in native microenvironment or in organotypic models. Whereby, HaCaT orthokeratotic keratinization will not ever achieved in organotypics unless certain media enrichment be performed.

1.4. Mobility

HaCaT migrates properly in scratch assays demonstrating its usefulness in wound healing models (Büth *et al.*; 2004). This cell line responds to collagen type I as well as fibronectin peptides either non-soluble, in a form of substratum-bound (haptotaxis), or in a soluble form (chemotaxis). Recognition of amino acidic RGD (Arg-Gly-Asp) sequence through its independent VLA-2/collagen receptor ($\alpha_2\beta_1$) might be implied (Scharffetter-Kochanek *et al.*; 1992). Degradative components of laminin 5 also interact with EGFR promoting chemotaxis. This interaction also occurs in invasive phase of skin cancer and in three-dimensional (3D) tissue culture systems built with HaCaT (Zinn *et al*.; 2006). Furthermore, the EGFR ligands as EGF, TGF-α, amphiregulin, epiregulin, heparin-binding EGF-like growth factor (HB-EGF) and heregulin-α, participates in NHK motility and proliferation during wound healing process (Hudson, McCawley; 1998) (Schelfhout *et al*.; 2002). Those EGFR ligands are released after cytokine stimulation. For example, as occurs in psoriatic skin, IL-22 induces the HB-EGF secretion in a STAT3-ERK1/2 dependent manner in HaCaT cultures (Luo *et al*.; 2016). Upon ligand binding, EGFR dimerizes and the tyrosine kinase activity appears leading to cross-phosphorylation, receptor internalization and initiation of its signaling pathway. Up regulation of phospholipases C-γ and D, extracellular signal-regulated kinase keratinocyte motility (ERK), Rac1 GTPase and phosphatidylinositol 3-kinase/Akt pathway contributes to keratinocyte motility and proliferation (Pastore *et al*.; 2008). Commented pathway leads to NF-κB activation, specially its c-REL subunit in HaCaT cells (Lorenz, Schön, Seitz; 2015).

EGFR activation also repress the MDC/CC17 (macrophage-derived chemokine/CC chemokine ligand 17) production and enhances the CCL22 production in HaCaT (Yano *et al*.; 2015). CCL22 is a potent chemoattractant for the CCR4-expressing cells such as Th2 cells. These pathways depend of glycogen synthase kinase-3 (GSK-3) presence as was demonstrated in both monolayer scratch-wounded cultures and in organotypics made with HaCaT (Koivisto *et al*.; 2006). Internalized EGFRs are recycled back to the cell membrane or proteolyzed in cytoplasm depending on the keratinocyte demands (Pastore *et al*.; 2008). Additional intracellular pathways have been associated with locomotion either in NHK or HaCaT. Reactive oxygen species (ROS)-nicotinamide adenine dinucleotide phosphate (NADPH) oxidase system activated by hepatocyte growth factor (HGF) and TGF-β1 has been proven (Nam *et al*.; 2010). Sonic hedgehog (SHH) might be related to HaCaT mobility too (Bigelow *et al*.; 2005). Finally, K6/K16 heteropolymer increase leads to the formation of lamellipodia in the direction of the movement (Trost *et al*.; 2010). Actin filaments also undergoes a reorientation co-localized with fructose-bisphosphate aldolase A (ALDOA) (Tochio *et al*.; 2010).

1.5. Lipid Synthesis

Epidermal lipids regulate skin barrier function by several mechanisms: are allocated between corneocytes in a laminar organization (i.e. bricks and mortar model), are present in a high molar relation, and have hydrophobic properties. During keratinization, the main cornified cell envelope lipids are made from glucosylceramides, free sterols, cholesterol sulphate and phospholipids. These lipids are presents in granular stratum at laminar bodies. Quoted components are *de novo* synthetized by keratinocytes or extracted from extra-cutaneous sources as blood circulation (e.g. trough lipid carriers as CD36 and LDL-receptor) (Elias, Feingold, Fluhr; 2006). Once secreted, lipids are processed by phospholipases A2 (PLA2) and steroid sulfatase when pH 7-7.3. Later, β-glucocerebrosidase and α-sphingomyelinase increase its activity as pH becomes acid (pH ~5) (Feingold; 2007). Lipid enriched lamellas in extracellular spaces of corneocytes are composed by 50% ceramides, 25% cholesterol and 15% free fatty acids (FFAs), with very little phospholipids (Feingold, Elias; 2014).

When confluency (e.g. 50%, 75% and 100%) and [Ca^{2+}] (e.g. 0.6 mM or 1.6 mM) variates in flask culture, HaCaT develops equivalent quantities of total major lipid classes in comparison to NHK (e.g. fatty acids and sphingolipids) (Schürer *et al.*; 1993). Nonetheless, at all stages of cellular confluence, HaCaT cholesterol production is more LDL-dependent than in NHK. Normal keratinocytes are lesser LDL-dependent only at 100% confluence. Like NHK, once HaCaT are exposed to insulin and EGF, increases its 3-hydroxy-3-methylglutaryl coenzyme A (HMG-CoA) synthase and reductase production by 2.5 and 6-fold, respectively. In isoprenoid/mevalonate pathway of cholesterol anabolism, those enzymes catalyze the HMG-CoA from acetoacethyl-CoA, and mevalonate from HMG-CoA, respectively (Harris *et al*.; 2000). Cholesterol is important in lipid lamellae establishment at horny layer. Importantly, at basal calcium condition (i.e. 0.6 mM), the three-foremost species of glycerophospholipids fraction are also larger in HaCaT, namely phosphatidyl-ethanolamine, -serine and –inositol.

Based on the lipid comparison with NHK, Schürer *et al.* conclude that HaCaT cells do not achieve a normal differentiated state, showing defects in terminal steps of cornification. HaCaT organotypics made on DED, rat/bovine collagen gels and polycarbonate (PC) based filters, showed severe impaired capacity to synthesize lipids. Some of them are present in epidermal hydrophobic lipid envelope, as free fatty acids, glucosphingolipids and ceramides. Triglycerides achieve higher amounts in collagen and PC compared with DED (Boelsma, Verhoeven, Ponec; 1999). In our research work, a FFAs analysis was

carried out, so in the table 1 is presented a FFAs fraction comparison between NHK and HaCaT, encountered by several authors.

Table 1. Comparison of free fatty acid (FFA) fraction between HaCaT cell line and other tissues.

FFA (wt%)	<C20						>C20			
	C12:0	C14:0	C16:0	C18:0	C18:1n9	C18:2n6	C20:0	C22:0	C24:0	Reference
Skin	- - -	6.2	28.3	14.8	32.8		1.4	10.5	7.7	Coon *et al*.; 1963
	<0	~2	~30	~50	~12	<0	~4	~10	~37	Norlén *et al*.; 1998
	- - -	- - -	10	8	C18 MUFAs = ~4.3 wt%		2	5	17	van Smeden *et al.*; 2014b
RHE on DED	- - -	- - -	14.7	19.8	14.3	- - -	5.7	8	21.8	Ponec *et al*.; 2001
RHE on PC	- - -	- - -	~12	~8	~5.5	~1	~3	~8.5	~22.5	Ponec *et al*.; 2003
HaCaT	- - -	0	32.6	26	26.2	2.7	0	0	3.5	Schürer *et al*.; 1993

FFA, free fatty acid; wt%, weight percent; RHE, reconstructed human epidermis; DED, de-epidermized dermis; PC; polycarbonate; <C20, short-chain fatty acids; >C20, long-chain fatty acids; MUFA, mono-unsaturated fatty acid.

Based on Table 1, it is possible to think that the two key enzymes required for *de novo* fatty acid synthesis, acetyl-CoA carboxylase and fatty acid synthase, are present in HaCaT. Oxidation of fatty aldehyde, mediated by fatty aldehyde dehydrogenase, have a minor role in the total fatty acid epidermal pool (Rizzo; 2011). Likely, this anabolic pathway, and other, also are present in HaCaT. Once synthetized, FFAs undergoes elongation, probably mediated by ELOVL (elongation of very long chain fatty acid-4) enzymes (e.g. ELOVL1 and 4). Desaturation is mediated, for example, by Stearoyl-CoA desaturase 2 (SCD2), as a crucial step to very long chain fatty acids anabolism (i.e. >C26) (Feingold, Elias; 2014).

1.6. Other Physiological Features

This session aims to show some additional features of HaCaT that makes it a good model to study the NHK biology. HaCaT cell line surface shows similarities in its adhesive properties with normal keratinocytes, even being used as skin attachment assays models to pathogens like *S. aureus* (Mempel *et al.*; 1998). This hypotetraploid cell line also constitutively synthetizes stem cell factor (SCF) in its two molecular forms (i.e. soluble or as membrane receptor). SCF production and secretion increases with time of culture as normal keratinocyte, suggesting the HaCaT potential use in studies of epidermal melanization (Grabbe *et al*.; 1996). For example, in co-cultures with melanocytes (Springer, Engelhart, Biesalski; 2003). HaCaT expresses proteins important in skin normal metabolically function (e.g. Nuclear $1,25(OH)_2D_3$ receptors (VDR) or retinoic acid 4-hydroxilase). Has been proposed as a model in studies of skin metabolism of vitamin D (Lehmann; 1997), its role in inflammation (Ravid *et al*; 2016), as well as retinoic acids skin metabolism (Marikar *et al*.; 1998). Compared with normal human stripped skin, HaCaT sheets made *in vitro* can synthetizes enough quantities of aminopeptidase to catalyze and to prevent xenobiotics skin penetration that are labile to this enzyme (e.g. bradykinin) (Boderke *et al*.; 1998). For illustration, like NHK, submerged monolayer cultures of HaCaT produce and increase the activity of xenobiotic metabolizing enzymes, like cytochrome P450 1 (CYP1) and N-acetyltransferase 1 (NAT1), after an *in vitro* xenobiotic challenge (e.g. para-phenylenediamine, 2-aminofluorene) (Bonifas *et al*.; 2010).

Regarding to wound healing, cultures of this human spontaneously transformed keratinocyte cell line, rapidly and massively translate functional inducible nitric oxide synthase (iNOS) and GTP-cyclohydrolase I (GTP-CH I), after stimulation with inflammatory cytokines as interleukin-1β (IL-1β), tumor necrosis factor alpha (TNF-α) and interferon gamma (IFN-γ). Something similar occurs at basal keratinocytes from edge of wounded normal skin (Frank *et al*.; 1998). HaCaT responds to comment cytokines in a normal

fashion. For case, TNF-α acts by interaction with either death domain-containing TNF-receptor 1 (TNF-R1) and by non-death domain-containing TNF-receptor 2 (TNF-R2). These two receptors create a positive feedback loop across ERK/JNK (extracellular signal-regulated kinase/c-Jun N-terminal kinase) pathway, inciting Early Growth Response-1 (EGR-1) activity. EGR-1 is a member of the zinc-finger transcription factors that mediates more production of IL-1α/β, IL-6 and TNF-α (Son *et al*.; 2008). Above cited signaling also exerts other important effects through NF-κB pathway as depletion of gap unions and translation decrease of functional connexin 43 (Cx43). Those events also occur during migration of NHK and inflammation (Tacheau *et al*.; 2008). When wound microenvironment is emulated by a hypoxic challenge in scratch assays, HaCaT also initiates Hsp90α (heat shock protein 90 alpha) releasing in a HIF-1 (hypoxia induced factor 1) dependent manner. In turn, cell migration and wound closing is stimulated via lipoprotein receptor-related protein-1 (LRP-1) (Zhang *et al*.; 2014). Artificial EGFR activation also leads to neural NOS (nNOS) and endothelial NOS (eNOS) functional isoforms synthesis in HaCaT, which are related with modulation of keratinocyte proliferation and melanogenesis (Boissel *et al.*; 2004) (Nakai *et al*.; 2009). Reepithelization in diabetes is altered, probably due to high glucose effect on intracellular nitric oxide (NO) levels, which suppress the keratinocyte proliferation. A similar effect on HaCaT cells was showed by Nakai *et al*. in 2003, who demonstrate a significantly iNOS increase in presence of high [glucose], with its accompanying effects. These works show HaCaT usefulness in diabetic skin model too.

The high resistance to oxidative stress of HaCaT differentiated states and its sensitivity to peroxynitrite in the basal phenotype has been proven (Bakondi *et al*.; 2003). HaCaT also responds to tumor necrosis factor (TNF)-related apoptosis-inducing ligand (TRAIL) establishing an inflammatory profile mediated by IL-8 releasing and IL-1 receptor antagonist (IL-1Ra) surface exposition (Leverkus *et al*.; 2003). The group of chemokines TARC/MDC (thymus and activation-regulated chemokine/macrophage-derived chemokine) are overexpressed in some skin disorders, playing a pivotal role in the infiltration of Th2 cells (e.g. atopic dermatitis). TARC/MDC are normally overexpressed in HaCaT and responds in the same way of normal epidermis to regulatory effects of IL-4, IL-13, and IFN-γ (i.e. re-distribution of cadherin/catenin proteins) (Fujii-Maeda *et al*.; 2004). Relatedly, adenylyl cyclase-cAMP system down regulates the TARC/MCD activity in HaCaT increasing the IFN-γ and TNF-α production (Qi *et al*.; 2009). Nevertheless, has been evinced that terminal gene expression profile (e.g. keratin 10, filaggrin, loricrin) of HaCaT cell line does not respond like NHK after T helper cell cytokines challenge (i.e. IFN-γ, IL-4, IL-17A and IL-22) (Seo *et al*.; 2012). Catepsin B, an enzyme related with matrix degradation in keratinocyte migration during wound healing, is also produced by HaCaT (Büth *et al*.; 2004).

Calcium intracellular metabolism is independent of its extracellular concentration in HaCaT (Shi, Isseroff; 1997) (Micallef *et al.*; 2009). Normally, it depends of external cues as purines and its derivatives (e.g. ATP, ADP, UTP, etc.). Insofar as, HaCaT express the purinoceptors 2 Y (e.g. $P2Y_2$, $P2Y_6$) which can induce transient intracellular calcium rise (e.g. 6.2±0.5), via $G_{q/11}$-phospholipase C (PLC)-$[Ca^{2+}]_i$ pathway (Lee *et al*.; 2001) (Yoshida *et al*.; 2006). Similar effects were obtained when HaCaT was exposed to parathyroid hormone-related protein (PTHrP), which potentiates the effects of ATP (Burrell *et al*.; 2007). HaCaT cultures also responds to corticotropin-releasing hormone (CRH). The CRHR is a housekeeping synthetized receptor that emulates the high sensory capability of epidermis for noxious stimuli. CRHR signaling promotes the local autocrine CRH/CRH-R loop involved in the local stress response pathway (Ruhland, de Villiers; 2001). In line, this cell line also produces IL-18 as a response to adrenocorticotropic hormone (ACTH) stimulation. These observations shed light into the use of HaCaT to study the interaction between hypothalamic–pituitary–adrenal axis and epidermal inflammatory mediators (Park *et al*.; 2007). Functional thyroid-stimulating hormone receptor (TSHR) also was evidenced. This finding

empowers the usefulness of HaCaT cells as a hypothalamic–pituitary-thyroid-skin axis research tool as well (Pattwell *et al*.; 2010). Furthermore, HaCaT also translates functional muscarinic receptors (i.e. M1 and M3). These receptors can be activated by acetylcholine leading to ADAM (A Disintegrin And Metalloproteinase) pathway. Then, once flotillin-1 and MMP3 (matrix metalloproteinase 3) are activated, agonistic EGF-like ligands are released by cell surface proteolysis. Commented process is known as triple-membrane-passing signal (TMP) pathway. EGFR is finally transactivated altering the proliferation and differentiation properties of this cell line as in normal epidermis (Ockenga *et al*.; 2014). Recent works also did demonstrate that HaCaT cell line is a good option as first step to evaluate the circadian behavior of the skin and its relationship with temperature (Spörl *et al*.; 2011) and the nuclear redox status (Ranieri *et al*.; 2015).

2. MATERIALS AND METHODS

2.1. Normal Human Dermal Fibroblasts Isolation and Culture

Full thickness skin biopsy (i.e. ~5 mm punch) of six consented patients was harvested from its retro auricular area. This procedure was done by qualified medical personnel associated with our laboratory (Laboratorio de Terapia Celular y Biobanco, IPS-Universitaria), in the context of an autologous dermal fibroblasts-based facial rejuvenation cell therapy. Customers were consulted, through an informed consent, for their willingness to use their surplus cells in research. Firstly, biopsy fat tissue was removed with sterile scissors, then dermal-epidermal tissue was cut into pieces of ~0.5 mm (named skin explants) and were placed into T25 culture flasks (Falcon™). Skin explants were dehydrated by air exposition for 20 minutes allowing flask surface attachment. Dulbecco´s Modified Eagle Medium (DMEM) supplemented with 10% (v/v) fetal bovine serum (FBS), 1% (v/v) penicillin-streptomycin (Pen-Strep) and 1% L-Glutamine (L-Glu), all from Lonza, was added. Flasks containing the explants where placed into incubator at standard conditions (37 °C, 5% CO_2, 99% relative humidity, RH). Medium change was done every two or three days. After fibroblasts outgrowth (~20 days), the cells were sub-cultured using 0.05%/0.02% (w/v) trypsin/EDTA (Sigma-Aldrich) and maintained with DMEM supplemented with 5% (v/v) *in house* produced human platelet lysate (hPL), 1% (v/v) Pen-Strep, and 1% L-Glu. Low dermal fibroblasts passages (1-3) were used in further experiments maintaining a split ratio of 1:2.

2.2. HaCaT Culture and Maintenance

HaCaT cells were grown submerged in complete medium: DMEM (high glucose, ~1.8 mM Ca^{2+}) supplemented with 10% (v/v) FBS, 1% (v/v) L-Glu and 1% (v/v) Pen-Strep, all from Gibco™. Sub-culturing was done with 0.25%/0.02% (w/v) trypsin/EDTA (Sigma-Aldrich), maintaining a split ratio of 1:4 between the passages 30 and 50 for experiments. Medium was renewed each two or three day.

2.3. Population Doubling Time and Cell Proliferation Assay

Nine serial dilutions of HaCaT were done beginning from $1{,}5x10^5$ cells. Initially, cells were counted in Neubauer´s chamber. After 18 h of incubation in standard conditions, cell number was estimated using 1 mg/mL yellow tetrazolium MTT (3- (4, 5 -dimethylthiazolyl - 2) - 2, 5 - diphenyltetrazolium bromide) (Thermo Fisher) dissolved in MEM without red phenol and L-glutamine (MEM-RP^-, Sigma-Aldrich). A linear regression relating cell number versus formazan crystals OD570 was carried out to cell number determination in further experiments. Population doubling time (PDT), defined as required time for a

culture to double in number, was determined for HaCaT cell line in three independent assays cultured in complete medium. Following American Type Culture Collection (ATCC) guidelines, generation of a growth cell curve in standard conditions was used to calculate the PDT with the formula $PDT = T(ln2/ln\ (X_e/X_b))$; where, *T* is incubation time in any units, X_b is the cell number at incubation time begins and X_e is the cell number at final point of incubation time. Start cell input was $3x10^3$ per well (n=5) in a 96-well flat-bottom plate (Greiner CELLSTAR®). Cell culture was monitored for 10 days and medium was exchanged each two or three day. A linear regression was carried out to determine the best two points where the population doubling number behaves linearly. Once PDT was determined, three independent cell proliferation assays (CPA) were done to evaluate the effect of used media on HaCaT proliferation. For CPAs, optimal cell density and the optimal incubation time were subtracted from PDTs assays. See *1. Statistical Supplemental Material*, to more technical details.

2.4. Dermal Equivalents

Corning® Transwell® polyester (polyethylene terephthalate, PET) membrane cell culture inserts (CLS3460) were used as supports in three different models to establish dermal equivalents. In the simplest model, HaCaT was directly cultured on PET membrane. Primary human fibroblasts were plated on the basolateral side just underneath the filter, as dermal equivalent. In a second model, fibroblast populated fibrin gels were erected on PET inserts membranes; then were used as dermal equivalent surfaces for HaCaT cells culture. Fibrin gels were made using research available fresh frozen plasma (FFP), discarded from blood bank belonging to the IPS-Universitaria. 350 µL of FFP were mixed with primary human dermal fibroblasts, 5 µL of tranexamic acid (Ropshon®) and 50 µL of thromboplastin (TP) as coagulant initiator. Mixture was incubated at standard conditions by 5 minutes. PET and fibrin methodological designs were original of this research. In a third model, rat tail collagen type I and type III mixture (CI+III), from Advanced Biomatrix (RatCol®), was used following fabricant recommendations. Briefly, cooled collagen type I and type III were mixed in a proportion of 2:1, thus chilled neutralization solution with human primary fibroblasts was added. After a gently agitation, the mixture was incubated by 1 hour at standard conditions until gel state was reached. Once fibrin and collagen gels were obtained, HaCaT cells were plated at three cell densities (see below).

2.5. Dermal-Epidermal Skin Equivalent Culture and Maintenance

As described above, PET, human fibrin or CI+III matrices populated with human primary fibroblasts were used to seed HaCaT on its top to generate dermal-epidermal organotypics (DEpOs). DEpOs were built in 12 well plates (Corning®), grown submerged for 7 days and were raised to the air-liquid interphase for 14 days to be analyzed. Two variants of culture supplemented media were used. A medium named QN composed by DMEM/Ham´s F12 (3:1) mixture supplemented with 10% FBS (Gibco®), 1% Pen-Strep (Lonza®), 1% L-Glu (Lonza®), 8 ng/mL cholera toxin (Life Technologies), 24 µg/mL adenine, 5 µg/mL insulin, 0.4 µg/mL hydrocortisone and 13 ng/mL triiodothyronine (all from Sigma). At day 7, recombinant human Epidermal Growth Factor (EGF, Gibco®) was added to QN medium at 10 ng/mL, which was called QC. To improve the firstly proposed QN-QC media based model, a protocol developed by Gangatirkar *et al*. in 2007 was proved with some modifications adjusted to our laboratory conditions and possibilities. Those researchers developed three types of media with different exposition time (every 7 days): a) Epidermalization Medium (EM): 3:1 1X DMEM/1X Ham´s F12, 0,3% FBS, 1% Pen-Strep, 1% L-Glu, 8 ng/mL cholera toxin, 24 µg/mL adenine, 5 µg/mL insulin, 5 µg/mL transferrin (Gibco®), 0,04 µg/mL selenium (Gibco®), 0.4 µg/mL hydrocortisone and 13 ng/mL triiodothyronine. b) Cornification Medium (CM): Same formulation that EM but 2% FBS. c) Maintenance Medium: EM formulation plus 1% FBS. As

we describe in results, Gangatirkar *et al*. media were only used in CPA measurements because its irrelevant behavior compared with QN-QC model. Three HaCaT densities were proved: $2x10^5$, $3x10^5$ or $4x10^5$ per insert (~1,3 cm^2); three fibroblasts proved densities were: 500, $1x10^3$ and $2x10^3$ per insert (~1,3 cm^2).

2.6. Histology and Immunohistochemistry

Samples were fixed in 10% neutral buffered formaldehyde (Sigma). Dehydration was carried out using the 70%-90%-100% ethanol sequence. Once dehydrated, samples were cleared by a typical xylene based sequence for specimens not more than 4 mm thick. Paraffin wax-based histological infiltration was done using liquid wax at 60 °C, cooling at 20°C. Infiltrated samples were correctly oriented in the mould to blocking out. Wax blocks containing the tissue specimens were removed from the mould to proceeds with microtome. Vertical slides (3-5 µm) were cut and stained with hematoxylin-eosin (H&E) or incubated with primary antibodies to immunohistochemistry. The following murine monoclonal anti-human antibodies from Abcam® were used as primary antibodies (all diluted 1:50): anti-cytokeratin 14 ([LL 002] ab7800), anti-cytokeratin 10 ([DE-K10] ab9026) and anti-filaggrin ([SPM 181] ab17808). Also, rabbit monoclonal anti-human antibodies were used as primary antibodies: anti-Ki67 (diluted 1:2000; ThermoFisher, RM-9106-S) and anti-Loricrin (diluted 1:50; Santa Cruz®; W-22 sc-133757). All antibodies were diluted in Tris buffer (pH 6). To improve the immunoreactivity of target antigens in formaldehyde fixed tissues, Thermo Scientific™ Lab Vision™ Citrate Buffer for Heat-Induced Epitope Retrieval (10X) (AP-9003-500) was used. In negative control sections phosphate-buffered saline (PBS, Sigma) was substituted for the primary antibody. Antibody reactions were revealed using UltraVision Quanto detection system HRP (Thermo; TL-125-QHL). Sections were counterstained with hematoxylin. Tissue control was normal skin to most of markers and tonsil to Ki-67. Light microscopy analysis and photography was done in an inverted microscope Carl Zeiss PrimoVert. Finally, a manual approximation to Ki-67 index calculation was carried out based on works of Safferling *et al*. (2013) and Kitagawa *et al.* (2014). The reported Ki-67 index were expressed as the mean of three independent experiments ± SD (see supplemental material, *4. Calculation of Ki-67 Index*).

2.7. Lipid Extraction and Gas Chromatography with Fire Ionization Detector (GC-FID)

Lipid extraction was conducted by the simple method described by Folch, Lees and Sloane in 1957. Briefly, after DEpOs mechanical homogenization, a mixture of chloroform/methanol (2:1) (all from Sigma) was added. Saline solution (NaCl 0,9%, CORPAUL®) was used to wash and separate the hydrophobic lipid fraction. After centrifugation, the process was repeated three times with chloroform phase only. Samples were stored at -20 °C. Analysis of fatty acid methyl esters (FAMEs) fraction by gas chromatography (GC) was done as was described by Bermúdez and Velásquez, 2014. An Agilent 6890N gas chromatograph with fire ionization detector (FID) and a capillary column (TR-CN100, 60 m x 250 µm x 0.20 µm ID) was used.

2.8. TEER Measurement and Lucifer Yellow Permeability Assay

After 21 culture days, DEpOs-integrity and its barrier function were evaluated by transepithelial electrical resistance (TEER) and the penetration rate of Lucifer yellow (LY), a paracellular integrity marker. Inserts containing DEpOs were washed with Ringer lactate (CORPAUL®) and submerged in Hank's Balanced Salt Solution (HBSS) with 25 mM 4-(2-hydroxyethyl)-1-piperazineethanesulfonic acid

(HEPES) (HBSS-HEPES, both from Gibco®), 1.5 mL basolateral and 500 µL apical. TEER was determined following the guidelines of Millicell® ERS-2 Voltohmmeter (Merck Millipore). Inserts were put in a new 12 well plate containing 1 mL of HBSS-HEPES per well, and 500 µL of 2 mM LY solution prepared in HBSS-HEPES, was added apically. Plate was incubated (37 °C, 5% CO_2, 99% RH) in agitation (50 rpm) by 30, 60, 90 and 120 minutes. A basolateral sample of 200 µL was taken at each time, replenishing with the same solution volume after harvesting. Fluorometric analysis was carried out in 96 well plate Greiner Black (Fluotrac™ 200) and determined in a Varioskan™ Flash Multimode Reader (ThermoFisher) at 480/530 nm, using HBSS-HEPES solution without LY as blank. All determinations were done four times, with three intra-assay replicates by each DEpO variant (i.e. PET, fibrin or CI+III).

2.9. DNA Content Assessing (Ploidy) by Flow Cytometry

DNA content measurements were based in a protocol described by Krueger and Wilson in 2011. Briefly, confluent fibroblasts (passage 1) and HaCaT at ~70% confluence (passage 36, 37 and 38) were collected ($1x10^6$ of cells) and fixed with 1 mL 70% ethanol (Merck®) overnight. Harvested cells were washed three times in phosphate buffer solution (PBS, Gibco®), with centrifugation (1500 rpm) between each wash. Staining was carried out by the addition of 300 µL of propidium iodide (50 µg/mL PI; Becton Dickinson, BD™). Cells were incubated in darkness, at room temperature, for 20 minutes. DNA QC Particles kit from BD™ was used to linearly determination of BD LSRFortessa™ cytometer (i.e. chicken erythrocyte nuclei) as well as setup and verification of the doublet discrimination function (i.e. calf thymocyte nuclei). PI signal was detected using a 630 nm long-pass filter. Results were analyzed by FlowJo 7.6 software to determine cell cycle phases distribution (i.e. pragmatic Watson approximation). Ploidy was determined by comparison with human primary fibroblasts. "Rule of three" was followed to generate reproducible valid results: 1) Do the measurements three times at the same day with the same sample. 2) Do the measurements three different days with the same sample. 3) Do the measurements three times with different samples (i.e. different HaCaT passages and primary fibroblasts from distinct individuals).

2.10. Statistical analysis

Normal behavior of data was proved for all assays using both Kolmogorov-Smirnov Test (K-S) with Lilliefors significance correction and the Shapiro-Wilk (S-W) test. Homogeneity of variances (i.e. homoscedasticity) was proved by Levene test. Based on normally and homoscedasticity outcomes, one factor ANOVA/Kruskal-Wallis and, if it was necessary, Bonferroni/Tamhane tests were used to compare mean values from independent groups. In most of the cases α=0.05 significance was assumed. All analyses were conducted using Excel v.10 and SPSS v.20. A detailed statistical analysis of PDT/CPA assays is showed in *1. Statistical Supplement Material* to illustrate the form to procedure with data of all quantitative assays.

3. RESULTS

In order to provide an optimal microenvironment that allows *in vitro* epidermis production, is obligatory to consider three pivotal matters: initial cell density, calcium concentration ($[Ca^{2+}]$) and growth factors. The initial input of both, HaCaT and human fibroblasts (i.e. $4x10^5$ and $2x10^3$ respectively), was fixed using bright field microscopy only in PET, due to its simplistic initial features. We assumed that proliferation and attachment properties would be potentiated in other two evaluated biopolymers, as

in effect it happened. Applied criterion to HaCaT was that it reached the total confluence at day 7 after culture (i.e. when air-liquid phase lifting was carried out). To fibroblasts, that it did maintain its growth and viability after 21 days of culture. [Ca^{2+}] was not possible to manipulate, so all assays were conducted at the fabricant calcium levels of used media. FBS concentrations tried by Gangatirkar *et al.* in media, also implicates [Ca^{2+}] variations. For instance, 2% FCS can include about 100 µM Ca^{2+}. Calcium gradient is a fact in human epidermis (higher at horny layer), and its molecular effect has not been totally elucidated. Differentiative effect of calcium high levels is improved by 100% culture confluence. Indeed, confluence in HaCaT cultures induces functional early terminal markers as K1 and K10 (Ryle *et al*.; 1989). So, as HaCaT growth is independent of [Ca^{2+}] (Micallef *et al.*; 2009) and its levels in used media did not variate during culture (i.e. QN and QC), more importance to EGF concentration and cellular confluence variables were given as well. Finally, it has been demonstrated that fibroblasts are a mesenchymal cell type that develops subpopulations. "Positional identity or memory" may be due to biological and physical differences in local microenvironment where they reside (Sriram, Bigliardi, Bigliardi-Qi; 2015). To minimize potential positional variation, retro auricular zone was only used as fibroblasts source.

3.1. HaCaT need 16.92±2.03 hours to divide in complete medium

To investigate the growth rate properties of our HaCaT cell line under used media and in agreement to DEpO optimal culture time elucidation, population doubling time (PDT, Fig. 3) and cell proliferation assay (CPA, Fig. 4) were performed. An ideal trend was expected following the ATCC guidelines (Fig.3A). Three experiments showed the same behavior in the obtained cell growth curves. Non-statistical differences were found in the cell number at the end of each incubation time and in calculated PDTs (Fig. 3B). Statistical and calculus details of PDT and CPA are available at *1. Statistical Supplemental Material*.

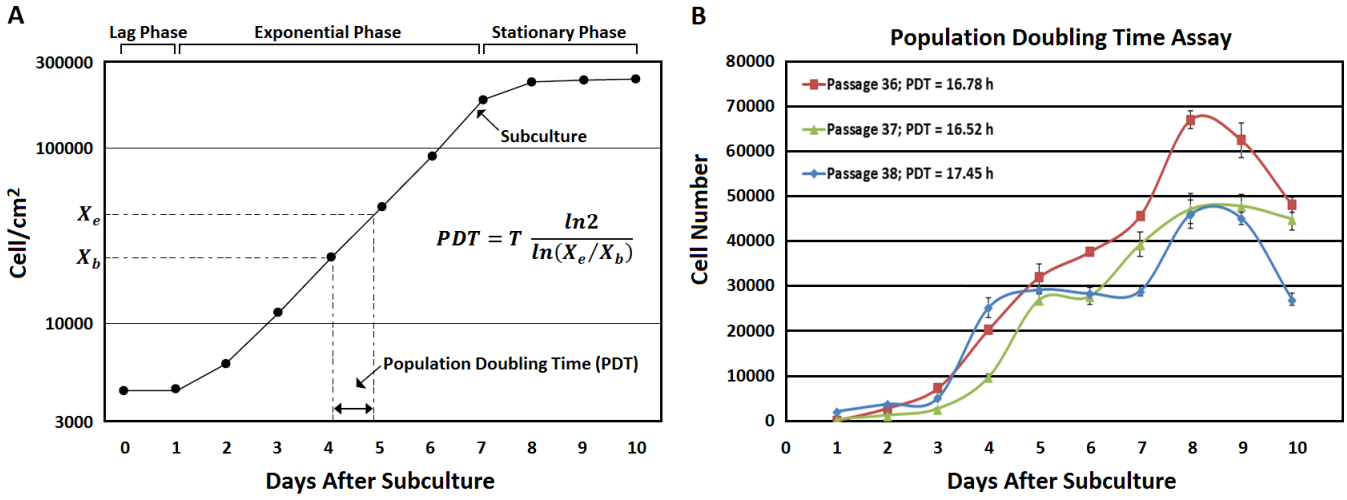

Figure 3. Population doubling time (PDT) assay of HaCaT cell line. **A.** Theoretical behavior of a cell culture following the ATCC guidelines. In a given condition, showed formula predicts the PDT of a specific cell type when growth between two points is linearly (e.g. X_b and X_e). **B.** HaCaT growth behavior for three PDT assays in three different and consecutive passages. Indistinctly cell passage, one factor ANOVA did suggest that there were no statistical differences between assays in the first eight days ($p > 0.01$). PDTs were calculated with cell numbers obtained between day 2 and day 4. Calculated 95% confidence interval using t-student approximation was 16.92±2.03 h ($\alpha/2$=0,025, n-1=2, see text). Five replies (n=5) by evaluated point (i.e. day in *x* axis) in each assay were made. Bars represents standard deviations.

All PDT curves did show a trend to cell growth rate decrease at day five. Two issues might be associated. First, nutrients decreasing in media (i.e. energetic stress) after massive mitosis at days three and four.

Negative cues to growth modulation, because well surface exhaustion (i.e. cell contact inhibition), might be implicated too (Martz, Steinberg; 1972). Researches that assessed the HaCaT susceptibility to contact inhibition, showed the same behavior at day 5 of culture (Morais *et al*.; 2017). R^2, calculated from linear function of the eight first points in each graphic, showed a good correlation ($R^2 > 0.85$). PDTs were calculated with cell number obtained between day 2 and day 4 as is proposed by the ATCC mathematical approximation. Cell division rate is normally distributed (Kubitschek; 1962). Gaussian distribution was ratified here by Kolmogorov-Smirnov Test (K-S) with Lilliefors significance correction and the Shapiro-Wilk (S-W) test. One factor ANOVA ($\alpha = 0.01$) was used to compare the three PDTs assays behavior. No statistically significant differences were found ($p > 0.01$). A 95% confidence interval (CI) to PDT was made applying the t-student statistic ($t_{(0.025;\ n=2)}$). Based in these results, was possible to conclude that the PDT for HaCaT, at 30-40 passages and cultured in complete medium, was 16.92±2,03 hours. This time correlates with reported by Boukamp *et al.* in 1997, where they found that PDT did reduce with passages (e.g. from ~23 h at P19 to ~16 h at P119).

In previous researches HaCaT viability and proliferation were dependent on insulin and EGF presence (Rekus; 2000). Nonetheless, here an ideal-like growth curve was obtained in medium without supplements and in high [Ca^{2+}] (Fig. 3). This result propose that this dependence is weakly. It is important to remember that used DMEM had ~1.8 mM [Ca^{2+}], a quantity considered high to NHK culture. In other words, HaCaT cells are susceptible to mitogenic stimuli of mentioned growth factors but are independent to them. Thus, was possible to conclude that HaCaT does not depends on high concentrations of exogenous growth factors (more than added by FBS) to maintain logarithmic growth phase. This feature is not present in NHK. Finally, once PDT was fixed, four days after HaCaT subculture were stablished as the best time to DEpOs construction.

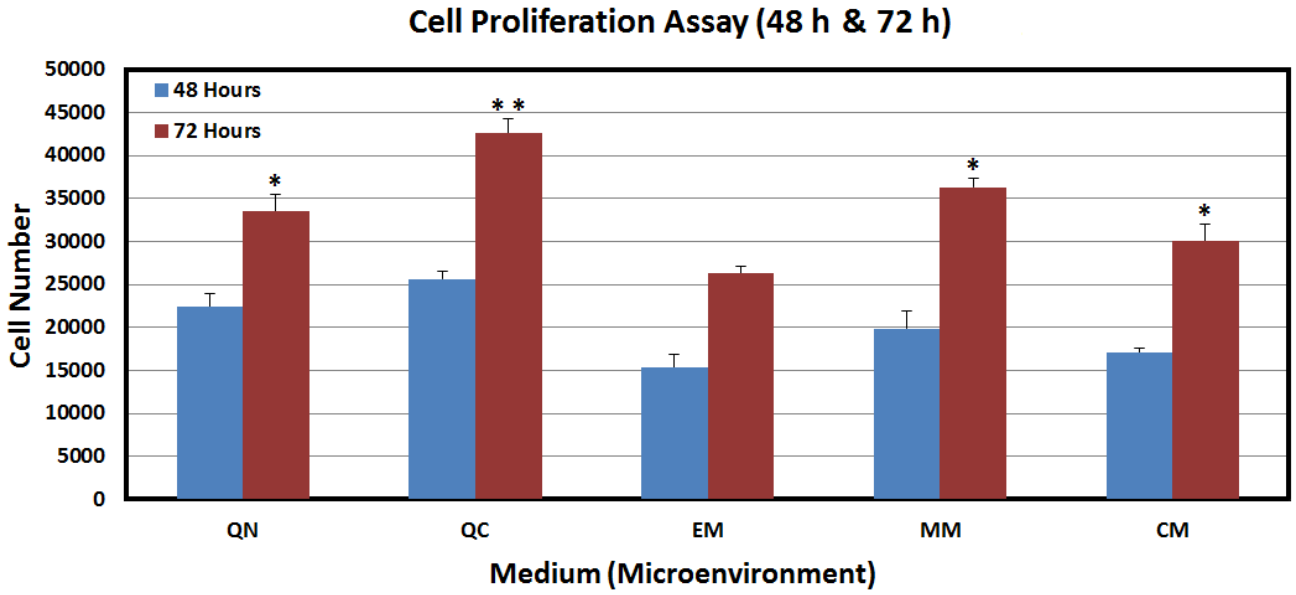

Figure 4. Cell proliferation assay (CPA) of HaCaT cell line. Showed data correspond to the first assay (passage 36). Several supplemented media were evaluated. QN and QC are the names of media used at our laboratory; they differ from each other by the presence of EGF content. EM (Epidermalization Medium), CM (Cornification Medium) and MM (Maintenance Medium) are media used by Gangatirkar *et al*. (2007). The pivotal difference between each one is the FBS concentration, 0.3% to EM, 2% to CM and 1% to MM. One factor ANOVA did suggest that there were statistical differences between treatments at 72 h of incubation ($p < 0.01$). Bonferroni test showed that QN, MM, and CM behaves in the same way (*, i.e. p value > α, 0.01). These three media were more potent mitogens than EM but lesser than QC (**). To conclude, QC medium was the most potent mitogenic tested medium. While was true that behavior at 48 h of incubation was similar, no statistical differences were found ($p > 0.01$). Each treatment had five replicates per assay (n=5). Three independent assays were done (passages 36, 37 and 38) with similar results.

To investigate the mitogenic effect of used media over HaCaT, CPA was implemented. The media used in this research, as well as the media used by Gangatirkar *et al*. (2007) were tested. Based on one factor ANOVA results, we did argue that there were statistical differences between used media after 72 hours of incubation (Fig. 4). Thus, Bonferroni test ratified that outcome, with a confidence of 99,99%. The unique treatments which behavior is not significantly different compared with each other are QN, MM, and CM (i.e. p value > α). Based on this find is possible to conclude that the three-mentioned media elicit more potent mitogenic effect on HaCaT cells (at passage 30-40) than EM, but lesser than QC. These results are in accordance with FBS and EGF concentration. QC was the medium with the highest concentration of both, 10% and ~10 ng/mL respectively. While was true that behavior at 48 h of incubation was similar, no statistical differences were found (Fig. 4). Finally, significantly mitogenic effect of 10 ng/mL EGF on HaCaT, after 36 hour of incubation, has been reported previously (Liang *et al*.; 2008).

3.2. Dermal-Epidermal Organotypics (DEpOs) reaches a parakeratotic cornification

After four days in submerged culture, HaCaT were detached by trypsinization to DEpOs construction. The former time was fixed from PDT assay (Fig. 3B). Three implemented dermal matrices were removed from Transwells® using a needle. Harvested tissues were fixed and immersed in paraffin to make microtomic cuts. Hemathoxilin and eosin (H&E) staining showed partial stratification in all matrices. Very few layers were observed in comparison with normal skin (Fig. 5, 6 and 7). After 21 days of culture, air-exposed DEpOs did not show classic histological features of keratinocyte differentiation. Microanatomy was the same regardless of three evaluated 3D tissue culture models. Flattened shape was present in all layers, not only in the uppermost. Enucleation never was observed (i.e. parakeratosis instead orthokeratosis). Cytoplasm was regular without evident granules or vesicles. No obvious hemidesmosomes were found (Fig. 5, 6 and 7). Obtained DEpOs histology in PET matrix showed microscopically features away from native skin (Fig. 5); but enormously similar to previously reported HaCaT sheets made on submerged polycarbonate (PC) membranes (Steinsträsser; 1994) (Boderke *et al*.; 1998).

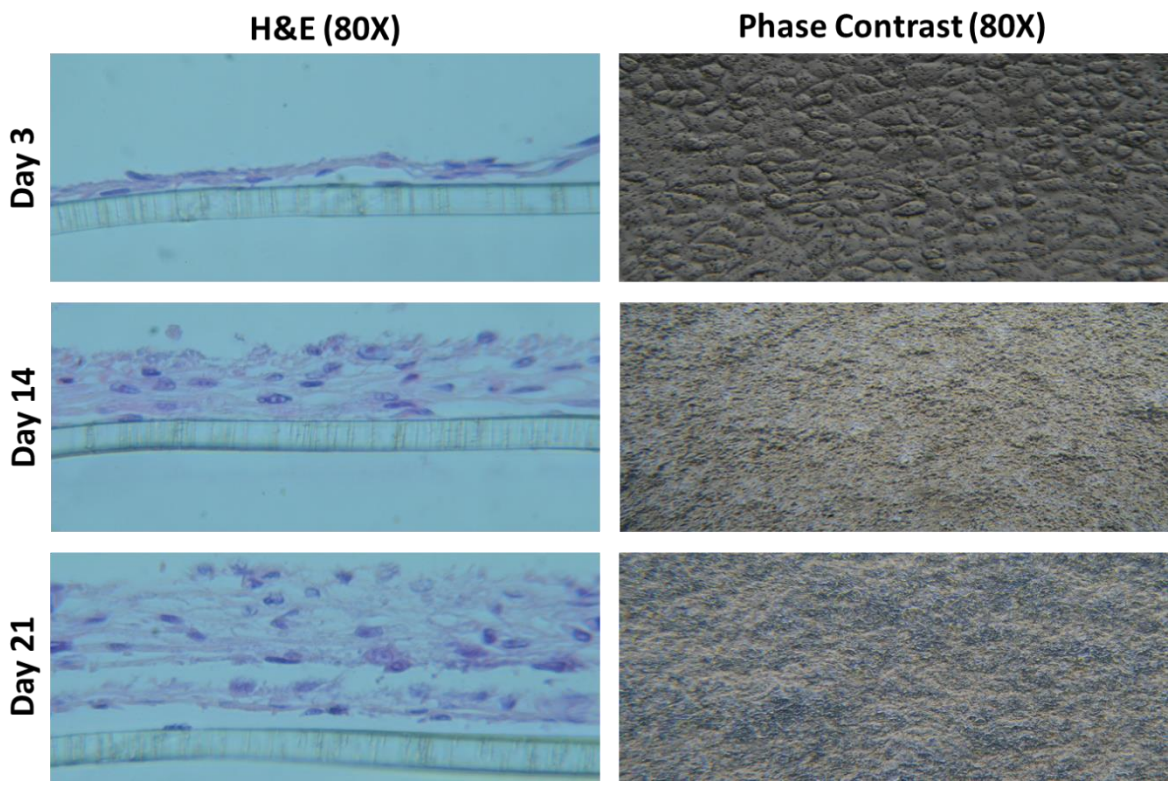

Figure 5. Hematoxylin and eosin (H&E) staining and microscopical phase contrast tracing of dermal-epidermal organotypics (DEpOs) built directly on polyethylene terephthalate (PET) membrane inserts. Once DEpOs construction was performed, three moments of culture were selected to tissue paraffin embedding (i.e. 3, 14 and 21 days). Partial stratification is achieved (7-8 layers). Flattening, massive nuclei losing and non-evident hemidesmosomes were found. Obtained morphology is resembled to HaCaT sheets erected over polycarbonate inserts (Boderke *et al*.; 1998). Phase contrast microscopy photos were taken at the same three moments. Those photos showed evident topological changes and the usefulness of PET to trace these models. PET based DEpOs histology was correlated with its topological changes photographically registered. Microanatomical features are compatible with parakeratosis, suggesting abnormal keratinization process. Fibroblasts have not been shown but they were present in basolateral side. n=5.

There are several benefits to use fibrin from fresh plasma as dermal matrix. Plasma have a low-cost because its easily obtainable resource. For example, from whole blood or plasma discarded units at blood banks. Plasma give us the possibility to produce an autologous skin equivalent transplant if it is necessary. Some works have previously shown that fibrin is a suitable substrate for keratinocyte cultivation and transplantation (Ronfard *et al*.; 2000) (Llames *et al*.; 2004) (Morales *et al*.; 2016). HaCaT expresses urokinase-type plasminogen activator receptor (uPA-R) which is related with accelerated plasminogen activation, detachment and normal keratinocyte migration during wound healing (Reinartz *et al*.; 1994). To prevent HaCaT detachment, we did inhibit plasmin using a lysine analogue named tranexamic acid. Thus, did expect that most of plasmin mediated protease activity was annulled. Fibrin based DEpOs revealed good stability throughout incubation time. As showed in the Fig. 6, normal stratification was not obtained. Apart of fibroblasts adhesion assays on fibrin lattices (Bizik, Harjula, Kankuri; 2010), we were not aware about other 3D tissue culture systems built with human fibrin, human primary fibroblasts and HaCaT.

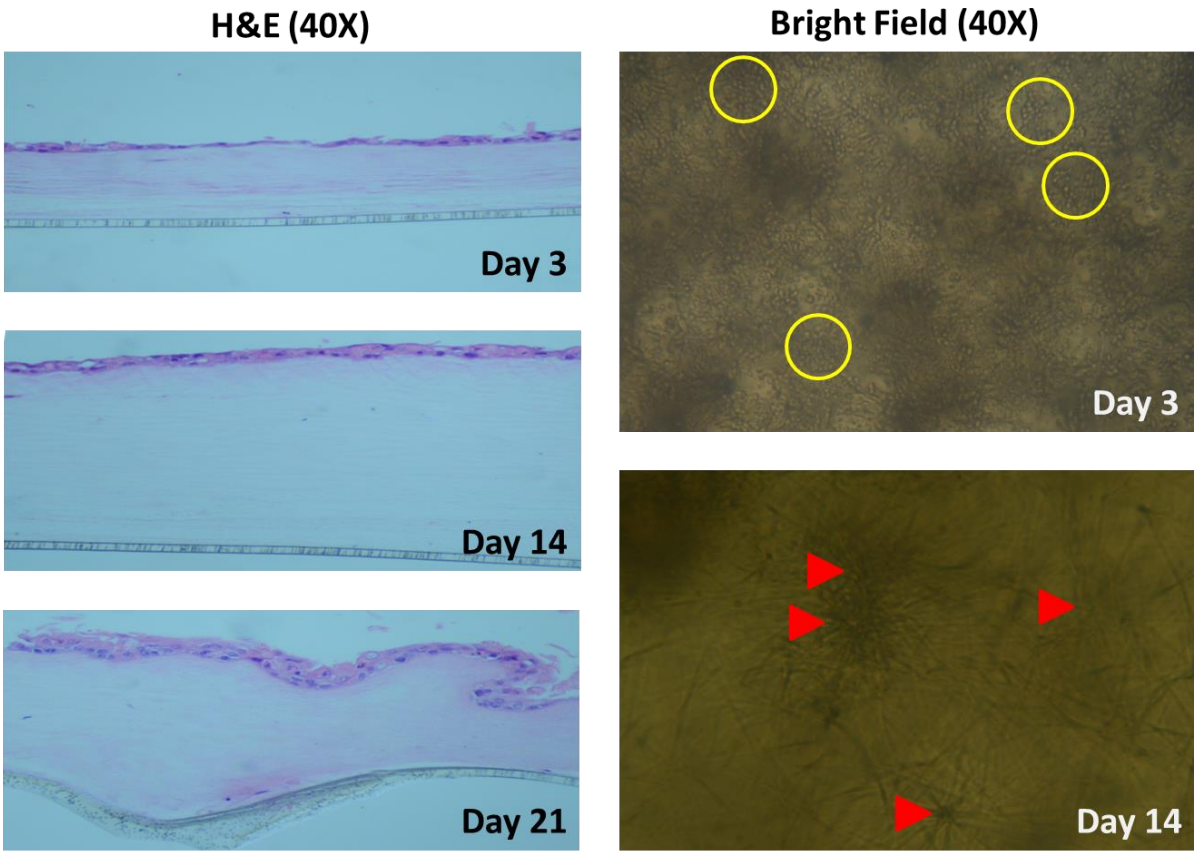

Figure 6. Hematoxylin and eosin (H&E) staining and microscopical phase contrast tracing of dermal-epidermal organotypics (DEpOs) built from human fibrin. Time harvesting and microscopical photos were the same of PET DEpOs. Partial stratification is achieved after 21 days of culture (2-4 layers). Flattening, massive nuclei losing and non-evident hemidesmosomes in H&E were compatible with an abnormal keratinization process (i.e. parakeratosis). Bright field microscopy photos showed attached HaCaT cells at day 3 (yellow circles) and fibroblasts colonies at day 14 (red arrowheads). Take epidermal stratum photos after day 7 was impossible. Something similar occurs with dermal stratum after day 14. Opacity was consequence of cell confluency. n=5.

More than 70% of normal dermis dry weight consists of collagen. Type I and Type III are the major collagens components (Chu *et al.*; 2006). Type I collagen has a molecular mass ~290 KDa and accounts for approximately 80% of total amount of dermis collagen. Type III collagen makes up approximately 10% of dermal collagen (Gelse, Pöschl, Aigner; 2003). Both type I and type III collagen form the extracellular fibers that are largely responsible for dermis tensile strength. Taken together those facts and the preparation steps proposed by Advanced Biomatrix (RatCol®), collagen I+III (CI+III) mixture protocol were designed. Unlike other evaluated matrices, all fibroblasts in CI+III matrix reach the insert bottom (Fig. 7, black head arrows). This fact suggests a slow gel formation rate (~1 h) in such a way that cell soma did not remain suspended into. Similar outcome was observed in all assays. Given the temporal scope of this research, correct it was not possible. So, gelation times proposed by fabricant remained unchangeable. Try to amend collagen mixture gelation in a future research is mandatory. Equidistant fibroblasts distribution facilitates mesenchymal-epidermis cross-talking. This issue is a pivotal aspect in artificial built epidermis (Schoop, Mirancea, Fusenig; 1999). Epidermal stratum features showed the same parakeratotic behavior as the other two matrices models. HaCaT-collagen based three-dimensional culture models made by others behaves analogous (Ryle *et al.*; 1989). More complex collagen mixtures models constructed from human, rat tail or bovine collagen and the same HaCaT passages (30-45), did leads to alike parakeratotic behavior. Nevertheless, layers quantity of epidermis was greater than our DEpOs (Boelsma, Verhoeven, Ponec; 1999).

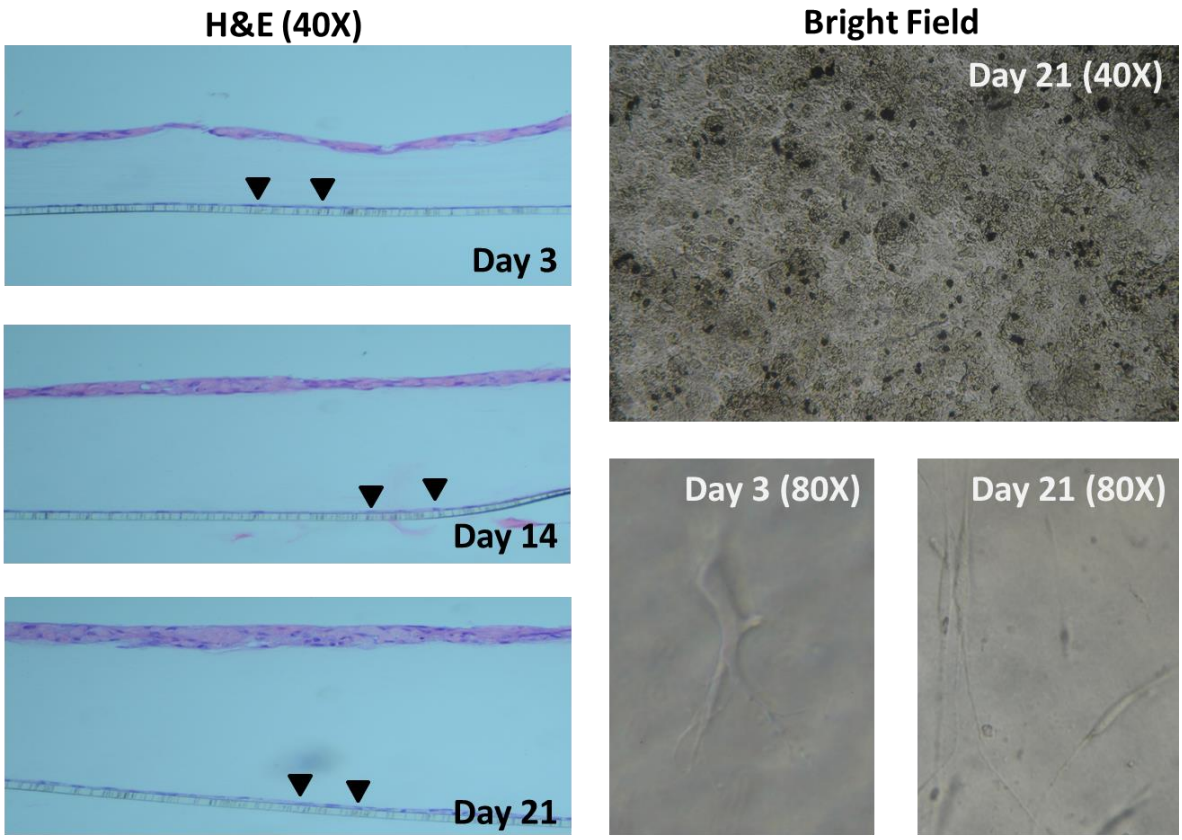

Figure 7. Hematoxylin and eosin (H&E) staining and microscopical phase contrast tracing of dermal-epidermal organotypics (DEpOs) built from rat tail collagen type I and III mixture. Time harvesting and microscopical photos were the same of PET DEpOs. H&E showed a partial stratification (3-5 layers). Flattening, massive nuclei losing and non-evident hemidesmosomes in H&E were compatible with an abnormal keratinization process (i.e. parakeratosis). Most of fibroblasts went to the bottom of inserts (black head arrows). Bright field microscopy showed the epidermal stratum at day 21. Zones with evident irregular morphology features are showed. Fibroblasts colonies at day 3 and 21 are showed (bright field microscopy). n=5.

Finally, an appropriate adhesion process and normal staining behavior on the three matrices was demonstrated by H&E outcome. Specifically, eosinophilic cytoplasm with basophilic nuclei. When HaCaT fails to adhere to a matrix undergoes a cell death type termed anoikis (da Silva *et al*.; 2015). If it was the case, viable cells could not be observed in DEpOs, but they were found as was showed in Fig. 5, 6 and 7.

To characterize the pattern of several epidermal differentiation markers in obtained tissues, immunohistochemistry was carried out (Fig. 8). Based in normal gene switching during keratinization, one marker by layer was detected. Ki-67 and K14 to basal layer, K10 to suprabasal/spinosum layer, filaggrin to granular layer and cornified layer was identified with loricrin staining (Chu *et al*.; 2005). DEpOs built on PET matrix reached a greater cell layers compared to other two evaluated systems. At the same time, PET based model was the farthest to the normal expression pattern (Fig. 8A-E). No Ki-67 labeling was found in the HaCaT nucleus (Fig. 8A). It can suggest the achieving of cell proliferation homeostasis like normal skin or a total abort of cell proliferation at day 21 of culture. Keratin 14 was the unique clearly observed (Fig. 8B). Weakly questionable keratin 10 (Fig. 8C, black arrowheads) and filaggrin (Fig. 8D, black arrowheads) was found. No loricrin was located on PET based DEpOs (Fig. 8E).

The best differentiation pattern was observed in fibrin based DEpOs, which showed a wild behavior (Fig. 8F-J). Ki-67, K14 and K10 were clearly detected (Fig. 8F, G & H). Filaggrin and loricrin showed a scattered

expression (Fig. 8I & J, yellow arrowheads). DEpOs made on CI+III mixture abort its differentiation process in what would be the spinosum layer (Fig. 8K-M). An irregular K10 staining was largely restricted to the uppermost layers (Fig. 8M). K10 has been observed in 3 weeks old cultures of HaCaT based organotypics. These models were made on native collagen (Ryle *et al*.; 1989) or rat tail collagen type I (Schoop, Mirancea, Fusenig; 1999). Irregular K10 staining outcome was hugely resembled to Boelsma, Verhoeven and Ponec work in 1999. Lesser K10 scattered location was observed in HaCaT-organotypics made on L929 populated collagen type I gels (Kehe *et al*.; 1999). No filaggrin or loricrin production was detected (Fig. 8N & O). Functional filaggrin translation, accompanied by a weakly loricrin production, has been reported in collagen type I gels co-cultured with HaCaT and primary human fibroblasts (Schoop, Mirancea, Fusenig; 1999).

Is important to mention that the genetic loricrin flux is sharply regulated and is strictly linked to keratinocyte terminal differentiation either in wild or artificial epidermis (Jang, Steinert; 2002). Thus the *in vitro* loricrin induction is especially complicated because the dynamics of transcription factors that determine its mRNA transcription is so stringently (see discussion). A weakly loricrin expression in most works with HaCaT has been documented (Boelsma, Verhoeven, Ponec; 1999) (Schoop, Mirancea, Fusenig; 1999) (Maas-Szabowski, Stärker, Fusenig; 2003) (Jung, Jung, Shin; 2016). All immunohistochemistry staining controls are showed in the supplemental material (Fig. 3S).

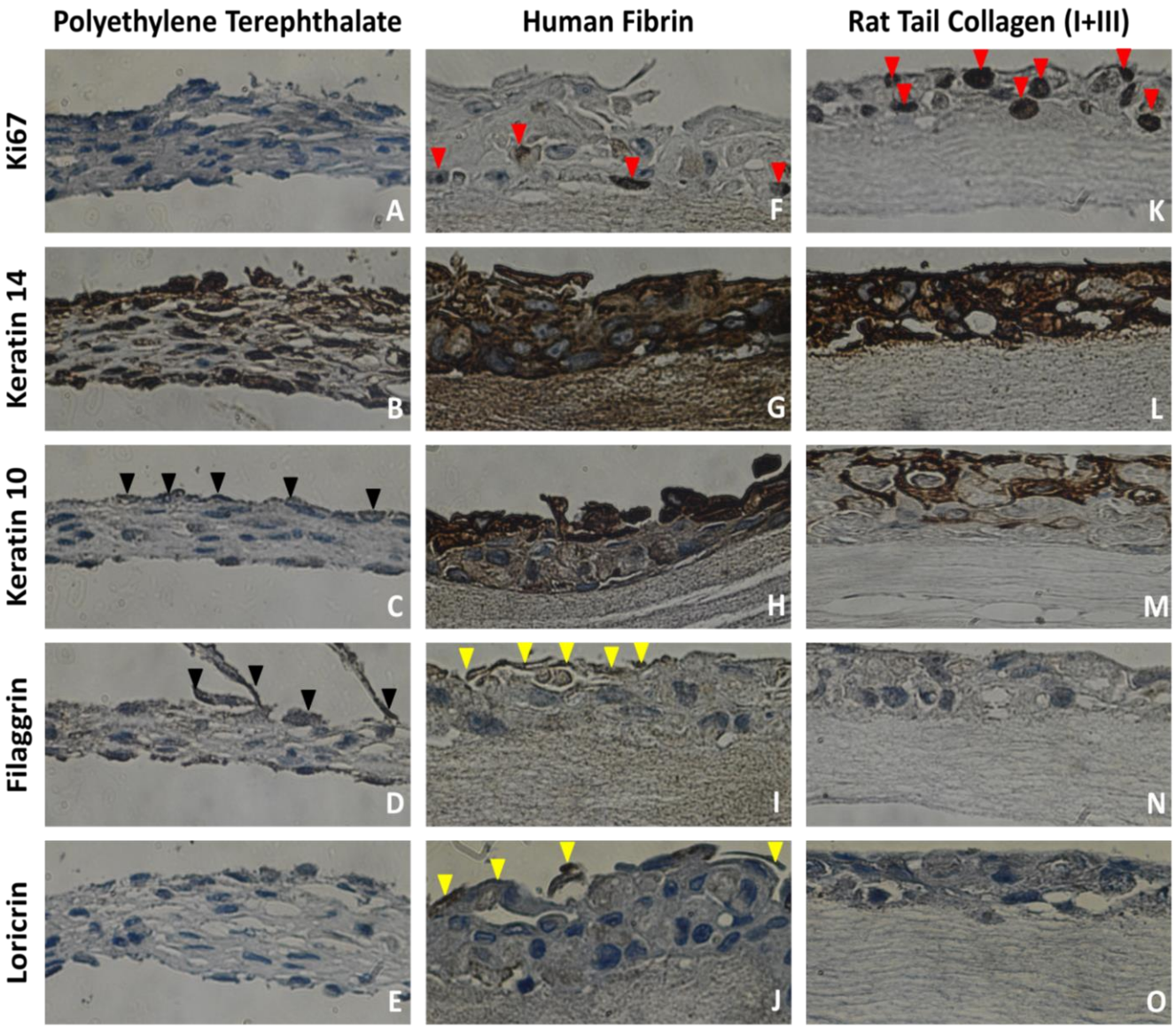

Figure 8. Immunohistochemistry analysis of formalin-fixed dermal-epidermal organotypics (DEpOs) after 21 days of culture, in the three evaluated matrices. PET based DEpOs (A-E) only clearly expressed keratin 14 (B). Keratin 10 (C) and filaggrin occurrence was doubtful (D; black arrowheads). Loricrin was not found (E). Ki-67 positive nuclei were not visible in PET based DEpOs (A) suggesting cell proliferation homeostasis or total proliferation abortion (see text). DEpOs built on fibrin matrix (F-J) was positive to Ki-67 (F, red arrowheads), keratin 14 (G) and keratin 10 (H). Filaggrin (I; yellow arrowheads) and loricrin (J; yellow arrowheads) were dimly positive. When DEpOs were made on rat tail collagen mixture (type I and type III; C I+III) (K-O) Ki-67 (K, red arrowheads), keratin 14 (L) and keratin 10 (M) presence were confirmed. Neither filaggrin (N) nor loricrin (O) were observed. All evaluated markers were produced in a wild fashion except keratin 14, which was located through epidermis, irrespective of used matrix type (B, G and L). All photos were made at 120X; n=3 per matrix type and marker.

Lastly, Ki-67 index calculated to each tested model was, respectively: <1±0.5% (PET), 23.1±4% (fibrin) and 42.5±7% (CI+III). Statistical analysis between Ki-67 indexes disclosed significantly differences in the same cited hierarchy (i.e. CI+III>Fibrin>PET). To a detailed description of Ki-67 index calculation see the item number four of supplemental material. Similar Ki-67 index found in CI+III system was reported on HaCaT-basal epidermal equivalent erected on DED at 10 ng/mL EGF (i.e. 44.9±15%) (Boelsma, Verhoeven, Ponec; 1999). Our experience has shown a Ki-67 index of ~2% to retro auricular normal skin (Morales *et al*.; 2016). Values reported are 0,8% to normal skin and >10% during hyperproliferative

disorders, such as actinic keratosis (23.7%) and squamous cell carcinomas (19.3%) (Khodaeiani *et al*.; 2013).

3.3. Dermal-Epidermal Organotypics (DEpOs) did not develop barrier function

Found free fatty acid (FFA) fraction was very low compared to both native skin and organotypics (see Table 1, Introduction). Proportions in our results, separated by chain length, were like previously reported works (Ponec, Boelsma, Weerheim; 2000). C16 and C18 were the most abundant (Fig. 9) (see Schürer *et al*.; 1993 in Table 1). Commercial reconstructed epidermis as Episkin, SkinEthic or EpiDerm™, which are made with NHK either on collagen or specially prepared inserts, showed a lesser quantity of FFAs (<6% of total lipids) in comparison with native skin (10% of total lipids) (Ponec *et al*.; 2000). Ponec and coworkers has been reported that reconstructed human epidermis have short-chain FFAs excess. C16-C18 sum (e.g. 48.9% on DED) is greater than C24-C26 FFAs sum (e.g. 28.7% on DED, see Table 1) (Ponec *et al*.; 2001) (Ponec *et al*.; 2003). Moreover, arachidic acid (C:20:0) was not present in DEpOs while 20-carbon poly unsaturated fatty acid (PUFA), termed arachidonic acid (AA; 20:4n6), does (Fig. 9). AA makes up ~9% of the total fatty acids in human epidermal phospholipids (i.e. second most prominent PUFA). Normally, epidermis have neither 6Δ- nor 5Δ-desaturases (Elias, Feingold, Fluhr; 2005). Thus, AA synthesis is not carried out and is considered an essential nutrient for the skin (Chapkin *et al*.; 1986). Desaturases mediates the linoleic acid (C18:2) conversion to γ-linolenic acid (C18:3) or the arachidic acid desaturation. The presence of AA but not arachidic acid in DEpOs suggest that HaCaT codify functional Δ-desaturases leading to arachidic acid exhaustion. FFAs like lauric acid (C12:0), myristic acid (C14:0) or linolenic acid (C18:2n6) did not show important quantities or variations between evaluated DEpOs. Earlier works found an intrinsic HaCaT impaired capacity to produce FFAs and an incomplete profile of ceramides (Ponec, Boelsma, Weerheim; 2000). Those lipids are crucial in formation of a proper barrier function.

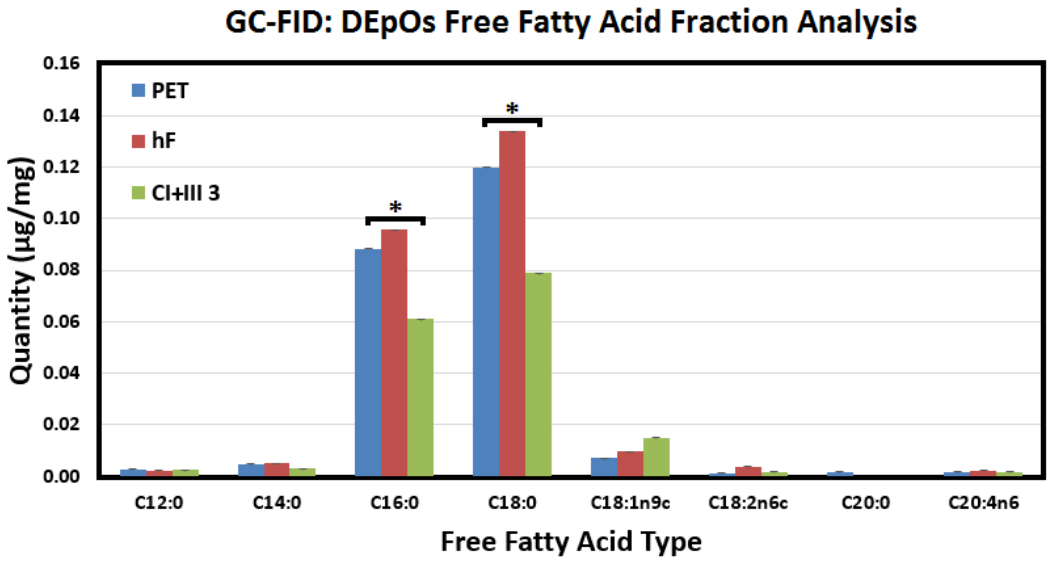

Figure 9. Free fatty acids (FFAs) fraction (C12-20) analysis of dermal-epidermal organotypics (DEpOs) after 21 days of culture. Gas Chromatography with Fire Ionization Detector (GC-FID) was used. Quantity of FFAs, measured in µg per mg of dry weight (i.e. dehydrated DEpO), revealed that C16:0 and C18:0 were the most abundant despite DEpO type (*). FFA fraction was significantly higher in polyethylene terephthalate (PET, blue) and human fibrin (hF, red) than in rat tail type I and III collagen mixture (CI+III, green). Arachidic acid (C20:0) was not found in most of analyzed DEpOs. Three independent assays (n=3) were carried out per each one of tested DEpOs models. *p>0.001.

Until here, we had been observed histological dissimilarities and low [FFAs] in comparison to native skin. Nonetheless, barrier function of DEpOs was appraised as an important physiologically feature. TEER measurements showed a pitiable resistance gaining (i.e. 30-50 Ohms) along culture time in all evaluated matrices (Fig. 10). Our low TEER values might suggest that cultures did not achieve total monolayer integrity. However, analysis of microtomic cuts by exhaustion did not revealed discontinuity (Fig. 5, 6 & 7). TEER reported values are >1000 Ohms (Ω) on the most "simple" models of epidermal equivalents. For example, epidermis made from NHK over PC (Kuninger, Gopinath, Newman; 2014). Similar values have been reported in skin organotypics erected on PET from human embryonic stem cells (hESCs) and induced pluripotent stem cells (iPSCs) (Petrova *et al*.; 2014). Interestingly, when submerged HaCaT monolayers were built on collagen® filter inserts and powered with KGM medium, TEER values were like ours. After 3 days of culture, registered TEER was 60 Ohm x cm^2. Medium was exchanged to DMEM supplemented with 15% FCS at day 5; so, TEER increase to 374 Ohm x cm^2 (Meyle *et al*.; 1999). Irrespective to used media, resistance measurements decreased until 30 Ohm x cm^2 between day 5 and 13 (Meyle *et al*.; 1999). These results suggest a poor TEER development of this cell line, probably due to its low TJs occurrence (Meyle *et al*.; 1999).

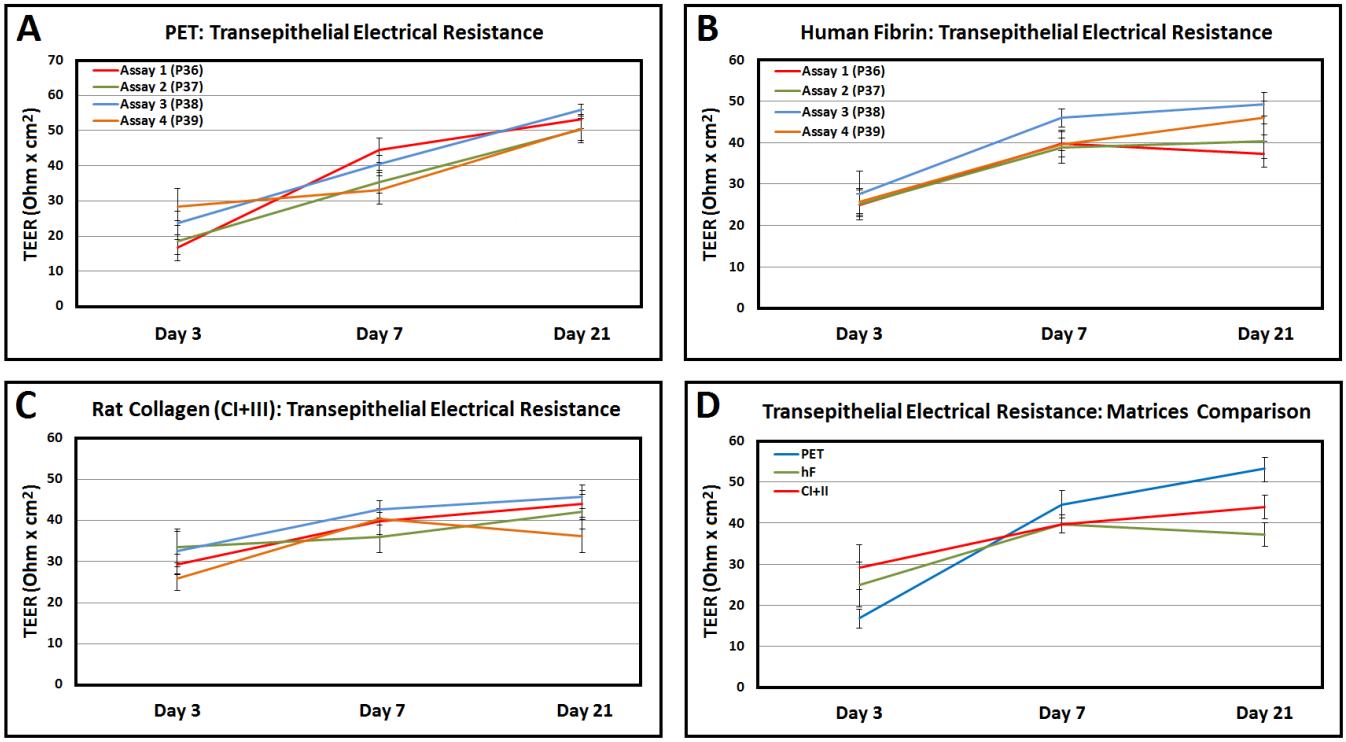

Figure 10. Transepithelial electrical resistance (TEER) measurement (in Ohms, Ω per cm^2) on dermal-epidermal organotypics (DEpOs). Three times of incubation period were evaluated. Three used dermal matrices are showed: Polyethylene terephthalate (PET, **A**), human fibrin (**B**) and rat tail collagen type I and III mixture (CI+III, **C**). One factor ANOVA ($p>0.001$) was applied. No significant differences between calculated means were found neither between assays nor matrices (**D**). Each measurement at each day was conducted in four different DEpOs (n=4) in independent assays. Standard deviation (SD) is indicated by bars.

Correlated with FFAs and TEER assays behavior, Lucifer yellow (LY) penetration assays showed that barrier function was not present (Fig. 11). Results indicates an active transport to the basolateral side, as suggested when curves of matrices without cells (controls) were compared (Fig. 11A, B & C). Because hydrophilic nature, LY molecule cannot enter passively to viable cells neither native skin nor cultured cells (Indra, Leid; 2011). In fact, LY must be internalized by artificial methods (Hanani; 2012). Some reports have demonstrated LY energy-dependent internalization by endocytosis in *Candida albicans*

(Basrai, Naider, Becker; 1990) and cultured rat atrial myocytes (Page *et al*.; 1994). These observations were made only in special conditions of culture as low [Ca^{2+}], low [glucose] or cooled environments. Quoted conditions were not present in our HaCaT or DEpOs cultures. Then, observed LY massive basolateral presence suggested us a potent paracellular transport mechanism. Tight junctions (TJs) might be involved but is an issue that should will be investigated. Finally, four independently LY permeability assay was carried out with consecutive HaCaT passages (P36-P39), obtaining similar results (see supplemental material, Fig. 2S).

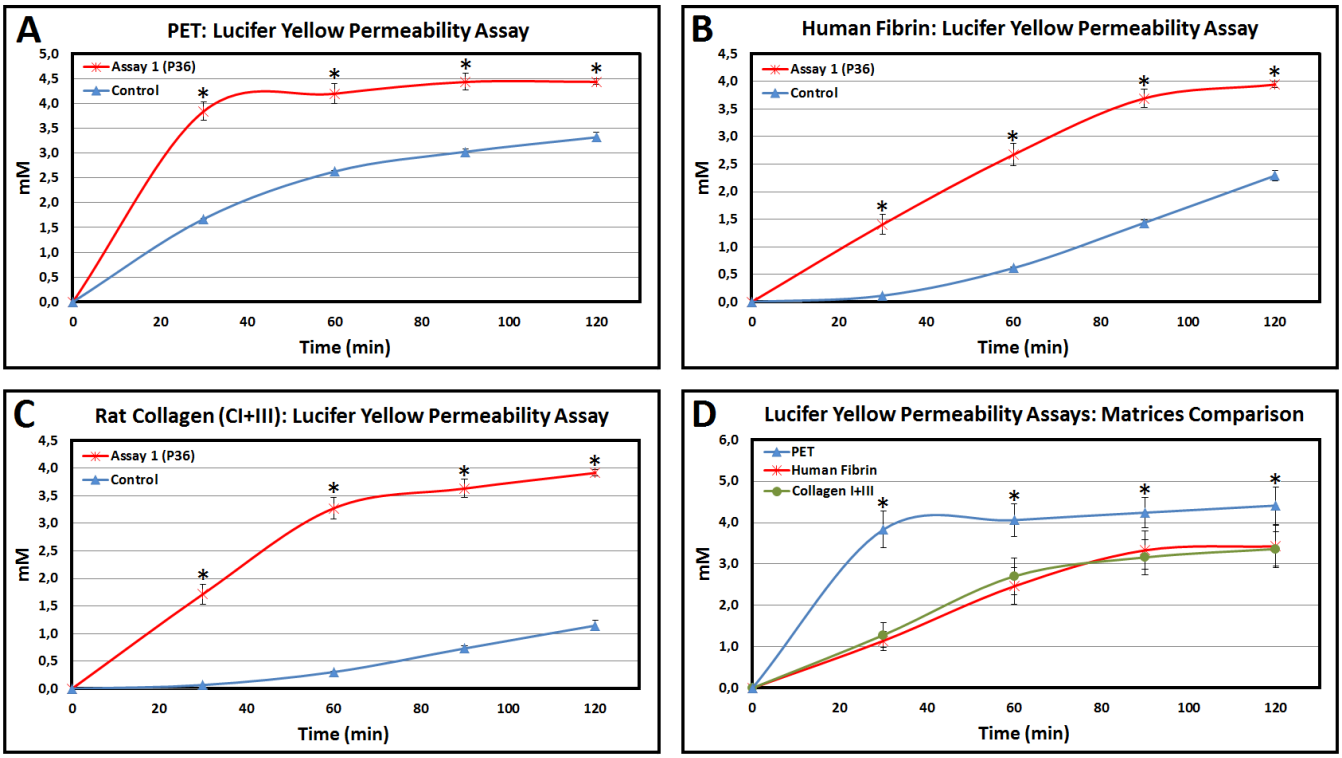

Figure 11. Lucifer yellow (LY) assay conducted over dermal-epidermal organotypics (DEpOs) after 21 days of culture. Three used dermal matrices are showed: Polyethylene terephthalate (PET, **A**), human fibrin (**B**) and rat tail collagen type I and III mixture (CI+III, **C**). One factor ANOVA showed significant differences between LY rate pass across DEpOs and the matrices without cells (control) in all proved models ($p>0.001$). An actively paracellular transport was suggested. The mild barrier function achieved by obtained epidermis in PET was statistically different compared to other two matrices (i.e. human fibrin and CI+III) (D). Each measurement at each day was conducted in four different DEpOs (n=4) in four different independent assays with similar results. P36, Passage 36; standard deviation (SD) is indicated by bars; *$p>0.001$.

It is important to highlight that the absence of barrier function was in total agreement with filaggrin absence (Fig. 8D, I, N) and low [FFAs] (Fig. 9). These are two important components of cornified envelope. Filaggrin alterations leads to severe changes in extracellular lamellar bilayer architecture of cornified envelope. It has been associated to impairments in corneocyte cohesion and a decreased permeability barrier function (e.g. atopic dermatitis) (Gruber; 2014). Functional filaggrin translation stimulus on HaCaT cultures improves its potential barrier function development (Oh *et al*.; 2016). In addition, equal FFA chain lengths distribution and its wild spatial stacking are necessary to achieve transitional "solid" phases on stratum corneum and normal skin barrier function development (Chen *et al*.; 2007). Well-ordered lipid lamellar phases are central to develop a functional barrier in epidermis reconstructed on DED, which was confirmed by small-angle X-ray diffraction (Ponec *et al*.; 2001). Finally, filaggrin breakdown products (e.g. urocanic acid, pyrrolidone carboxylic acid) upgrade acid conditions of epidermis assisted by the free fatty acids reaching an optimal pH to epidermal lipid synthesis enzymes (Jungersted; 2014).

3.5. Used HaCaT are hypotetraploid with at least two genetically heterogeneous populations

Above presented results led us to hypothesize a non-homogeneous HaCaT population. Firstly, parakeratosis and its associated abnormal metabolically features. In second place, the observed shadows in contrast phase and clear spaces in bright field photos (Fig. 5, 6 & 7) suggests us a variable cell phenotype in epidermis stratum. To investigate the presence of possible HaCaT subpopulations, DNA content assay, by PI staining and flow cytometry was conducted. Two populations different in size and granularity were found (Fig. 12A). Pragmatic Watson approximation cell cycle model was possible to apply to each one (Fig. 12B and C). Both populations were different in its DNA content. Cells of two found populations were hypotetraploids compared to human primary fibroblasts (Fig. 11D). Further analysis in consecutive passages suggested that high genome instability was present in used HaCaT cell line. DNA content was gained during mitosis, resulting in a lot of chromosome collection (Fig. 11E). It was evidenced by significantly increasing of coefficient of variation or widening in PI fluorescence intensity peaks (Fig. 11D, orange line).

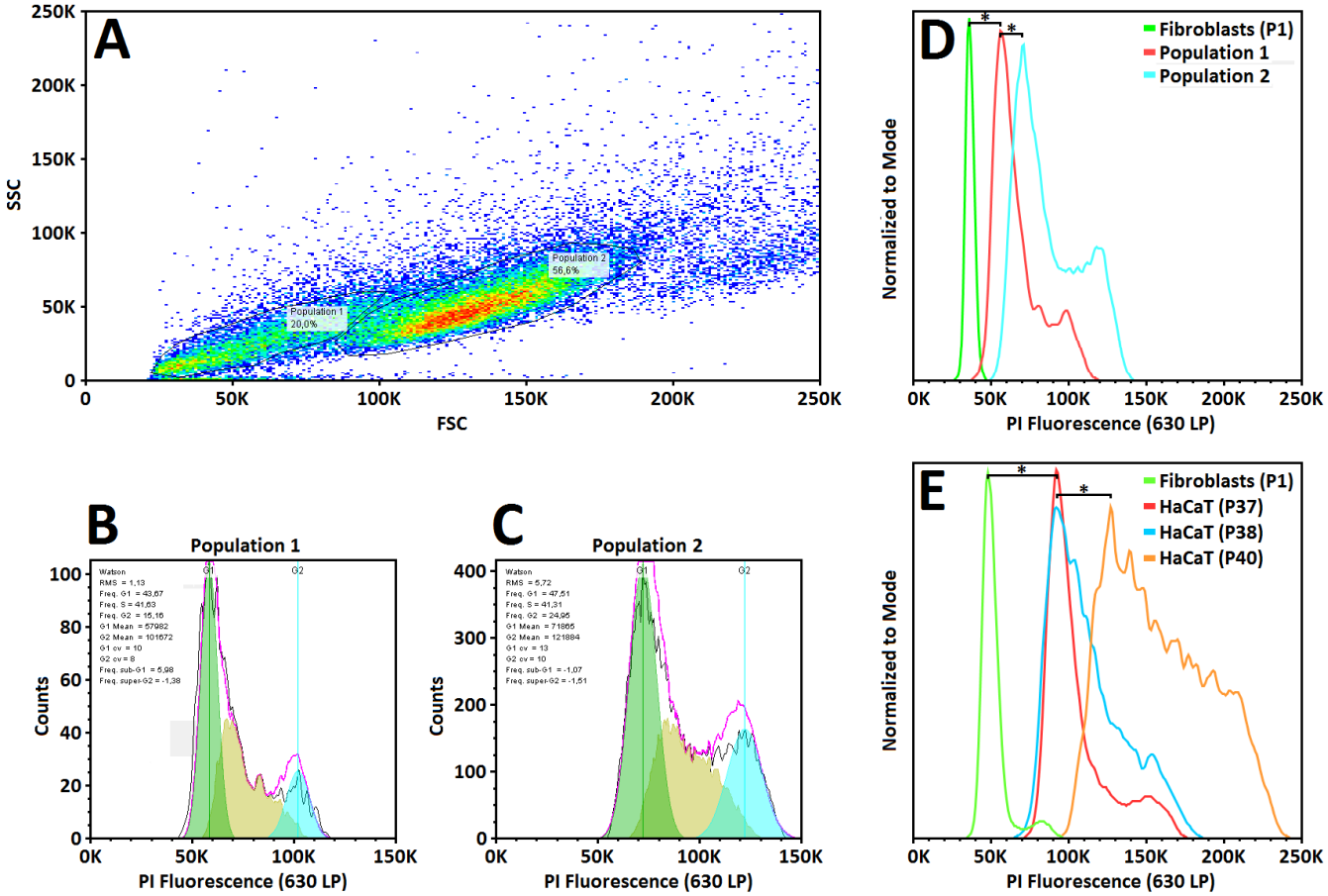

Figure 12. HaCaT DNA content analysis by propidium iodide (PI) staining and flow cytometry. **A.** Two populations (1 and 2) from the same culture (passage 37) were discriminated when granularity (side scatter light, SSC) and size (forward scatter light, FSC) were crossed. These populations fix the cell cycle model when were constrained to pragmatic Watson approximation (**B**, **C**). **B.** Population 1 was nearer to theoretical expected sum (purple line) (root mean square (RMS) was 1.13). Most of cells were in G1 and S phase as well. G1≈44%, S≈42% and G2≈15%. **C.** Population 2 was farther to theoretical expected sum (RMS=5.72). Most of cells were in G1 and S phases. G1≈47%, S≈41% and G2≈25%. **D.** Comparison between diploid human fibroblasts (passage 1) and HaCaT found populations. Population 1 was more hypotetraploid and lesser frequent in cell number than Population 2. **E.** DNA content measurements of consecutive HaCaT passages (P37, P38 & P39). Increase of coefficient of variation and its associated widening of PI fluorescence intensity peaks (P40, orange line), suggest

massively changes in DNA content and a high genome instability. Three assays were carried out with similar results. Propidium iodide (PI) fluorescence was measured by a 630-long pass filter (630 LP). *p>0.001 (Kruskal-Wallis test).

Massively changes in DNA ploidy and genome mutation rates was previously demonstrated in the same passage range (P30-50) (Boukamp *et al.*; 1998). Cell cycle distribution of HaCaT cells showed that two found populations were in division state. Near half of the cells were allocated in synthesis (S) phase (Fig. 11B and C). Other researchers have been proven that HaCaT cell line generates at least two populations. These are differentiable by their behavior in culture once they are challenged to differentiate with high [Ca^{2+}] (>1.2mM) (Micallef *et al*.; 2010). In afore quoted research, one HaCaT population was more committed and had a lesser proliferation potential than the other. Aberrant changes on DNA content was not hypothesized as a possible causal event to those outcomes.

4. DISCUSSION

Most reported 3D tissue culture systems made with HaCaT cell line achieve a pseudo-horny layer at day 21 of culture. It holds its nuclei (i.e. parakeratosis). Some studies had reported that those nuclei undergo DNA fragmentation as in normal early horny layer (Kehe *et al*.; 1999). Even so, normal epidermal morphology in HaCaT organotypics (i.e. orthokeratosis) was never obtained (Breitkreutz *et al*.; 1998) (Schoop, Mirancea, Fusenig; 1999) (Boelsma, Verhoeven, Ponec; 1999) (Maas-Szabowski, Stärker, Fusenig; 2003) (Stark *et al*.; 2004) (Jung, Jung, Shin; 2016). After transplantation, HaCaT 3D cultures becomes nearly orthokeratotic only with further incubation (e.g. 2-3 weeks). In contrast, NHKs requires ~6 days to differentiate once are grafted in surface transplants researches (Breitkreutz *et al.*; 1998). Excessively needed time to reach orthokeratosis on surface transplants might indicate a gradual sensitivity reduction of HaCaT to paracrine differentiation factors from underlying mesenchyme (i.e. dermis). For instance, HaCaT does not respond in the same way of NHK to extracellular rise of Ca^{2+}. Neither increases the p21 levels nor stops its growth in a S100C/A11 dependent manner (Sakaquchi *et al*.; 2003). Quoted variables increase in NHK when cell proliferation is stopped by [Ca^{2+}] rising and are cellular criteria to cornification beginning (Walker *et al*.; 2006). Curiously, p21 increases after low-dose radiation exposure (LDR; ≤100 cGy) if HaCaT cells are cultured in low Ca^{2+} conditions (Hahn *et al*.; 2016). HaCaT also has a reduced capacity to release factors that normally stimulates fibroblasts in early skin reepithelization (e.g. IL-1). Increase of genetic aberration frequency might be associated (e.g. translocations and deletions). Bearing in mind the HaCaT abnormal behavior in comparison with NHK, we hypothesize some causal aspects of our poor results compared with other researchers. Based on epidermis and HaCaT biology exposed in introduction, four aspects must be considered: dermal-epidermal cross-talking, [EGF], [Ca^{+}] and different HaCaT populations. Topological and mechanical effects of used polymers are briefly considered.

4.1. Poor dermal-epidermal double paracrine signaling (cross-talking) in DEpOs partially explain its parakeratotic development

Cross-talking between dermal fibroblasts and keratinocytes has been demonstrated in normal skin ontogenesis (Chu *et al*.; 2005). Emulate cross-talking *in vitro* allows to improve the stratification process of NHK (Stark *et al*.; 2004) (Boehnkea *et al*.; 2007), but also of HaCaT based organotypics (Schoop, Mirancea and Fusenig; 1999). Co-cultures of primary fibroblasts and HaCaT did indicate that this cell line responds satisfactory to fibroblasts cues. Moreover, that proinflammatory cytokines orchestrates, in turn, the fibroblasts responsiveness degree (Shephard *et al*.; 2004). Cross-talking probably entails the

basement membrane components deposition beginning (e.g. collagen IV) (Wojtowicz *et al.*; 2014). Before to consider the paracrine issue in artificial skin, it must be considered: fibroblasts initial input, its body region source and its colonies morphology.

Stratification level of HaCaT sown on gels, made from rat tail collagen type I, did depend of fibroblast start input. An epidermal thickness increase tendency was correlated with the number of fibroblasts in the collagen gel (Schoop, Mirancea and Fusenig; 1999). While commented research group did use 10^5, $2x10^5$ and $5x10^5$ fibroblasts/mL we use ~$9x10^3$ fibroblasts/mL. As was presented in results, we fixed the fibroblasts initial input based on confluence reached in PET at day 21, the reported mitogenic effects of used biopolymers and in our experience in fibrin based DEpOs (Morales *et al*.; 2016). So, the results presented here suggest us that fibroblasts number must be standardized to each model. Secondly, some reports propose that the number of keratinocytes layers produced in artificial epidermis is in function of used fibroblasts subpopulation (Sriram, Bigliardi, Bigliardi-Qi; 2015). Yamaguchi *et al*. shown, in 1999, that hyperkeratosis and a massively expression of its marker (i.e. keratin 9) was elicited when palmoplantar fibroblasts were seeded in coculture models with non-palmoplantar primary keratinocytes. HaCaT stratification level depends lesser than NHK to fibroblasts subpopulation variations in collagen based organotypics (Stark *et al*.; 2004). Lastly, aggregation is also crucial in the role of fibroblasts on keratinocyte fate. For instance, dermal papilla is a specialized fibroblasts cluster that drive the hair follicle formation from skin epidermal cells (Kang *et al*.; 2012). Through its adherent junctions, fibroblasts clustering stabilizes the extracellular matrix–integrin interactions during wound healing. These contacts promote wound closure after fibroblasts differentiation into myofibroblasts and its further contraction (da Rocha-Azevedo, Grinnell; 2013). Firstly, even if fibroblasts aggregates did appear into fibrin (Fig. 6) and collagen (Fig. 7), neither dermal papilla like structures nor matrix contraction were observed. This suggest us a clonal origin of colonies. Furthermore, no hyperplasic-like behavior as nemosis, a malignant fibroblast aggregation, was detected (Räsänen *et al*.; 2008) (Räsänen, Vaheri; 2010).

After a cutaneous insult, fibrin clot is suddenly formed and some chemotactic mediators of inflammation are released (e.g. fibrinopeptides, complement peptides like C3a, C5a and C5b67). Neutrophils are recruited, phagocytize pathogens and are activated, secreting macrophage inflammatory proteins (MIP-1 α/β). Activated macrophages produces the major proinflammatory cytokines, IL-1, IL-6, TNF-α, to proceeds with acute inflammation (Werner, Krieg, Smola; 2007) (Safferling *et al*.; 2013). IL-1 activates local fibroblasts, which begins to generate matrix metalloproteinases (MMPs) and to release KGF/FGF7 (keratinocyte growth factor/fibroblast growth factor-7) and other cytokines (e.g. EGF, IGF, TNF-β, GM-CSF) (Eming, Martin, Tomic-Canic; 2014). Finally, MMPs carry out remodeling and TNF-α promotes collagen deposition, using fibrin as scaffold. Secreted extracellular matrix or "wound bed", is then repopulated by keratinocytes (Werner, Krieg, Smola; 2007). KGF/FGF7 initiates the double paracrine signaling between mesenchyme and epidermis during wound healing. Nonetheless, it is considered that keratinocytes, through IL-1α and TGF-α, govern reepithelization in organotypics (Fig. 13a) (Werner, Krieg, Smola; 2007). Fibroblasts release IL-8 once are stimulated by IL-1α. An IL-8 autocrine positive loop is established (Fig. 13a). It potentiates its release and give way to others as IL-6 and granulocyte colony-stimulating factor (G-CSF) (Fig. 13c) (Menon *et al*.; 2012). Lastly, IL-6 and G-CSF acts as paracrine effectors over keratinocytes to stimulate self-production. A second autocrine positive loop is created (Fig. 13d) (Safferling *et al*.; 2013).

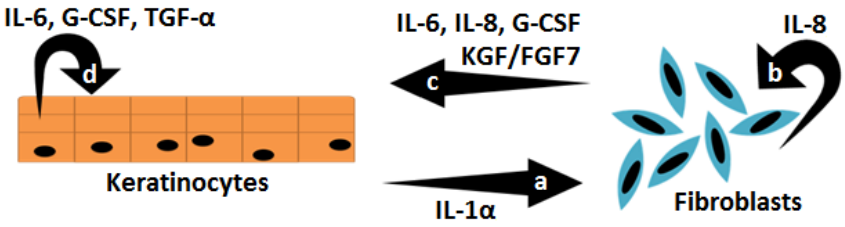

Figure 13. Cross-talking between keratinocytes and fibroblasts in cutaneous reepithelization. See the text to a detailed description. Inspired by (Safferling *et al*.; 2013).

Having in mind the commented paracrine network, let us start by saying that IL-1α is not massively produced by HaCaT (Ruhland, de Villiers; 2001). So, IL-6, IL-8, G-CSF and KGF, probably, were not significantly synthetized by fibroblasts in our dermal-epidermal organotypic cultures. Furthermore, whether previously mentioned factors were present in our DEpOs, HaCaT cannot respond to them due to its little cognate receptors production (i.e. G-CSF-R/CD114 and KGFR) (Capone *et al*.; 2000) (Maas-Szabowski, Stärker, Fusenig; 2003). IL-1α, IL-8 and TGF-α signaling finish with the translocation of NF-κB from cytoplasm to nucleus (Takao *et al*.; 2003) (Lewis *et al*.; 2006). This transcription factor stops keratinocyte proliferation by the induction of cyclin-dependent kinase inhibitor $p21^{CIP1/WAF1}$ and p27 (Borowiec *et al*.; 2013) (Seitz *et al*.; 2000). Expression inhibition of epidermal mitogen Cyclin-dependent kinase 4 (CDK4) is involved too (Zhang *et al*.; 2005). Once basal keratinocytes proliferation is stopped, differentiation process begins. This entails, for example, ending and suppression of JNK pathway, which leads to motility detention and G1/0 arrest. Transcription of cornification associated genes (e.g. cell-cell tight junctions components as zonula occludens-1, ZO-1) is stopped. At the end, stratification is done and cornified envelope is generated. Commented pattern has been revealed by DNA microarrays both in NHKs (Gazel *et al*.; 2006) and in cultured HaCaT (Minakami *et al*.; 2015). Reports from several laboratories have shown that NF-κB signaling pathway is abnormal in HaCaT cells (Chaturvedi *et al*.; 2001). It undergoes a high and unprovoked constitutive activity (Lewis *et al*.; 2006). So, on the one hand, few surface receptors on HaCaT can explain its resistance to differentiation stimuli and its high proliferative potential. Conversely, the high NF-κB activity aver a differentiative phenotype as well.

TGF-α production is also depleted in HaCaT, but it remains sensitive to (Game *et al*.; 1992). Maas-Szabowski, Stärker and Fusenig declare in 2003, that the addition of TGF-α to used medium might increases G-CSF and KGF receptors production. At the same time, addition of IL-1α could empower the synthesis and secretion of mesenchymal mentioned growth factors, improving the HaCaT differentiation in dermal-epidermal organotypics (Maas-Szabowski, Stärker, Fusenig; 2003). Others studies also had found the role of other dermal-epidermal growth factors, as epimorphin, that mediates early HaCaT commitment in organotypics (Okugawa, Hirai; 2008). This protein could be also depleted in our fibrin and CI+III models because of its poor fibroblasts distribution throughout gels (Fig. 6 & 7).

4.2. EGF effect on HaCaT probably did induce a hyperproliferative phenotype

CPA results in part explain the DEpOs histological (Fig. 5, 6 & 7) and immunohistochemical (Fig. 9) findings. As is showed in Fig. 4, QC medium cause a potent mitogenic effect in HaCaT cells compared with other proved media. This outcome is probably owing to EGF addition. An ideal epidermal differentiation medium or reagent must suppress or reduce lateral cell rate proliferation (parallel to basement membrane), with a concomitant initiation of slower asymmetrical cell division (perpendicular to basement membrane) (Lechler, Fuchs; 2005). The most important keratinocyte proliferation transductor is the EGFR (or also termed Erythroblastic Leukemia Viral Oncogene Homolog B1, ErbB1) (Peus, Hamacher, Pittelkow; 1997) (Jost, Kari, Rodeck; 2000). EGFR is functional in HaCaT (Kaufmann,

Thiel; 2002). This type-1 tyrosine kinase is the target of both TGF-α (from keratinocytes) and EGF (from blood). Quoted ligands are homolog proteins characterized by possess a triple loop structure belayed by three intramolecular cysteine bridges (Jost, Kari, Rodeck; 2000). EGFR-dependent events are complex. Have more than one ligand, synergize with other EGFR family members (i.e. ErbB family) but also can undergoes transactivation (e.g. from G-protein-coupled receptors, integrins, and cytokine receptors) (Pastore *et al*.; 2008).

Once activated, changes in cell phenotype depends on linked ligand and specific microenvironment, which may lead to EGFR variations of its cooperative arrays (Jost, Kari, Rodeck; 2000). Briefly, when EGF is bind, EGFR (ErbB1) form a heterodimer with ErbB2. The tyrosine kinase activity generates phosphorylated specific tyrosine residues inside the cytoplasmic tail and provide docking sites for SH2 (Src Homology-2) and PTB (Phosphotyrosine Binding) domain-containing proteins. Myriad of pathways can be initiated: PLC-γ (Phospholipase-C-gamma), Dok2 (Docking Protein-2), FAK (Focal Adhesion Kinase), STATs (Signal Transducer and Activator of Transcription), E3B1 (EPS8 Binding Protein)/ABI1 (Abl-Interactor-1), Paxillin, Caveolin, E-Cadherin and Catenin-β. Among others, an essential transductor of EGFR-Ras pathway, is GRB2 (Growth Factor Receptor-Bound Protein-2, a SH2 protein). Shortly, GRB2 binds to phosphotyrosines 1068 and 1086 at EGFR cytoplasmic tail → Ras/Raf → PI3K (Phosphatidylinositol 3-Kinase) → Hydrolysis of PIP2 (Phosphatidylinositol (4,5)-bisphosphate) → Intracellular Ca^{2+} release and PKC (Protein Kinase-C) activation → NF-κB (Nuclear Factor-KappaB)-dependent transcription (QIAGEN; 2013). In keratinocyte, EGFR can promote three highly related effects, cell survival (e.g. by Dok2/Akt), proliferation (e.g. by PLC-γ/NF-κB or GRB2/Ras-Raf/c-Myc) and migration (e.g. by FAK1 or paxillin). Conversely, differentiation is also stimulated conducing to keratinocyte death by cornification (e.g. by STAT3) (Blumenberg; 1997) (Pastore *et al*.; 2008). EGFR signaling induce anti-apoptotic molecules as Bcl-XL (e.g. through PLC-γ/phosphatidylinositol 3/kinase–Akt pathway). Nonetheless, when its tyrosine kinase activity is suppressed, HaCaT or NHK proliferation is stopped leading off to terminal differentiation (Rekus; 2000) (Peus, Hamacher, Pittelkow; 1997). For instance, after suprabasal desmoglein 1 (DSG1) translation, proliferative effect of EGFR is suppressed, triggering the differentiation process (Getsios *et al.*; 2009). Consistently, Wnt5a/β-catenin pathway suppress cell proliferation and induce genes related with keratinization (e.g. keratin 1 and loricrin) (Popp *et al*.; 2014).

Normally, EGFR is present in basal layer, where is involved in epidermis growth control. During skin disorders, is up-regulated thorough layers and is correlated with parakeratosis and hyperproliferation (e.g. psoriasis, squamous cell carcinoma) (Jost, Kari, Rodeck; 2000). Both the use and the effect of EGF in 3D skin cultures are controversial. Is accepted that EGF behaves as a potent mitogen in NHK and HaCaT, but at the same time this growth factor can be important in early keratinization steps.

EGF inhibits some mitogenic receptors (e.g. insulin-like growth factor binding protein 3, IGFBP-3) and its associated ligands (e.g. insulin-like growth factor I, IGF-I) expression, possibly provoking HaCaT early cornification (Wraight, Werther; 1995). EGF can initiate deposition of the major basement membrane component, laminin 5, a necessary step in the normal epidermis ontogenesis (Zinn *et al*.; 2006). EGF, together with insulin, also elicits the HMG-CoA synthase, an enzyme important in epidermal cholesterol anabolism (Harris *et al*.; 2000).

Despite EGF role in cornification initial steps, this growth factor has a preponderantly mitogenic effect on keratinocyte as was commented above. EGF blocks the differentiation genes codification, as K1/K10, in NHK and HaCaT (Rekus; 2000), fact that correlates with our results (Fig. 9C, H, M). HaCaT transfected

with EGF decline sharply the caspase 3 and cyclin D1 levels accelerating the G1 cell cycle phase and improving its proliferation rate (Tao *et al*.; 2013). EGF (20 ng/mL) conduces to keratin intermediate filaments reorganization to proliferate and migrate in HaCaT cells (Moch *et al*.; 2013). Ponec *et al*. work unveiled, in 1997, that in presence of 10 ng/mL EGF, organotypics built with DED and primary human keratinocytes, did develop an epidermis without suprabasal keratins (i.e. K1 and K10). No differentiable stratum granulosum or stratum corneum were found. Moreover, these strata were rich in nuclear remnants and triglyceride droplets (Ponec *et al*.; 1997). Those results possibly are associated with an EGF mediated hyperproliferative effect. Similar results were found in bovine collagen and HaCaT cell line (passage 30-45) based organotypics incubated in presence of 1 ng/mL EGF. These tissues did produce a multilayered epithelium 2 weeks after air exposure with weakly similarities equated to wild human epidermis (Boelsma, Verhoeven, Ponec; 1999). Indeed, the same work reported an increase of Ki-67 index in stratum basale. When HaCaT epidermis was produced on DED and incubated without growth factors Ki-67= 35.2±6.5%. When cultures were supplemented with 10 ng/mL EGF, Ki-67 = 44.9±15%. EGF also mediates the suppression of K1, K10 and involucrin in submerged HaCaT monolayer cultures (Rekus; 2000). In the same way, Hu *et al*. (2012) transfected HaCaT with hEGF to improve its functional translation and secretion. When cells were cultured on the top of type I collagen gels, did generates a parakeratotic tissue almost the same that obtained by us in CI+III based DEpOs (i.e. 2-3 layers with flattened cells) (Hu *et al*.; 2012). Bigelow *et al*. demonstrate that EGF activates EGFR and exerts a synergistic effect on sonic hedgehog pathway bringing on HaCaT infiltrative behavior at basal layer of collagen organotypic co-cultures as occur in basal cell carcinoma, which confirms a predominantly mitogenic effects of EGF in HaCaT (Bigelow *et al*.; 2005). Works carried out in HaCaT cultures stimulated with EGF advises that intracellular pathway of this molecule is accompanied by the biosynthesis of early growth response-1 (EGR-1) and c-Jun transcription factors (Rössler, Thiel; 2004). Those proteins lead to expression of pro-mitotic proteins as PPAR β/δ (peroxisome proliferator-activated receptors beta and delta), which in fact, increase HaCaT proliferation (Liang *et al*.; 2008). Curiously related, some researchers encountered that PPAR β/δ complex can enhance other gene activities (e.g. ANGPTL4, angiopoietin-like protein 4) that can cause a modest inhibition of cell proliferation and HaCaT apoptosis, suggesting an ambivalent role of this protein complex in the skin (Borland *et al*.; 2011). Finally, was probably that EGF effect on HaCaT did induce a hyperproliferative phenotype instead a differentiative, leading to an abnormal epidermal keratinization process in our DEpOs.

4.3. High used [Ca^{2+}] and [EGF] might synergistically acts leading to a pro-mitotic HaCaT phenotype

EGF effects should be counteracted by elevated calcium concentration in all used media. Ca^{2+} gradient in human epidermis is non-linear, the lowest concentration is reached in the supra-basal and in early spinosum layers. Basal layer has a higher concentration. In the late spinosum, granular and corneous compartments occur an abrupt increase (Leinonen *et al*.; 2009). Based on Ca^{2+} gradient, most recent protocols have reached to a simplified [Ca^{2+}] switching consensus in culture conditions to potentiate proliferation firstly (<0.1mM) and terminal commitment further (> 1mM). Some authors claim that the abrupt change to high Ca^{2+} levels is suitable to induce, study and determine the Ca^{2+}-dependent genes. But, in turn, that is not a good model for eliciting and studying the G1/0 arrest and terminal commitment of *in vitro* primary keratinocytes based organotypics (Borowiec *et al*.; 2013). Even external high [Ca^{2+}] is an essential component to provoke artificial cornification, it must be accompanied with high serum and low temperature switching, as in normal human skin (Borowiec *et al*.; 2013). For example, HaCaT cells grown under medium (0.7 mM) and high (1.2 mM) [Ca^{2+}], early translate functional profilaggrin. At the same time, quoted Ca^{2+} levels, maintain HaCaT proliferative properties despite of IGFBP-3 production

decline. IGF-I ligand and receptor are normally limited to basal keratinocytes. So, at high [Ca^{2+}], IGF-I/IGFBP-3 level expression is maintained, carrying out to a disarticulated gene switching in keratinization after air-lifting (Edmondson, Werther, Wraight; 2001).

Used media in our research contained high calcium concentrations (see fabricant technical sheet). HaCaT shows a good adaptation and further relative independence to [Ca^{2+}] (Micallef *et al.*; 2009). Despite this, was possibly that extracellular Ca^{2+} leads to an increasing of the intracellular [Ca^{2+}]. This cation can enhance some molecular processes such as PLC activity and, thereupon, the cell proliferative behavior instead of differentiative phenotype (Haase *et al*.; 1997). In fact, when HaCaT was cultured in low calcium conditions (with Ca^{2+}-depleted FBS) during three weeks, they switch off K1 and involucrin basal expression. Spindle shape and suppression of tight junctions cell-cell unions also appears like to EpiASCs maintained in low calcium medium (Deyrieux, Wilson; 2007).

Some observations can explain the response of HaCaT to low calcium conditions. For example, intracellular low calcium levels (0.05 mM) allows the normal translation of functional Yin-Yang-1. YY1 is a member of the GLI-Krüppel family of transcription factors, that maintain HaCaT in a basal proliferative phenotype. Increases to 0.35 mM [Ca^{2+}] down-regulates YY1 and start the HaCaT differentiation. Specifically, loricrin codification, a major component of the epidermis cornified cell envelope (Xu *et al*.; 2004) (Taguchi *et al*., 2011). Intracellular [Ca^{2+}] increasing is “interpreted” by HaCaT as a stress signal. This also leads to heterodimerization of the calcium- and arachidonic acid (AA)-binding proteins S100A8 and S100A9. This heterodimer provokes the NADPH-oxidase activation, ROS generation, NF-κB nucleus translocation and expression of cytokines related with proliferation and mobility (e.g. IL-8) (Benedyk *et al*.; 2007) (Nuki *et al*.; 2008). Production of cytokines involved in growth suppression and differentiation markers induction (e.g. involucrin and filaggrin) also are stimulated (Voss *et al*.; 2011). Increased intracellular [Ca^{2+}] can leads to S100A6 excess activity (a S100 family member also known as calcyclin). S100A6 is related with basal keratinocyte proliferation due to its role in G1 to S cell cycle phase transition (Ito, Kizawa; 2001). When HaCaT overexpressing S100A6 was committed to differentiate on collagen type I gels. Ki-67 generation did increase, keratin 14 remained normal but keratin 10 was diminished and loricrin suppressed (Ito, Kizawa; 2001). Commented trend is spectacularly similar to our results, irrespective analyzed model (Fig. 9). Cytoplasmic Ca^{2+} increasing in keratinocyte triggers the profilaggrin dephosphorylation and proteolysis, a fundamental event in cornification (Harding, Aho, Bosko; 2013). Commented proteolysis carries to profilaggrin N-terminal domain (PND) releasing. PND has an S100 domain and has been observed interacting with loricrin and K10 in HaCaT (Yoneda *et al*.; 2012). Consistent with these observations, and compared to organotypics made with NHK, Stoll, Zhao and Elder demonstrate, in 1998, that EGF did stimulates transcription of CaN19. This protein, also named S100A2, works as an effector of the regenerative hyperplasia pathway of epidermal differentiation, a form of parakeratotic adult skin morphogenesis common in wound healing process.

In contrast, works with high EGF concentrations (10 nM) found that its signaling alters the intracellular [Ca^{2+}] leading to m-calpain activation, α-spectrin cleavage and HaCaT cells apoptosis (Inoue *et al*.; 2004). HaCaT transient changes in free cytosolic calcium promotes short actin filaments formation too. These structures alter the HaCaT cells volume and their regulatory response to external conditions (Blase *et al*.; 2009). So, the high used [EGF] and [Ca^{2+}], probably led us to observed high proliferative activity measured by CPA as well as Ki-67 calculated index in DEpOs.

4.4. Potential role of fibrin and collagen in HaCaT hyperproliferation and DEpOs parakeratosis

Comparison of calculated Ki-67 index suggest that fibrin and collagen did exert a pro-mitotic effect on HaCaT. This effect may be due to 3D matrices capacity to adsorb growth factors but also to mechanotransduction issues. All used matrices have different elasticity, stiffness and topography. Intact skin is continuously exposed to an anisotropic tensile stress. It has been evidenced that these mechanical forces promote signaling pathways related with keratinocyte proliferation. To illustrate, mitogen-activated protein kinase (MAPK), protein kinase C (PKC), extra-cellular signal-related kinase (ERK), protein kinase B (PKB or Akt) and matrix metalloprotease 9 (MMP9) (Evans *et al*.; 2013). HaCaT seeded on bovine collagen type I-polycaprolactone nanofiber gels, were exposed to air-liquid interphase and a mechanical stimulation simultaneously (i.e. radial strain for 1 min every 30 min). A stratum corneum characterized by up-regulation of terminal markers like filaggrin and loricrin was generated (Jung, Jung, Shin; 2016). Biology under HaCaT response to mechanical stimuli suggest a massive cytosolic influx of Ca^{2+} via cell membrane distortion, followed by ATP release. Activation of PY2 receptor leads to a sudden massive mitosis and switch on of genes associated to cornification (Takada, Furuya, Sokabe; 2014). Recent studies about mechanotransduction on collagen type I gels populated with NHK and fibroblasts, suggest that the thicker epidermal layer obtained after mechanical stress is related with a major and better deposition of laminin 5 and collagen IV/VII in the basal layer, compared with equivalents not subjected to stretch stimulation (Tokuyama *et al*.; 2015). Epidermal pattern incited by dermal papillae peaks, known as rete ridges, also has been emulated in NHK based organotypics. Rete ridges like structure improves the cornification quality of artificial epidermis (Clement, Moutinho, Pins; 2013). Finally, while fibrin and CI+III could promote proliferation on HaCaT in comparison with PET, the absence of mechanical stress, together with high [EGF] and [Ca^{2+}], keep off its potential benefic effects in terminal differentiation.

4.5. Genetic heterogeneous HaCaT population may explain its poor differentiation in DEpOs

Flow cytometry results showed evident hypotetraploidy as was early reported (Boukamp *et al*.; 1997). At 30-50 passages this cell line undergoes an importantly genetic alteration increase without a gross chromosomal imbalance (Boukamp *et al.*; 1997). Some evidence prove that genome instability experimented by HaCaT cells may be ascribed to spatial reorganization of telomere repeat-binding factor 2 (TRF2). To evade chromosomal end-to-end fusions, TRF2 maintains the loop structure and integrity of telomeres during all cell cycle phases (de Lange; 2004). During mitosis, TRF2 shows an additional concentration around chromosomes evading massive chromosomal DNA exchange. So, overexpression of factors as c-myc in HaCaT (Cerezo *et al*.; 2003), carries out to redistribution of TRF2, leading to telomeric aggregates that causes genomic instability and massive genomic alterations (Ermler *et al*.; 2004).

In other way, Micallef *et al*. did observe that cultured HaCaT at high calcium concentration (1.2 mM) developed two sub-populations. These were separable by sedimentation field-flow fractionation. One of them had a high proliferative phenotype while the other was committed and had a lower proliferative activity therefore (Micallef *et al*.; 2010). As flow cytometry had been showing (Fig. 12), two well differentiated cell populations were present in our HaCaT cell line cultures. These populations can be resolved by its granularity/size (Fig. 12A), cell cycle distribution (Fig. 12B and C) and by its DNA content (Fig. 12D). In fact, aberrant genetic events increase spectacularly between above commented passages range, as was disclosed by the gaining of PI fluorescence between passages (Fig. 12E). In this research, we used HaCaT at passages 30-50. So is expectable, based on PI based DNA analysis, that we did built

our DEpOs starting from a heterogenous population of HaCaT. So, if there were most than one group of cells within cultures, with variable proliferation rates, is expectable that an unorganized development process was carried out. Indeed, overexpression of proliferative phenotype elements (e.g. c-myc and telomerase) leads to a poor stratification process without a clearly horny layer in HaCaT based organotypics (Cerezo *et al*.; 2003).

4.6. [EGF], [Ca^{2+}] and HaCaT heterogeneous population could act synergistically altering the keratinization

Barrier function is derived from the final corneocytes based structure known as cornified envelope. Keratins bundles are joined by filaggrin. Formed intermediate filaments are interweaved and reinforced by a protein amalgam composed from crosslinked involucrin, loricrin, small proline rich proteins, tricohyaline and repetin. Cross-liking is mediated by transglutaminases (Candi, Schmidt, Melino; 2005). At the end, lipids are integrated to cornified envelope. ω-hydroxy-ceramides are esterified to the glutamine-glutamate-rich regions of structural proteins present in extra cellular space (i.e. involucrin mainly, but other as desmoplakin and periplakin). A lamellar structure termed corneocyte lipid envelope is produced (van Smeden *et al*.; 2014a) (Elias *et al*.; 2014). So, analyzed variables (i.e. [EGF], [Ca^{2+}] and HaCaT heterogeneous population), could act synergistically altering the stratification expected finding, which in turn can also explain the absence of barrier function in DEpOs.

Non-detectable barrier function is correlated with the absence or so weakly expression of terminal differentiation markers. As was showed in Fig. 9 filaggrin and loricrin have a reduced or inexistent presence in all obtained DEpOs despite used matrix type (Fig. 9D, E, I, J, N, O). Filaggrin role in barrier function is controversial. Using a lentivirus small-hairpin RNA, filaggrin gene expression was knockdown in NHKs from abdominal dermolipectomy. Those NHKs were used to reconstructs human epidermis on PC filters. Thus, barrier function and keratinocyte differentiation were severely altered as occurs in epidermis of atopic patients (Pendaries *et al*.; 2014). In contrast, the barrier function was not affected in epidermis reconstructed on transwells sensitized with 100 mg/mL rat-tail collagen and made from NHK that did not express filaggrin (Niehues *et al*.; 2016).

In the other hand, when loricrin undergoes genetic mutations lead to Vohwinkel syndrome with ichthyosis, a skin disorder characterized by an abnormal barrier function (Schmuth *et al*.; 2004). Loricrin is rich in glycine, serine, and cysteine residues that represent near of 80% of total cornified envelope proteins (Nithya, Radhika, Jeddy; 2015). Briefly, in undifferentiated keratinocytes, loricrin gene is repressed by Jun-B, Sp3, cAMP response element-binding (CREB), Activator protein 2 (AP-2)-like protein (termed the keratinocyte-specific repressor-1, KSR-1) and YY1 transcription factors (Jang, Steinert; 2002) (Xu *et al*.; 2004). Once keratinization begins, aforecited transcription factors switch-off. Thus, Sp1 and c-Jun levels are increased, an unidentified regulator protein bind to loricrin promoter and p300/CREB1-binding protein (CBP) is recruited to start with its transcription (Jang, Steinert; 2002). Mentioned loricrin-associated events are regulated by mechanical forces (Jung, Jung, Shin; 2016), EGFR activity (Popp *et al*.; 2014), $p21^{CIP1/WAF1}$ levels (Di Cunto *et al*.; 1998), and by intracellular [Ca^{2+}] and its down-regulation effect over S100A6 and YY1 (Ito, Kizawa; 2001) (Xu *et al*.; 2004) (Taguchi *et al*., 2011). Once translated, filaggrin, loricrin and K10 interacts not only physically but also at genetic flux level in a cooperative way. Knockdown of profilaggrin N-terminal domain (PND), which co-localize with K10, in an organotypic skin culture model caused loss of filaggrin and loricrin expression (Yoneda *et al*.; 2012). When HaCaT filaggrin production was downregulated with small interfering RNAs, loricrin synthesis was diminished together with EGFR, E-cadherin, and occluding, all implied in barrier function (Nakai *et al.*;

2012). To conclude, reduced sensitivity of HaCaT to differentiate, non-ideal conditions in our culture conditions and the highly regulated genetic flux of evaluated terminal differentiation markers can explain its absence or weakly presence either in our DEpOs (Fig. 8) or in previously works (Boelsma, Verhoeven, Ponec; 1999) (Schoop, Mirancea, Fusenig; 1999) (Maas-Szabowski, Stärker, Fusenig; 2003) (Yoneda *et al*.; 2012) (Jung, Jung, Shin; 2016).

Since used HaCaT cells were genetically heterogeneous and was exposed to non-ideal media, it was expectable that its lipid anabolism was abnormal too. For illustration, the diminished HaCaT sensitivity to growth factors as insulin and EGF. These ligands stimulate the activity of some enzymes implied in lipid metabolism as HMG-CoA synthase/reductase. So, the altered response to those factors might also conducts to lipid reduced biosynthesis (e.g. mevalonate) (Harris *et al*.; 2000). HaCaT based organotypics developed by Boelsma, Verhoeven and Ponec in 1999 depicted a lipid profile very similar to NHK cultured in submerged condition. These results did suggest an inactivation of normal enzymes involved in lipid synthesis during cornification and a basal proliferative over differentiative phenotype as well. Skin is an active site of lipid anabolism (e.g. 25% of total body cholesterol synthesis occurs in skin). Fatty acids and cholesterol are required for cutaneous homeostasis. In general, the major skin lipid are ceramides (50%), followed by cholesterol (25%) and free fatty acids (FFA, 15%) (Elias, Feingold, Fluhr; 2005). Composition of free fatty acid (FFA) fraction reported on skin human stratum corneum varies in chain length between C16 and C24. Approximately, in decreasing quantity order, C26:0 (25%), C25:0 (10%), C24:0 (31%), C18:0 (8%), C16:0 (7%) (Table 1) (Weerheim, Ponec; 2001). HaCaT-based artificial epidermis constructed over matrices populated with normal human dermal fibroblasts, showed lower quantities of FFAs fraction (~5%) compared with normal epidermis (~8%) (Ponec, Boelsma, Weerheim; 2000) (Ponec *et al*.; 2000). These results remain the same irrespective used media, matrix (i.e. DED, filter inserts, collagen gels) or incubation time (i.e. 3-5 weeks) (Boelsma, Verhoeven, Ponec; 1999). As far as minor than reported concentrations, a similar distribution per type of FFAs was found here. C16 and C18 were the most frequent in the C12-C20 range in all analyzed DEpOs models (Fig. 9). Fatty acid composition of 100% confluent HaCaT cultures showed that C16-C18 sum (i.e. 92.6%) was greater than C20-C26 (i.e. 7.4%) (Schürer *et al*.; 1993).

Above fact and the slight barrier function found, was in agreed with some reports where shorter chain FFAs (e.g. C16, C18 or C20) acquires a poor spatial order in stratum corneum altering the barrier function of skin (van Smeden *et al*.; 2014a). Lateral organization of lipids in wild lamellae begins with a low density, disordered, liquid phase. While FFA density increase, some lipid populations achieve a hexagonal organization and, at the end, a very dense-orthorhombic-organization is reached (van Smeden *et al*.; 2014a). Orthorhombic lamellar packing depends of ceramides:cholesterol:FFAs ratio and long chain FFAs. This spatial association was not achieved in reconstructed epidermis, where lipids reach just a hexagonal lamellar packing (Ponec, Boelsma, Weerheim; 2000). In contrast, the spatial orientation raised by ceramides and medium-chain FFAs (i.e. C22 & C24) improves skin barrier properties (Uchiyama *et al*.; 2016). Additionally, in culture with fetal calf serum (FCS), NHK as well as HaCaT, acquires low quantities of linoleic acid and a relatively high content of oleic acid, which is very different compared with normal freshly skin. It has been suggested that the medium supplementation with essential fatty acids and its use in HaCaT cultures can be improve the cited abnormal behavior (Schürer *et al.*; 1993). Despite all above, some reports assert that all molecular machinery that regulates lipid synthesis in committed HaCaT are present and behaves as normal keratinocytes in differentiation, namely liver X receptor alpha/beta (LXRα/β) (Hong *et al.*; 2010) and its associated down-stream regulator termed sterol-regulatory element-binding protein-1c (SREBP-1c) (Yokoyama *et al*.; 2009).

In accordance with low FFA fraction content (Fig. 9) and the poor impedance level achieved by DEpOs (Fig. 10), the Lucifer yellow (LY) permeability assay suggest not just non-barrier function but an active paracellular transport of LY to basolateral side. Paracellular transport properties of all epithelia is determined by tight junctions (TJs) and its role in permeability of skin has been widely reported (Kirschner *et al*.; 2010) (Kirschner *et al*.; 2013) (Brandner *et al*.; 2015). TJs correct assemble is only present in orthokeratosis. When inflammation occurs, horny layer desquamation is accelerated and parakeratosis appears. Concomitant with this phenomenon, TJs are reorganized to serve as tunnels throughout extensions from Langerhans cells pass, getting better the antigen presentation process (Kubo *et al*.; 2009) (Ouchi *et al*.; 2011). Involved reorganization of TJs leads to alteration of normal barrier function of epidermis (Kubo *et al*.; 2009). As all our DEpOs were parakeratotic, TJs reorganization is expected in a way that structures like tunnels were found leading to a massively LY transport to basolateral side in insert system, such as was observed (Fig. 11). In fact, poor TEER values registered on submerged HaCaT monolayers has been ascribed to few TJs occurrence (Meyle *et al*.; 1999).

5. IMPROVEMENT PROPOSALS

It has been shown that HaCaT cell line allows a more reproducible and consistent results in the study of cellular and molecular changes during early cornification process paralleled to primary keratinocytes. NHKs shows high variability associated to individual features as body region or age. Results showed here, as in other works, claims to a poor phenotype stability that depends highly on culture environment conditions from start to finish. As was argued early in the first HaCaT 3D tissue culture system, this cell line is so sensitive to microenvironment. A carefully medium formulation is mandatory (Ryle *et al.*; 1989). Based on our laboratory experience (Morales *et al.*; 2016) and other researchers, we expected that HaCaT will possess the necessary genetic and cellular epidermal differentiation repertoire to generate epidermis properly. Nonetheless, it is required to characterize genetically the utilized HaCaT cell line. Is important confirm the presence and function, for example, of epidermal differentiation complex (EDC), allocated at 1q21 (Abhishek, Palamadai; 2016). Obtained results strongly argues that is required to do a rigorous adjustment of calcium concentration thorough the assay as was proposed everywhere (Breitkreutz *et al*.; 1993) (Borowiec *et al.*; 2013). Furthermore, is possible to enrich the used media with some additives to try to circumvent the problem of HaCaT loss of sensitivity to differentiation cues. Several compounds have been proposed: ethanolamine, phosphoethanolamine (Wille *et al*.; 1984), ascorbic acid (Smola, Thiekötter, Fusenig; 1993), soluble laminin 5r (Hormia *et al*.; 1995), linoleic acid, transferrin (Boelsma, Verhoeven, Ponec; 1999), IL-1α, TGF- α (Maas-Szabowski, Stärker, Fusenig; 2003), Ginsenoside Re (Oh *et al*.; 2016).

Other "exotic" strategies about culture media can be proved in the future. For example, Rekus did observe that, after two days of growth factor withdrawal, HaCaT cells initiate terminal differentiation, concomitant with loss of clonogenic potential (Rekus, 2000). Nakai *et al*. reports a similar behavior in 2016, after incubation of HaCaT culture by 12 hours in PBS. Starvation led to filaggrin and loricrin expression increase, suggesting cornification start. So, once 100% culture confluence is reached in DEpOs, is possibly to exchange to proliferation medium. Incubate for 2 or 3 days to trigger differentiation, performs air-liquid lifting and change to conditioned medium. These procedures should be performed carefully because apoptosis or loss of the HaCaT ability to grow at confluent density can appear (Rekus; 2000). Additionally, basal conditions (i.e. low $[Ca^{2+}]$ medium without growth factors) in HaCaT cultures cause, in its latent form, TGF-β releasing. This is a potent mitosis inhibitor. Thus, when $[Ca^{2+}]$ is raised (e.g. QN or QC), this negative cell growth regulator can be activated (Kato *et al*.; 1995).

Consistent with these observations, extended culture (> 3 weeks) in low Ca^{2+} conditions (~0.03 mM) and in low confluence (< 85%) leads to a basal keratinocyte behavior of HaCaT. This basal phenotype responds very well to extracellular [Ca^{2+}] increasing (2.8 mM) and confluency stimuli (> 85%) (i.e. K1 and involucrin translation) (Deyrieux, Wilson; 2007).

6. CONCLUSIONS & FUTURE REMARKS

Current medicine need to replenish lost skin and scientific research calls for replace animal skin assays models with alternative test methods. These two situations have led us to development of three dimensional models of human skin. In general, classic *in vitro* reconstructed skin consists of NHK seeded over fibroblast-populated dermal matrices. HaCaT is a human, spontaneously immortalized and hypotetraploid keratinocyte cell line. This cells historically have been used to study early cornification molecular events both in submerged or in organotypic type cultures. We used HaCaT to try to mimicry the basic functions of NHK proliferation and differentiation. HaCaT based dermal-epidermal organotypics (DEpOs) were erected on three kind of dermal matrices populated with primary fibroblasts, namely: polyethylene terephthalate (PET), human fibrin (hF) and rat tail collagen Type I and Type III (CI+III). HaCaT growth properties were analyzed by cell enumeration based in formazan production (PDT and CPA); its differentiation characteristics (after 21 day of culture) were evaluated by H&E, immunohistochemistry, TEER, LY permeability assay and lipid GC-FID; DNA content was assessed by PI staining and flow cytometry. Together, the results obtained here permit us to conclude:

1. HaCaT populating doubling time (PDT) on passages 30-40 is 16.92±2.03 hours, incubated in complete medium at standard conditions (37 °C, 5% CO_2 and 99% RH).

2. EGF (10 ng/mL) is a potent mitogen that increases HaCaT rate proliferation, as cell proliferation assay (CPA) suggested.

3. Used HaCaT cell line was composed by at least two population, distinguishable by its DNA content, size and granularity in a propidium iodide (PI) based flow cytometry.

4. Used [EGF] and [Ca^{2+}] probably exerts a synergistical proliferative effect on HaCaT leading to a hyperproliferative phenotype (i.e. short PDT, high Ki-67 index and poor production of terminal differentiation markers as filaggrin and loricrin) and a parakeratotic epidermis (i.e. nuclei thorough layers) in built DEpOs.

5. Obtained parakeratotic DEpOs, by here proposed protocol, did not develop neither barrier function (i.e. poor lipid profile and poor expression of terminal differentiation markers related with this function, as filaggrin and loricrin) nor impedance properties (i.e. low TEER values), but showed an active paracellular transport (i.e. high lateral Lucifer yellow transport rates).

6. Here proposed protocol to provoke keratinization on HaCaT based DEpOs is not optimal. It causes an abnormal stratification process characterized by parakeratosis. Modifications in [Ca^{2+}], [EGF] and fibroblasts number are mandatory to improve it.

Based on showed results and conclusions, a modified protocol can be proposed. Briefly, HaCaT basal phenotype should be promoted by its culturing at low [Ca^{2+}] (<0.2 mM) for at least three weeks. Once a

basal obvious phenotype is achieved, consecutive sub-culturing should be made to stabilizes cell line DNA content. Flow cytometry cell sorting to obtain a clonal strain can accelerate the clonal step. As soon as stabilized and cultured at 20% confluence, four incubation days are enough to do sub-culturing (i.e. when ~70% confluence is achieved). $4x10^5$ HaCaT cells must be sown on top of dermal equivalents. First seven days on submerged culture must be carried out with QC (0.2 mM Ca^{2+} and 10 ng/mL EGF), thus, air-liquid raising is done. Is necessary be sure that total confluence is accomplished. Following 14 days in air-liquid interphase culture must be done with basolateral addition of QN enriched with 5 ng/mL IL-1α and 2 ng/mL TGF-α as Maas-Szabowski, Stärker and Fusenig (2003) recommends. Other additives as SP600125 (50 µM), an inhibitor of c-Jun NH_2-terminal protein kinase (JNK), can potentiates HaCaT terminal differentiation as it has been reported previously (Kitagawa *et al*.; 2014). Finally, fibroblast number in dermal gels models must be standardized, starting, for instance, with 10^4 cells.

PRESENTATIONS AND SCIENTIFIC PRODUCTION

Design, results and conclusions of this work were exposed at "Seminario VII de Ciencias Básicas Biomédicas" (November 15-17, 2016). A version of this work to a possible original research paper is in construction.

ACKNOWLEDGMENTS

We would like to thank Gabriel Jaime Merizalde Soto for his expert technical assistance and linguistically manuscript revision, Luis Alfonso Correa Londoño and Beatriz Eugenia Vieco Durán for his help in histological cuts and stains, Mauricio Rojas López for his advice and help to design and execute the DNA content and cell cycle analysis. We also wish to extend our thanks to IPS-Universitaria to allow postgraduate students work in its installations.

FUNDING

This work was supported by grants from Sistema General de Regalías 2013-2016: "Biobanco regional Antioquia, Optimización de la captación y mejoramiento de la calidad de componentes anatómicos: una opción al alcance de todos". Student associated costs were supported by university scholarship from Escuela de Microbiología, academic resolution 2748 (March 20, 2014) (Universidad de Antioquia) and Sistema General de Regalías (2013-2016 grant).

REFERENCES

Abhishek S, Palamadai Krishnan S. Epidermal Differentiation Complex: A Review on Its Epigenetic Regulation and Potential Drug Targets. Cell J. 2016; 18(1): 1-6.

Auger FA, Berthod F, Moulin V, Pouliot R, Germain L. Tissue-engineered skin substitutes: from *in vitro* constructs to in vivo applications. Biotechnol Appl Biochem. 2004; 39(Pt 3): 263-275.

Arrigo AP, Ducasse C. Expression of the anti-apoptotic protein Hsp27 during both the keratinocyte differentiation and dedifferentiation of HaCaT cells: expression linked to changes in intracellular protein organization? Exp Gerontol. 2002; 37(10-11): 1247-1255.

Bakondi E, Gönczi M, Szabó E, Bai P, Pacher P, Gergely P, Kovács L, Hunyadi J, Szabó C, Csernoch L, Virág L. Role of intracellular calcium mobilization and cell-density-dependent signaling in oxidative-stress-induced cytotoxicity in HaCaT keratinocytes. J Invest Dermatol. 2003; 121(1): 88-95.

Balin AK, Fisher AJ, Anzelone M, Leong I, Allen RG. Effects of establishing cell cultures and cell culture conditions on the proliferative life span of human fibroblasts isolated from different tissues and donors of different ages. Exp Cell Res. 2002; 274(2): 275-287.

Basrai MA, Naider F, Becker JM. Internalization of lucifer yellow in Candida albicans by fluid phase endocytosis. J Gen Microbiol. 1990; 136(6): 1059-1065.

Bello YM, Falabella AF, Eaglstein WH. Tissue-engineered skin. Current status in wound healing. Am J Clin Dermatol. 2001; 2(5): 305-313.

Benedyk M, Sopalla C, Nacken W, Bode G, Melkonyan H, Banfi B, Kerkhoff C. HaCaT keratinocytes overexpressing the S100 proteins S100A8 and S100A9 show increased NADPH oxidase and NF-kappaB activities. J Invest Dermatol. 2007; 127(8): 2001-2011.

Bermúdez JA, Velásquez CM. Perfil de ácidos grasos libres (AGL) en suero de jóvenes colombianos con obesidad y síndrome metabólico. Arch Latinoam Nutr. 2014; 64(4): 248-257.

Bieging KT, Mello SS, Attardi LD. Unravelling mechanisms of p53-mediated tumour suppression. Nat Rev Cancer. 2014; 14(5): 359-370.

Bigelow RL, Jen EY, Delehedde M, Chari NS, McDonnell TJ. Sonic hedgehog induces epidermal growth factor dependent matrix infiltration in HaCaT keratinocytes. J Invest Dermatol. 2005; 124(2): 457-465.

Bin Mh Busra MF, Chowdhury SR, Bin Ismail F, Bin Saim A, Idrus RH. Tissue-Engineered Skin Substitute Enhances Wound Healing after Radiation Therapy. Adv Skin Wound Care. 2016; 29(3): 120-129.

Bizik J, Harjula A, Kankuri E (inventors). Regenerative Matrix Comprising Cells Activated by Nemosis and/or Factors Released from such Cells. Asiatic, European and African patent. WO/2010/112678 (PCT/FI2010/050256). 31.03.2010

Blase C, Becker D, Kappel S, Bereiter-Hahn J. Microfilament dynamics during HaCaT cell volume regulation. Eur J Cell Biol. 2009; 88(3): 131-139.

Blumberg M. Keratinocyte Differentiation and Activation. Acta Derm Venereol. 1997; 6(4): 127-135.

Boderke P, Boddé HE, Ponec M, Wolf M, Merkle HP. Mechanistic and quantitative prediction of aminopeptidase activity in stripped human skin based on the HaCaT cell sheet model. J Investig Dermatol Symp Proc. 1998; 3(2): 180-184.

Boelsma E, Gibbs S, Faller C, Ponec M. Characterization and comparison of reconstructed skin models: morphological and immunohistochemical evaluation. Acta Derm Venereol. 2000; 80(2): 82-88.

Boelsma E, Verhoeven MC, Ponec M. Reconstruction of a human skin equivalent using a spontaneously transformed keratinocyte cell line (HaCaT). J Invest Dermatol. 1999; 112(4): 489-498.

Boehnkea K, Miranceaa N, Pavesioc A, Fuseniga NE, Boukampa P, Starka HJ. Effects of fibroblasts and microenvironment on epidermal regeneration and tissue function in long-term skin equivalents. Eur J Cell Biol. 2007; 86(11-12): 731-746

Boissel JP, Ohly D, Bros M, Gödtel-Armbrust U, Förstermann U, Frank S. The neuronal nitric oxide synthase is upregulated in mouse skin repair and in response to epidermal growth factor in human HaCaT keratinocytes. J Invest Dermatol. 2004; 123(1): 132-139.

Bonifas J, Hennen J, Dierolf D, Kalmes M, Blömeke B. Evaluation of cytochrome P450 1 (CYP1) and N-acetyltransferase 1 (NAT1) activities in HaCaT cells: implications for the development of in vitro techniques for predictive testing of contact sensitizers. Toxicol In Vitro. 2010; 24(3): 973-980.

Boraldi F, Annovi G, Tiozzo R, Sommer P, Quaglino D. Comparison of *ex vivo* and *in vitro* human fibroblast ageing models. Mech Ageing Dev. 2010; 131(10): 625-635.

Borland MG, Khozoie C, Albrecht PP, Zhu B, Lee C, Lahoti TS, Gonzalez FJ, Peters JM. Stable over-expression of PPARβ/δ and PPARγ to examine receptor signaling in human HaCaT keratinocytes. Cell Signal. 2011; 23(12): 2039-2050.

Borowiec AS, Delcourt P, Dewailly E, Bidaux G. Optimal Differentiation of *in vitro* Keratinocytes Requires Multifactorial External Control. PLoS One. 2013; 8(10): e77507.

Böttcher-Haberzeth S, Biedermann T, Reichmann E. Tissue engineering of skin. Burns. 2010; 36(4): 450-460.

Boukamp P, Petrussevska RT, Breitkreutz D, Hornung J, Markham A, Fusenig NE. Normal keratinization in a spontaneously immortalized aneuploid human keratinocyte cell line. J Cell Biol. 1988; 106(3): 761-771.

Boukamp P, Popp S, Altmeyer S, Hülsen A, Fasching C, Cremer T, Fusenig NE. Sustained nontumorigenic phenotype correlates with a largely stable chromosome content during long-term culture of the human keratinocyte line HaCaT. Genes Chromosomes Cancer. 1997; 19(4): 201-214.

Brandner JM, Zorn-Kruppa M, Yoshida T, Moll I, Beck LA, De Benedetto A. Epidermal tight junctions in health and disease. Tissue Barriers. 2015; 3(1-2): e974451.

Breitkreutz D, Schoop VM, Mirancea N, Baur M, Stark HJ, Fusenig NE. Epidermal differentiation and basement membrane formation by HaCaT cells in surface transplants. Eur J Cell Biol. 1998; 75(3): 273-286.

Breitkreutz D, Stark HJ, Plein P, Baur M, Fusenig NE. Differential modulation of epidermal keratinization in immortalized (HaCaT) and tumorigenic human skin keratinocytes (HaCaT-ras) by retinoic acid and extracellular Ca^{2+}. Differentiation. 1993; 54(3): 201-217.

Brooks RF. Variability in the cell cycle and the control of proliferation. In: John PCL (Editor). The cell cycle. US: Cambridge University Press; 1981. p. 35-62.

Burrell HE, Simpson AW, Mehat S, McCreavy DT, Durham B, Fraser WD, Sharpe GR, Gallagher JA. Potentiation of ATP- and bradykinin-induced $[Ca^{2+}]c$ responses by PTHrP peptides in the HaCaT cell line. J Invest Dermatol. 2008; 128(5): 1107-1115.

Büth H, Wolters B, Hartwig B, Meier-Bornheim R, Veith H, Hansen M, Sommerhoff CP, Schaschke N, Machleidt W, Fusenig NE, Boukamp P, Brix K. HaCaT keratinocytes secrete lysosomal cysteine proteinases during migration. Eur J Cell Biol. 2004; 83 (11-12): 781-795.

Candi E, Schmidt R, Melino G. The cornified envelope: a model of cell death in the skin. Nat Rev Mol Cell Biol. 2005; 6(4): 328-340.

Capone A, Visco V, Belleudi F, Marchese C, Cardinali G, Bellocci M, Picardo M, Frati L, Torrisi MR. Up-modulation of the expression of functional keratinocyte growth factor receptors induced by high cell density in the human keratinocyte HaCaT cell line. Cell Growth Differ. 2000; 11(11): 607-614.

Cerezo A, Stark HJ, Moshir S, Boukamp P. Constitutive overexpression of human telomerase reverse transcriptase but not c-myc blocks terminal differentiation in human HaCaT skin keratinocytes. J Invest Dermatol. 2003; 121(1): 110-119.

Chapkin RS, Ziboh VA, Marcelo CL, Voorhees JJ. Metabolism of essential fatty acids by human epidermal enzyme preparations: evidence of chain elongation. J Lipid Res. 1986; 27(9): 945-954.

Chaturvedi V, Qin JZ, Denning MF, Choubey D, Diaz MO, Nickoloff BJ. Abnormal NF-kappaB signaling pathway with enhanced susceptibility to apoptosis in immortalized keratinocytes. J Dermatol Sci. 2001; 26(1): 67-78.

Chen X, Kwak S, Lafleur M, Bloom M, Kitson N, Thewalt J. Fatty acids influence "solid" phase formation in models of stratum corneum intercellular membranes. Langmuir. 2007; 23(10): 5548-5556.

Choi M, Lee C. Immortalization of Primary Keratinocytes and Its Application to Skin Research. Biomol Ther (Seoul). 2015; 23(5): 391-399.

Chu DH, Haake AR, Holbrook K, Loomis CA. Estructura y Desarrollo de la Piel. In: Fitzpatrick TB, Freedberg IM, Eisen AZ, Wolff K (Directors). Dermatología en Medicina General Vol. I. 6a ed. Argentina: Médica Panamericana; 2005. p. 64-97.

Clement AL, Moutinho TJ Jr, Pins GD. Micropatterned dermal-epidermal regeneration matrices create functional niches that enhance epidermal morphogenesis. Acta Biomater. 2013; 9(12): 9474-9484.

Coon WM, Wheatley VR, Herrmann F, Mandol L. Free Fatty Acids of the Skin Surface and Barrier Zone in Normal and Abnormal Keratinization. J Invest Dermatol. 1963; 41: 259-264.

da Rocha-Azevedo B, Grinnell F. Fibroblast morphogenesis on 3D collagen matrices: the balance between cell clustering and cell migration. Exp Cell Res. 2013; 319(16): 2440-2446.

da Silva RA, Sammartino F, Planello AC, Line SR, de Souza AP. HaCaT anchorage blockade leads to oxidative stress, DNA damage and DNA methylation changes. Biochem Biophys Rep. 2015; 2: 94-102.

Damour O, Augustin C, Black AF. Applications of reconstructed skin models in pharmaco-toxicological trials. Med Biol Eng Comput. 1998; 36(6): 825-832.

de Lange T. T-loops and the origin of telomeres. Nat Rev Mol Cell Biol. 2004; 5(4): 323-329.

De Wever B, Kurdykowski S, Descargues P. Human Skin Models for Research Applications in Pharmacology and Toxicology: Introducing NativeSkin, the ‘‘Missing Link’’ Bridging Cell Culture and/or Reconstructed Skin Models and Human Clinical Testing. Applied In Vitro Toxicology. 2015; 1(1): 26-32.

Debels H, Hamdi M, Abberton K, Morrison W. Dermal Matrices and Bioengineered Skin Substitutes: A Critical Review of Current Options. Plast Reconstr Surg Glob Open. 2015; 3(1): 63-72.

Deyrieux AF, Wilson VG. *In vitro* culture conditions to study keratinocyte differentiation using the HaCaT cell line. Cytotechnology. 2007; 54(2): 77-83.

Di Cunto F, Topley G, Calautti E, Hsiao J, Ong L, Seth PK, Dotto GP.Inhibitory function of p21Cip1/WAF1 in differentiation of primary mouse keratinocytes independent of cell cycle control. Science. 1998; 280(5366): 1069-1072.

Edmondson SR, Werther GA, Wraight CJ. Calcium regulates the expression of insulin-like growth factor binding protein-3 by the human keratinocyte cell line HaCaT. J Invest Dermatol. 2001; 116(4): 491-497.

Elias PM, Feingold KR, Fluhr JW. La piel como órgano protector. In: Fitzpatrick TB, Freedberg IM, Eisen AZ, Wolff K (Directors). Dermatología en Medicina General Vol. I. 6a ed. Argentina: Médica Panamericana; 2005. p. 120-132.

Elias PM, Gruber R, Crumrine D, Menon G, Williams ML, Wakefield JS, Holleran WM, Uchida Y. Formation and functions of the corneocyte lipid envelope (CLE). Biochim Biophys Acta. 2014; 1841(3): 314-318.

Eming SA, Martin P, Tomic-Canic M. Wound repair and regeneration: mechanisms, signaling, and translation. Sci Transl Med. 2014; 6(265): 265sr6.

Evans ND, Oreffo RO, Healy E, Thurner PJ, Man YH. Epithelial mechanobiology, skin wound healing, and the stem cell niche. J Mech Behav Biomed Mater. 2013; 28: 397-409.

Feingold KR, Elias PM. Role of lipids in the formation and maintenance of the cutaneous permeability barrier. Biochim Biophys Acta. 2014; 1841(3): 280-294.

Ermler S, Krunic D, Knoch TA, Moshir S, Mai S, Greulich-Bode KM, Boukamp P. Cell cycle-dependent 3D distribution of telomeres and telomere repeat-binding factor 2 (TRF2) in HaCaT and HaCaT-myc cells. Eur J Cell Biol. 2004; 83(11-12): 681-690.

Feingold KR. Thematic review series: skin lipids. The role of epidermal lipids in cutaneous permeability barrier homeostasis. J Lipid Res. 2007; 48(12): 2531-2546.

Flaxman BA. Cell identification in primary cell cultures from skin. In Vitro. 1974; 10(1): 112-118.

Frank S, Kolb N, Werner ER, Pfeilschifter J. Coordinated induction of inducible nitric oxide synthase and GTP-cyclohydrolase I is dependent on inflammatory cytokines and interferon-gamma in HaCaT keratinocytes: implications for the model of cutaneous wound repair. J Invest Dermatol. 1998; 111(6): 1065-1071.

Folch J, Lees M, Sloane GH. A simple method for the isolation and purification of total lipides from animal tissues. J Biol Chem. 1957; 226(1): 497-509.

Fujii-Maeda S, Kajiwara K, Ikizawa K, Shinazawa M, Yu B, Koga T, Furue M, Yanagihara Y. Reciprocal regulation of thymus and activation-regulated chemokine/macrophage-derived chemokine production by interleukin (IL)-4/IL-13 and interferon-gamma in HaCaT keratinocytes is mediated by alternations in E-cadherin distribution. J Invest Dermatol. 2004; 122(1): 20-28.

Fusenig NE, Boukamp P. Multiple stages and genetic alterations in immortalization, malignant transformation, and tumor progression of human skin keratinocytes. Mol Carcinog. 1998; 23(3): 144-158.

Game SM, Huelsen A, Patel V, Donnelly M, Yeudall WA, Stone A, Fusenig NE, Prime SS. Progressive abrogation of TGF-beta 1 and EGF growth control is associated with tumour progression in ras-transfected human keratinocytes. Int J Cancer. 1992; 52(3): 461-470.

Gangatirkar P, Paquet-Fifield S, Li A, Rossi R, Kaur P. Establishment of 3D organotypic cultures using human neonatal epidermal cells. Nat Protoc. 2007; 2(1): 178-186.

Gazel A, Banno T, Walsh R, Blumenberg M. Inhibition of JNK promotes differentiation of epidermal keratinocytes. J Biol Chem. 2006; 281(29): 20530-20541.

Geer DJ, Swartz DD, Andreadis ST. In vivo model of wound healing based on transplanted tissue-engineered skin. Tissue Eng. 2004; 10(7-8): 1006-1017.

Gelse K, Pöschl E, Aigner T. Collagens: structure, function, and biosynthesis. Adv Drug Deliv Rev. 2003; 55(12): 1531-1546.

Getsios S, Simpson CL, Kojima S, Harmon R, Sheu LJ, Dusek RL, Cornwell M, Green KJ. Desmoglein 1-dependent suppression of EGFR signaling promotes epidermal differentiation and morphogenesis. J Cell Biol. 2009; 185(7): 1243-1258.

Ghaderi R, Haghighi F. Mutations of p53 Gene in Skin Cancers: a Case Control Study. Iran J Med Sci. 2007; 33(1): 5-8.

Gomez DE, Armando RG, Farina HG, Menna PL, Cerrudo CS, Ghiringhelli PD, Alonso DF. Telomere structure and telomerase in health and disease (review). Int J Oncol. 2012; 41(5): 1561-1569.

Grabbe J, Welker P, Rosenbach T, Nürnberg W, Krüger-Krasagakes S, Artuc M, Fiebiger E, Henz BM. Release of stem cell factor from a human keratinocyte line, HaCaT, is increased in differentiating versus proliferating cells. J Invest Dermatol. 1996; 107(2): 219-224.

Gruber R. Morphology of Filaggrin-Depleted Epidermis. In: Thyssen JP, Maibach HI (Editors). Filaggrin - Basic Science, Epidemiology, Clinical Aspects and Management. Berlin Heidelberg: Springer-Verlag; 2014. p. 9-21.

Chu DH, Haake AR, Holbrook K, Loomis CA. Estructura y Desarrollo de la Piel. In: Fitzpatrick TB, Freedberg IM, Eisen AZ, Wolff K (Directors). Dermatología en Medicina General Vol. I. 6a ed. Argentina: Médica Panamericana; 2005. p. 64-97.

Haase I, Liesegang C, Binting S, Henz BM, Rosenbach T. Phospholipase C-mediated signaling is altered during HaCaT cell proliferation and differentiation. J Invest Dermatol. 1997; 108(5): 748-752.

Hahn HJ, Youn HJ, Cha HJ, Kim K, An S, Ahn KJ. Single Low-Dose Radiation Induced Regulation of Keratinocyte Differentiation in Calcium-Induced HaCaT Cells. Ann Dermatol. 2016; 28(4): 433-437.

Hanani M. Lucifer yellow - an angel rather than the devil. J Cell Mol Med. 2012; 16(1):22-31.

Harding CR, Aho S, Bosko CA. Filaggrin - revisited. Int J Cosmet Sci. 2013; 35(5): 412-423.

Harris IR, Höppner H, Siefken W, Farrell AM, Wittern KP. Regulation of HMG-CoA synthase and HMG-CoA reductase by insulin and epidermal growth factor in HaCaT keratinocytes. J Invest Dermatol. 2000; 114(1): 83-87.

Härle-Bachor C, Boukamp P. Telomerase activity in the regenerative basal layer of the epidermis inhuman skin and in immortal and carcinoma-derived skin keratinocytes. Proc Natl Acad Sci U S A. 1996; 93(13): 6476-6481.

Hayflick L. The Limited *in vitro* Lifetime of Human Diploid Cell Strains. Exp Cell Res. 1965; 37: 614-636.

Hormia M, Falk-Marzillier J, Plopper G, Tamura RN, Jones JC, Quaranta V. Rapid spreading and mature hemidesmosome formation in HaCaT keratinocytes induced by incubation with soluble laminin-5r. J Invest Dermatol. 1995; 105(4): 557-561.

Hong I, Rho HS, Kim DH, Lee MO. Activation of LXRα induces lipogenesis in HaCaT cells. Arch Pharm Res. 2010; 33(9): 1443-1449.

Hu DH, Zhang ZF, Zhang YG, Zhang WF, Wang HT, Cai WX, Bai XZ, Zhu HY, Shi JH, Tang CW. A potential skin substitute constructed with hEGF gene modified HaCaT cells for treatment of burn wounds in a rat model. Burns. 2012; 38(5): 702-712.

Hudson LG, McCawley LJ. Contributions of the epidermal growth factor receptor to keratinocyte motility. Microsc Res Tech. 1998; 43(5): 444-455.

Indra AK, Leid M. Epidermal permeability barrier measurement in mammalian skin. Methods Mol Biol. 2011; 763: 73-81.

Inoue A, Yamazaki M, Ishidoh K, Ogawa H. Epidermal growth factor activates m-calpain, resulting in apoptosis of HaCaT keratinocytes. J Dermatol Sci. 2004; 36(1): 60-62.

IATT (Interagency Task Team) on Male Circumcision. Information Package on Male Circumcision and HIV Prevention [Web]. World Health Organization, WHO; 15 December 2015 [access 6 September 2016] http://www.who.int/hiv/pub/malecircumcision/infopack/en/

Isnard N, Fodil I, Robert L, Renard G. Modulation of cell-phenotype during *in vitro* aging: Glycosaminoglycan biosynthesis by skin fibroblasts and corneal keratocytes. Exp Gerontol. 2002; 37(12): 1379-1387.

Ito M, Kizawa K. Expression of calcium-binding S100 proteins A4 and A6 in regions of the epithelial sac associated with the onset of hair follicle regeneration. J Invest Dermatol. 2001; 116(6): 956-963.

Jang SI, Steinert PM. Loricrin expression in cultured human keratinocytes is controlled by a complex interplay between transcription factors of the Sp1, CREB, AP1, and AP2 families. J Biol Chem. 2002; 277(44): 42268-42279.

Jost M, Kari C, Rodeck U. The EGF receptor - an essential regulator of multiple epidermal functions. Eur J Dermatol. 2000; 10(7): 505-510.

Jung MH, Jung SM, Shin HS. Co-stimulation of HaCaT keratinization with mechanical stress and air-exposure using a novel 3D culture device. Sci Rep. 2016; 6: 33889.

Jungersted JM. Stratum Corneum Lipids and Filaggrin. Gruber R. Morphology of Filaggrin-Depleted Epidermis. In: Thyssen JP, Maibach HI (Editors). Filaggrin - Basic Science, Epidemiology, Clinical Aspects and Management. Berlin Heidelberg: Springer-Verlag; 2014. p. 23-27.

Kaji K, Ohta T, Horie N, Naru E, Hasegawa M, Kanda N. Donor age reflects the replicative lifespan of human fibroblasts in culture. Hum Cell. 2009; 22(2): 38-42.

Kan M, Yamane I. *In vitro* proliferation and lifespan of human diploid fibroblasts in serum-free BSA-containing medium. J Cell Physiol. 1982; 111(2): 155-162.

Kang BM, Kwack MH, Kim MK, Kim JC, Sung YK. Sphere formation increases the ability of cultured human dermal papilla cells to induce hair follicles from mouse epidermal cells in a reconstitution assay. J Invest Dermatol. 2012; 132(1): 237-239.

Katagata Y, Aoki T, Kondo S. Detecting expression of keratins 8/18 in human HaCaT keratinocytes. J Dermatol Sci. 1999; 19(2): 139-143.

Kato M, Ishizaki A, Hellman U, Wernstedt C, Kyogoku M, Miyazono K, Heldin CH, Funa K. A human keratinocyte cell line produces two autocrine growth inhibitors, transforming growth factor-beta and insulin-like growth factor binding protein-6, in a calcium- and cell density-dependent manner. J Biol Chem. 1995; 270(21): 12373-12379.

Kaufmann K, Thiel G. Epidermal growth factor and thrombin induced proliferation of immortalized human keratinocytes is coupled to the synthesis of Egr-1, a zinc finger transcriptional regulator. J Cell Biochem. 2002; 85(2): 381-391.

Kehe K, Abend M, Kehe K, Ridi R, Peter RU, van Beuningen D. Tissue engineering with HaCaT cells and a fibroblast cell line. Arch Dermatol Res. 1999; 291(11): 600-605.

Khodaeiani E, Fakhrjou A, Amirnia M, Babaei-Nezhad S, Taghvamanesh F, Razzagh-Karimi E, Alikhah H. Immunohistochemical evaluation of p53 and Ki67 expression in skin epithelial tumors. Indian J Dermatol. 2013; 58(3): 181-187.

Kirschner N, Houdek P, Fromm M, Moll I, Brandner JM. Tight junctions form a barrier in human epidermis. Eur J Cell Biol. 2010; 89(11): 839-842.

Kirschner N, Rosenthal R, Furuse M, Moll I, Fromm M, Brandner JM. Contribution of tight junction proteins to ion, macromolecule, and water barrier in keratinocytes. J Invest Dermatol. 2013; 133(5): 1161-1169.

Kitagawa N, Inai Y, Higuchi Y, Iida H, Inai T. Inhibition of JNK in HaCaT cells induced tight junction formation with decreased expression of cytokeratin 5, cytokeratin 17 and desmoglein 3. Histochem Cell Biol. 2014; 142(4): 389-399.

Koivisto L, Jiang G, Häkkinen L, Chan B, Larjava H. HaCaT keratinocyte migration is dependent on epidermal growth factor receptor signaling and glycogen synthase kinase-3alpha. Exp Cell Res. 2006; 312(15): 2791-2805.

Kretlow JD, Jin YQ, Liu W, Zhang WJ, Hong TH, Zhou G, Baggett LS, Mikos AG, Cao Y. Donor age and cell passage affects differentiation potential of murine bone marrow-derived stem cells. BMC Cell Biol. 2008; 9: 60.

Krueger SA, Wilson GD. Cytometric DNA Analysis of Human Cancers and Cell Lines. In: Cree IA (Editor). 2ª ed. Methods and Protocols: Cancer Cell Culture. London: Humana Press (Springer); 2011. p. 359-370.

Kubitschek HE. Normal distribution of cell generation rate. Exp Cell Res. 1962; 26: 439-450.

Kubo A, Nagao K, Yokouchi M, Sasaki H, Amagai M. External antigen uptake by Langerhans cells with reorganization of epidermal tight junction barriers. J Exp Med. 2009; 206(13): 2937-2946.

Küchler S, Strüver K, Friess W. Reconstructed skin models as emerging tools for drug absorption studies. Expert Opin Drug Metab Toxicol. 2013; 9(10): 1255-1263.

Kühne S, Ockenga W, Banning A, Tikkanen R. Cholinergic transactivation of the EGFR in HaCaT keratinocytes stimulates a flotillin-1 dependent MAPK-mediated transcriptional response. Int J Mol Sci. 2015; 16(3): 6447-6463.

Kuninger DT, Gopinath S, Newman RA. A DIY Model for Generation of Robust 3D Epidermal Skin Equivalents Composed of Normal Human Primary Epidermal Keratinocytes. Life technologies (Thermo). 2014.

Kwon YW, Kwon KS, Moon HE, Park JA, Choi KS, Kim YS, Jang HS, Oh CK, Lee YM, Kwon YG, Lee YS, Kim KW. Insulin-like growth factor-II regulates the expression of vascular endothelial growth factor by the human keratinocyte cell line HaCaT. J Invest Dermatol. 2004; 123(1): 152-158.

Lane DP. p53, guardian of the genome. Nature. 1992; 358(6381): 15-16.

Lechler T, Fuchs E. Asymmetric cell divisions promote stratification and differentiation of mammalian skin. Nature. 2005; 437(7056): 275-280.

Lee WK, Choi SW, Lee HR, Lee EJ, Lee KH, Kim HO. Purinoceptor-mediated calcium mobilization and proliferation in HaCaT keratinocytes. J Dermatol Sci. 2001; 25(2): 97-105.

Lehmann B. HaCaT cell line as a model system for vitamin D3 metabolism in human skin. J Invest Dermatol. 1997; 108(1): 78-82.

Lehman TA, Modali R, Boukamp P, Stanek J, Bennett WP, Welsh JA, Metcalf RA, Stampfer MR, Fusenig N, Rogan EM, Harris CC. p53 mutations in human immortalized epithelial cell lines. Carcinogenesis. 1993; 14(5): 833-839.

Leinonen PT, Hägg PM, Peltonen S, Jouhilahti EM, Melkko J, Korkiamäki T, Oikarinen A, Peltonen J. Reevaluation of the normal epidermal calcium gradient, and analysis of calcium levels and ATP receptors in Hailey-Hailey and Darier epidermis. J Invest Dermatol. 2009; 129(6): 1379-1387.

Lennon DP, Schluchter MD, Caplan AI. The effect of extended first passage culture on the proliferation and differentiation of human marrow-derived mesenchymal stem cells. Stem Cells Transl Med. 2012; 1(4): 279-288.

Leverkus M, Sprick MR, Wachter T, Denk A, Bröcker EB, Walczak H, Neumann M. TRAIL-induced apoptosis and gene induction in HaCaT keratinocytes: differential contribution of TRAIL receptors 1 and 2. J Invest Dermatol. 2003; 121(1): 149-155.

Lewis DA, Hengeltraub SF, Gao FC, Leivant MA, Spandau DF. Aberrant NF-kappaB activity in HaCaT cells alters their response to UVB signaling. J Invest Dermatol. 2006; 126(8): 1885-1892.

Liang P, Jiang B, Yang X, Xiao X, Huang X, Long J, Zhang P, Zhang M, Xiao M, Xie T, Huang X. The role of peroxisome proliferator-activated receptor-beta/delta in epidermal growth factor-induced HaCaT cell proliferation. Exp Cell Res. 2008; 314(17): 3142-3151.

Llames SG, Del Rio M, Larcher F, García E, García M, Escamez MJ, Jorcano JL, Holguín P, Meana A. Human plasma as a dermal scaffold for the generation of a completely autologous bioengineered skin. Transplantation. 2004; 77(3): 350-355.

Lorenz VN, Schön MP, Seitz CS. The c-Rel subunit of NF-κB is a crucial regulator of phenotype and motility of HaCaT keratinocytes. Arch Dermatol Res. 2015; 307(6): 523-530.

Luo S, Liu X, Zheng Y, Xu W, Ni H, Li Y, Liu Q. Interleukin-22 upregulates HB-EGF expression in HaCaT cells via JAK2/STAT3 and ERK1/2 signalling. Exp Dermatol. 2015; 24(9): 713-714.

Maas-Szabowski N, Stark HJ, Fusenig NE. Keratinocyte growth regulation in defined organotypic cultures through IL-1-induced keratinocyte growth factor expression in resting fibroblasts. J Invest Dermatol. 2000; 114(6): 1075-1084.

Maas-Szabowski N, Stärker A, Fusenig NE. Epidermal tissue regeneration and stromal interaction in HaCaT cells is initiated by TGF-alpha. J Cell Sci. 2003; 116(Pt 14): 2937-2948.

MacNeil S. Progress and opportunities for tissue-engineered skin. Nature. 2007; 445 (7130): 874-880.

Mahabal S, Konala VB, Mamidi MK, Kanafi MM, Mishra S, Shankar K, Pal R, Bhonde R. Sequential cultivation of human epidermal keratinocytes and dermal mesenchymal like stromal cells *in vitro*. Cytotechnology. 2016; 68(4): 1009-1018.

Marikar Y, Wang Z, Duell EA, Petkovich M, Voorhees JJ, Fisher GJ. Retinoic acid receptors regulate expression of retinoic acid 4-hydroxylase that specifically inactivates all-trans retinoic acid in human keratinocyte HaCaT cells. J Invest Dermatol. 1998; 111(3): 434-439.

Martz E, Steinberg MS. The role of cell-cell contact in "contact" inhibition of cell division: a review and new evidence. J Cell Physiol. 1972; 79(2): 189-210.

Mathes SH, Ruffner H, Graf-Hausner U. The use of skin models in drug development. Adv Drug Deliv Rev. 2014; 69-70: 81-102.

Mempel M, Schmidt T, Weidinger S, Schnopp C, Foster T, Ring J, Abeck D. Role of Staphylococcus aureus surface-associated proteins in the attachment to cultured HaCaT keratinocytes in a new adhesion assay. J Invest Dermatol. 1998; 111(3): 452-456.

Menon SN, Flegg JA, McCue SW, Schugart RC, Dawson RA, McElwain DL. Modelling the interaction of keratinocytes and fibroblasts during normal and abnormal wound healing processes. Proc Biol Sci. 2012; 279(1741): 3329-3338.

Meyle J, Gültig K, Rascher G, Wolburg H. Transepithelial electrical resistance and tight junctions of human gingival keratinocytes. J Periodontal Res. 1999; 34(4): 214-222.

Micallef L, Battu S, Pinon A, Cook-Moreau J, Cardot PJ, Delage C, Simon A. Sedimentation field-flow fractionation separation of proliferative and differentiated subpopulations during Ca^{2+}-induced differentiation in HaCaT cells. J Chromatogr B Analyt Technol Biomed Life Sci. 2010; 878(15-16): 1051-1058.

Micallef L, Belaubre F, Pinon A, Jayat-Vignoles C, Delage C, Charveron M, Simon A. Effects of extracellular calcium on the growth-differentiation switch in immortalized keratinocyte HaCaT cells compared with normal human keratinocytes. Exp Dermatol. 2009; 18(2): 143-151.

Minakami M, Kitagawa N, Iida H, Anan H, Inai T. p38 Mitogen-activated protein kinase and c-Jun NH2-terminal protein kinase regulate the accumulation of a tight junction protein, ZO-1, in cell-cell contacts in HaCaT cells. Tissue Cell. 2015; 47(1): 1-9.

Moch M, Herberich G, Aach T, Leube RE, Windoffer R. Measuring the regulation of keratin filament network dynamics. Proc Natl Acad Sci U S A. 2013; 110(26): 10664-10669.

Morales M, Pérez D, Correa L, Restrepo L. Evaluation of fibrin-based dermal-epidermal organotypic cultures for *in vitro* skin corrosion and irritation testing of chemicals according to OECD TG 431 and 439. Toxicol In Vitro. 2016; 36: 89-96.

Morais MC, Stuhl I, Sabino UA, Lautenschlager WW, Queiroga AS, Tortelli TC, Chammas R, Suhov Y, Ramos AF. Stochastic model of contact inhibition and the proliferation of melanoma *in situ*. PNAS. 2017; 30(20): 1-6.

Nakai K, Yoneda K, Hosokawa Y, Moriue T, Presland RB, Fallon PG, Kabashima K, Kosaka H, Kubota Y. Reduced expression of epidermal growth factor receptor, E-cadherin, and occludin in the skin of flaky tail mice is due to filaggrin and loricrin deficiencies. Am J Pathol. 2012; 181(3): 969-977.

Nakai K, Yoneda K, Moriue T, Igarashi J, Kosaka H, Kubota Y. HB-EGF-induced VEGF production and eNOS activation depend on both PI3 kinase and MAP kinase in HaCaT cells. J Dermatol Sci. 2009; 55(3): 170-178.

Nakai K, Yoneda K, Nakagawa T, Moriue T, Kubota Y. Phosphate buffered saline induces filaggrin expression in a human epidermal keratinocyte cell line (HaCaT cells). J Dermatol Sci. 2016; 84(1): e137

Nam HJ, Park YY, Yoon G, Cho H, Lee JH. Co-treatment with hepatocyte growth factor and TGF-β1 enhances migration of HaCaT cells through NADPH oxidase-dependent ROS generation. Exp Mol Med. 2010; 42(4): 270-279.

Netzlaff F, Lehr CM, Wertz PW, Schaefer UF. The human epidermis models EpiSkin, SkinEthic and EpiDerm: an evaluation of morphology and their suitability for testing phototoxicity, irritancy, corrosivity, and substance transport. Eur J Pharm Biopharm. 2005; 60(2): 167-178.

Niehues H, Schalkwijk J, van Vlijmen-Willems IM, Rodijk-Olthuis D, van Rossum MM, Wladykowski E, Brandner JM, van den Bogaard EH, Zeeuwen PL. Epidermal equivalents of filaggrin null keratinocytes do not show impaired skin barrier function. J Allergy Clin Immunol. 2016. pii: S0091-6749(16): 31116-2.

Nolte CJ, Oleson MA, Bilbo PR, Parenteau NL. Development of a stratum corneum and barrier function in an organotypic skin culture. Arch Dermatol Res. 1993; 285(8): 466-474.

Norlén L, Nicander I, Lundsjö A, Cronholm T, Forslind B. A new HPLC-based method for the quantitative analysis of inner stratum corneum lipids with special reference to the free fatty acid fraction. Arch Dermatol Res. 1998; 290(9): 508-516.

Nukui T, Ehama R, Sakaguchi M, Sonegawa H, Katagiri C, Hibino T, Huh NH. S100A8/A9, a key mediator for positive feedback growth stimulation of normal human keratinocytes. J Cell Biochem. 2008; 104(2): 453-464.

Nyame TT, Chiang HA, Leavitt T, Ozambela M, Orgill DP. Tissue-Engineered Skin Substitutes. Plast Reconstr Surg. 2015; 136(6): 1379-1388.

Nithya S, Radhika T, Jeddy N. Loricrin - an overview. J Oral Maxillofac Pathol. 2015; 19(1): 64-68.

Ockenga W, Kühne S, Bocksberger S, Banning A, Tikkanen R. Epidermal growth factor receptor transactivation is required for mitogen-activated protein kinase activation by muscarinic acetylcholine receptors in HaCaT keratinocytes. Int J Mol Sci. 2014; 15(11): 21433-12454.

Oh Y, Lim HW, Kim K, Lim CJ. Ginsenoside Re improves skin barrier function in HaCaT keratinocytes under normal growth conditions. Biosci Biotechnol Biochem. 2016: 1-3.

Okugawa Y, Hirai Y. Overexpression of extracellular epimorphin leads to impaired epidermal differentiation in HaCaT keratinocytes. J Invest Dermatol. 2008; 128(8): 1884-1893.

Ouchi T, Kubo A, Yokouchi M, Adachi T, Kobayashi T, Kitashima DY, Fujii H, Clausen BE, Koyasu S, Amagai M, Nagao K. Langerhans cell antigen capture through tight junctions confers preemptive immunity in experimental staphylococcal scalded skin syndrome. J Exp Med. 2011; 208(13): 2607-2613.

Page E, Goings GE, Upshaw-Earley J, Hanck DA. Endocytosis and uptake of lucifer yellow by cultured atrial myocytes and isolated intact atria from adult rats. Regulation and subcellular localization. Circ Res. 1994; 75(2): 335-346.

Papp H, Czifra G, Lázár J, Gönczi M, Csernoch L, Kovács L, Bíro T. Protein kinase C isozymes regulate proliferation and high cell density-mediated differentiation in HaCaT keratinocytes. Exp Dermatol. 2003; 12(6): 811-824.

Park HJ, Kim HJ, Lee JY, Cho BK, Gallo RL, Cho DH. Adrenocorticotropin hormone stimulates interleukin-18 expression in human HaCaT keratinocytes. J Invest Dermatol. 2007; 127(5): 1210-1216.

Pastore S, Mascia F, Mariani V, Girolomoni G. The epidermal growth factor receptor system in skin repair and inflammation. J Invest Dermatol. 2008; 128(6): 1365-1374.

Pattwell DM, Lynaugh KJ, Watson RE, Paus R. HaCaT keratinocytes express functional receptors for thyroid-stimulating hormone. J Dermatol Sci. 2010; 59(1): 52-55.

Pendaries V, Malaisse J, Pellerin L, Le Lamer M, Nachat R, Kezic S, Schmitt AM, Paul C, Poumay Y, Serre G, Simon M. Knockdown of filaggrin in a three-dimensional reconstructed human epidermis impairs keratinocyte differentiation. J Invest Dermatol. 2014; 134(12): 2938-2946.

Petrova A, Celli A, Jacquet L, Dafou D, Crumrine D, Hupe M, Arno M, Hobbs C, Cvoro A, Karagiannis P, Devito L, Sun R, Adame LC, Vaughan R, McGrath JA, Mauro TM, Ilic D. 3D *In vitro* model of a functional epidermal permeability barrier from human embryonic stem cells and induced pluripotent stem cells. Stem Cell Reports. 2014; 2(5): 675-689.

Peus D, Hamacher L, Pittelkow MR. EGF-receptor tyrosine kinase inhibition induces keratinocyte growth arrest and terminal differentiation. J Invest Dermatol. 1997; 109(6): 751-756.

Ponec M, Gibbs S, Pilgram G, Boelsma E, Koerten H, Bouwstra J, Mommaas M. Barrier function in reconstructed epidermis and its resemblance to native human skin. Skin Pharmacol Appl Skin Physiol. 2001; 14 Suppl 1: 63-71.

Ponec M, Boelsma E, Weerheim A. Covalently bound lipids in reconstructed human epithelia. Acta Derm Venereol. 2000; 80(2): 89-93.

Ponec M, Boelsma E, Weerheim A, Mulder A, Bouwstra J, Mommaas M. Lipid and ultrastructural characterization of reconstructed skin models. Int J Pharm. 2000; 203(1-2): 211-225.

Ponec M, Weerheim A, Lankhorst P, Wertz P. New acylceramide in native and reconstructed epidermis. J Invest Dermatol. 2003; 120(4): 581-588.

Ponec M, Gibbs S, Weerheim A, Kempenaar J, Mulder A, Mommaas AM. Epidermal growth factor and temperature regulate keratinocyte differentiation. Arch Dermatol Res. 1997; 289(6): 317-326.

Popp T, Steinritz D, Breit A, Deppe J, Egea V, Schmidt A, Gudermann T, Weber C, Ries C. Wnt5a/β-Catenin Signaling Drives Calcium-Induced Differentiation of Human Primary Keratinocytes. J Invest Dermatol. 2014; 134(8): 2183-2191.

Poumay Y, Dupont F, Marcoux S, Leclercq-Smekens M, Hérin M, Coquette A. A simple reconstructed human epidermis: preparation of the culture model and utilization in *in vitro* studies. Arch Dermatol Res. 2004; 296(5): 203-211.

Poumay Y, Coquette A. Modelling the human epidermis *in vitro*: tools for basic and applied research. Arch Dermatol Res. 2007; 298(8): 361-369.

Pruniéras M, Régnier M, Woodley D. Methods for cultivation of keratinocytes with an air-liquid interface. J Invest Dermatol. 1983; 81(1 Suppl): 28s-33s.

Qi XF, Kim DH, Yoon YS, Li JH, Song SB, Jin D, Huang XZ, Teng YC, Lee KJ. The adenylyl cyclase-cAMP system suppresses TARC/CCL17 and MDC/CCL22 production through p38 MAPK and NF-κB in HaCaT keratinocytes. Mol Immunol. 2009; 46(10): 1925-1934.

QIAGEN [sede Web]. Duesseldorf: QIAGEN; 2013 [access 20 March 2017]. EGF Pathway. Available at https://www.qiagen.com/us/shop/genes-and-pathways/pathway-details/?pwid=145

Ranieri D, Avitabile D, Shiota M, Yokomizo A, Naito S, Bizzarri M, Torrisi MR. Nuclear redox imbalance affects circadian oscillation in HaCaT keratinocytes. Int J Biochem Cell Biol. 2015; 65: 113-124.

Räsänen K, Salmenperä P, Baumann M, Virtanen I, Vaheri A. Nemosis of fibroblasts is inhibited by benign HaCaT keratinocytes but promoted by malignant HaCaT cells. Mol Oncol. 2008; 2(4): 340-348.

Räsänen K, Vaheri A. Proliferation and motility of HaCaT keratinocyte derivatives is enhanced by fibroblast nemosis. Exp Cell Res. 2010; 316(10): 1739-1747.

Ratushny V, Gober MD, Hick R, Ridky TW, Seykora JT. From keratinocyte to cancer: the pathogenesis and modeling of cutaneous squamous cell carcinoma. J Clin Invest. 2012; 122(2): 464-472.

Ravid A, Shenker O, Buchner-Maman E, Rotem C, Koren R. Vitamin D Induces Cyclooxygenase 2 Dependent Prostaglandin E2 Synthesis in HaCaT Keratinocytes. J Cell Physiol. 2016; 231(4): 837-843.

Rekus MT. Characterization of growth and differentiation of a spontaneously immortalized keratinocyte cell line (HaCaT) in a defined, serum-free culture system [Dissertation]. Düsseldorf: Heinrich-Heine-Universität Düsseldorf; 2000.

Reinartz J, Link J, Todd RF, Kramer MD. The receptor for urokinase-type plasminogen activator of a human keratinocyte line (HaCaT). Exp Cell Res. 1994; 214(2): 486-498.

Rheinwald JG, Green H. Serial cultivation of strains of human epidermal keratinocytes: the formation of keratinizing colonies from single cells. Cell. 1975; 6(3): 331-343.

Rizzo WB. The role of fatty aldehyde dehydrogenase in epidermal structure and function. Dermatoendocrinol. 2011; 3(2): 91-99.

Ronfard V, Rives JM, Neveux Y, Carsin H, Barrandon Y. Long-term regeneration of human epidermis on third degree burns transplanted with autologouscultured epithelium grown on a fibrin matrix. Transplantation. 2000; 70(11): 1588-1598.

Rössler OG, Thiel G. Brain-derived neurotrophic factor-, epidermal growth factor-, or A-Raf-induced growth of HaCaT keratinocytes requires extracellular signal-regulated kinase. Am J Physiol Cell Physiol. 2004; 286(5): C1118-C1129.

Ruhland A, de Villiers EM. Opposite regulation of the HPV 20-URR and HPV 27-URR promoters by ultraviolet irradiation and cytokines. Int J Cancer. 2001; 91(6): 828-834.

Ryle CM, Breitkreutz D, Stark HJ, Leigh IM, Steinert PM, Roop D, Fusenig NE. Density-dependent modulation of synthesis of keratins 1 and 10 in the human keratinocyte line HaCaT and in ras-transfected tumorigenic clones. Differentiation. 1989; 40(1): 42-54.

Safferling K, Sütterlin T, Westphal K, Ernst C, Breuhahn K, James M, Jäger D, Halama N, Grabe N. Wound healing revised: a novel reepithelialization mechanism revealed by *in vitro* and in silico models. J Cell Biol. 2013; 203(4): 691-709.

Sakaguchi M, Miyazaki M, Takaishi M, Sakaguchi Y, Makino E, Kataoka N, Yamada H, Namba M, Huh NH. S100C/A11 is a key mediator of Ca^{2+}-induced growth inhibition of human epidermal keratinocytes. J Cell Biol. 2003; 163(4): 825-835.

Scharffetter-Kochanek K, Klein CE, Heinen G, Mauch C, Schaefer T, Adelmann-Grill BC, Goerz G, Fusenig NE, Krieg TM, Plewig G. Migration of a human keratinocyte cell line (HaCaT) to interstitial collagen type I is mediated by the alpha 2 beta 1-integrin receptor. J Invest Dermatol. 1992; 98(1): 3-11.

Schelfhout VR, Coene ED, Delaey B, Waeytens AA, De Rycke L, Deleu M, De Potter CR. The role of heregulin-alpha as a motility factor and amphiregulin as a growth factor in wound healing. J Pathol. 2002; 198(4): 523-533.

Schoop VM, Mirancea N, Fusenig NE. Epidermal organization and differentiation of HaCaT keratinocytes in organotypic coculture with human dermal fibroblasts. J Invest Dermatol. 1999; 112(3): 343-353.

Scholzen T, Gerdes J. The Ki-67 protein: from the known and the unknown. J Cell Physiol. 2000; 182(3): 311-322.

Schmuth M, Fluhr JW, Crumrine DC, Uchida Y, Hachem JP, Behne M, Moskowitz DG, Christiano AM, Feingold KR, Elias PM. Structural and functional consequences of loricrin mutations in human loricrin keratoderma (Vohwinkel syndrome with ichthyosis). J Invest Dermatol. 2004; 122(4): 909-922.

Schneider EL, Shorr SS. Alteration in cellular RNAs during the *in vitro* lifespan of cultured human diploid fibroblasts. Cell. 1975; 6(2): 179-184.

Schürer N, Köhne A, Schliep V, Barlag K, Goerz G. Lipid composition and synthesis of HaCaT cells, an immortalized human keratinocyte line, in comparison with normal human adult keratinocytes. Exp Dermatol. 1993; 2(4): 179-185.

Seitz CS, Deng H, Hinata K, Lin Q, Khavari PA. Nuclear factor kappaB subunits induce epithelial cell growth arrest. Cancer Res. 2000; 60(15): 4085-4092.

Senthilkumar PK, Robertson LW, Ludewig G. PCB153 reduces telomerase activity and telomere length in immortalized human skin keratinocytes (HaCaT) but not in human foreskin keratinocytes (NFK). Toxicol Appl Pharmacol. 2012; 259(1): 115-123.

Seo MD, Kang TJ, Lee CH, Lee AY, Noh M. HaCaT Keratinocytes and Primary Epidermal Keratinocytes Have Different Transcriptional Profiles of Cornified Envelope-Associated Genes to T Helper Cell Cytokines. Biomol Ther (Seoul). 2012; 20(2): 171-176.

Shephard P, Martin G, Smola-Hess S, Brunner G, Krieg T, Smola H. Myofibroblast Differentiation Is Induced in Keratinocyte-Fibroblast Co-Cultures and Is Antagonistically Regulated by Endogenous Transforming Growth Factor-β and Interleukin-1. Am J Pathol. 2004; 164(6): 2055-2066.

Shi B, Isseroff RR. Intracellular calcium oscillations in cell populations of ras-transfected I-7 subline of human HaCaT keratinocytes. J Invest Dermatol. 1997; 109(6): 765-769.

Smola H, Thiekötter G, Fusenig NE. Mutual induction of growth factor gene expression by epidermal-dermal cell interaction. J Cell Biol. 1993; 122(2): 417-429.

Son SW, Min BW, Lim Y, Lee YH, Shin SY. Regulatory mechanism of TNFα autoregulation in HaCaT cells: the role of the transcription factor EGR-1. Biochem Biophys Res Commun. 2008; 374(4): 777-782.

Speidel D. The role of DNA damage responses in p53 biology. Arch Toxicol. 2015; 89(4): 501-517.

Spörl F, Schellenberg K, Blatt T, Wenck H, Wittern KP, Schrader A, Kramer A. A circadian clock in HaCaT keratinocytes. J Invest Dermatol. 2011; 131(2): 338-348.

Springer M, Engelhart K, Biesalski HK. Effects of 3-isobutyl-1-methylxanthine and kojic acid on cocultures and skin equivalents composed of HaCaT cells and human melanocytes. Arch Dermatol Res. 2003; 295(2): 88-91.

Sriram G, Bigliardi PL, Bigliardi-Qi M. Fibroblast heterogeneity and its implications for engineering organotypic skin models *in vitro*. Eur J Cell Biol. 2015; 94(11): 483-512.

Stark HJ, Baur M, Breitkreutz D, Mirancea N, Fusenig NE. Organotypic keratinocyte cocultures in defined medium with regular epidermal morphogenesis and differentiation. J Invest Dermatol. 1999; 112(5): 681-691.

Stark HJ, Szabowski A, Fusenig NE, Maas-Szabowski N. Organotypic cocultures as skin equivalents: A complex and sophisticated in vitro system. Biol Proced Online. 2004; 6: 55-60.

Stark HJ, Willhauck MJ, Mirancea N, Boehnke K, Nord I, Breitkreutz D, Pavesio A, Boukamp P, Fusenig NE. Authentic fibroblast matrix in dermal equivalents normalises epidermal histogenesis and dermoepidermal junction in organotypic co-culture. Eur J Cell Biol. 2004; 83(11-12): 631-645.

Steinsträsser I. The organized HaCaT cell culture sheet: A model approach to study epidermal peptide drug metabolism [Dissertation]. Aachen: Swiss Federal Institute of Technology Zurich (Shaker Verlag); 1994.

Stoll SW, Zhao X, Elder JT. EGF stimulates transcription of CaN19 (S100A2) in HaCaT keratinocytes. J Invest Dermatol. 1998; 111(6): 1092-1097.

Tacheau C, Laboureau J, Mauviel A, Verrecchia F. TNF-alpha represses connexin 43 expression in HaCat keratinocytes via activation of JNK signaling. J Cell Physiol. 2008; 216(2): 438-444.

Taguchi S, Kawachi Y, Ishitsuka Y, Fujisawa Y, Furuta J, Nakamimura Y, Xu X, Ikebe D, Kato M, Otsuka F. Overexpression of the transcription factor Yin-Yang-1 suppresses differentiation of HaCaT cells in three-dimensional cell culture. J Invest Dermatol. 2011; 131(1): 37-45.

Takada H, Furuya K, Sokabe M. Mechanosensitive ATP release from hemichannels and Ca^{2+} influx through TRPC6 accelerate wound closure in keratinocytes. J Cell Sci. 2014; 127(Pt 19): 4159-4171.

Takao J, Yudate T, Das A, Shikano S, Bonkobara M, Ariizumi K, Cruz PD. Expression of NF-kappaB in epidermis and the relationship between NF-kappaB activation and inhibition of keratinocyte growth. Br J Dermatol. 2003; 148(4): 680-688.

Tao K, Bai XZ, Zhang ZF, Shi JH, Hu XL, Tang CW, Hu DH, Han JT. Construction of the tissue engineering seed cell (HaCaT-EGF) and analysis of its biological characteristics. Asian Pac J Trop Med. 2013; 6(11): 893-896.

Tochio T, Tanaka H, Nakata S, Hosoya H. Fructose-1,6-bisphosphate aldolase A is involved in HaCaT cell migration by inducing lamellipodia formation. J Dermatol Sci. 2010; 58(2): 123-129.

Tokuyama E, Nagai Y, Takahashi K, Kimata Y, Naruse K. Mechanical Stretch on Human Skin Equivalents Increases the Epidermal Thickness and Develops the Basement Membrane. PLoS One. 2015; 10(11): e0141989.

Trost A, Desch P, Wally V, Haim M, Maier RH, Reitsamer HA, Hintner H, Bauer JW, Onder K. Aberrant heterodimerization of keratin 16 with keratin 6A in HaCaT keratinocytes results in diminished cellular migration. Mech Ageing Dev. 2010; 131(5): 346-353.

Uchiyama M, Oguri M, Mojumdar EH, Gooris GS, Bouwstra JA. Free fatty acids chain length distribution affects the permeability of skin lipid model membranes. Biochim Biophys Acta. 2016; 1858(9): 2050-2059.

van der Veen JW, Hodemaekers H, Reus AA, Maas WJ, van Loveren H, Ezendam J. Human relevance of an in vitro gene signature in HaCaT for skin sensitization. Toxicol In Vitro. 2015; 29(1): 81-84.

van Smeden J, Janssens M, Gooris GS, Bouwstra JA. The important role of stratum corneum lipids for the cutaneous barrier function. Biochim Biophys Acta. 2014a; 1841(3): 295-313.

van Smeden J, Janssens M, Kaye EC, Caspers PJ, Lavrijsen AP, Vreeken RJ, Bouwstra JA. The importance of free fatty acid chain length for the skin barrier function in atopic eczema patients. Exp Dermatol. 2014b; 23(1): 45-52.

Vangipuram M, Ting D, Kim S, Diaz R, Schüle B. Skin punch biopsy explant culture for derivation of primary human fibroblasts. J Vis Exp. 2013; (77): e3779.

Voss A, Bode G, Sopalla C, Benedyk M, Varga G, Böhm M, Nacken W, Kerkhoff C. Expression of S100A8/A9 in HaCaT keratinocytes alters the rate of cell proliferation and differentiation. FEBS Lett. 2011; 585(2): 440-446.

Walker D, Sun T, MacNeil S, Smallwood R. Modeling the effect of exogenous calcium on keratinocyte and HaCaT cell proliferation and differentiation using an agent-based computational paradigm. Tissue Eng. 2006; 12(8): 2301-2309.

Wang H, Van Blitterswijk CA, Bertrand-De Haas M, Schuurman AH, Lamme EN. Improved enzymatic isolation of fibroblasts for the creation of autologous skin substitutes. In Vitro Cell Dev Biol Anim. 2004; 40(8-9): 268-277.

Weerheim A, Ponec M. Determination of stratum corneum lipid profile by tape stripping in combination with high-performance thin-layer chromatography. Arch Dermatol Res. 2001; 293(4): 191-199.

Werner S, Krieg T, Smola H. Keratinocyte-fibroblast interactions in wound healing. J Invest Dermatol. 2007; 127(5): 998-1008.

Wilson VG. Growth and differentiation of HaCaT keratinocytes. Methods Mol Biol. 2014; 1195: 33-41.

Wille JJ Jr, Pittelkow MR, Shipley GD, Scott RE. Integrated control of growth and differentiation of normal human prokeratinocytes cultured in serum-free medium: clonal analyses, growth kinetics, and cell cycle studies. J Cell Physiol. 1984; 121(1): 31-44.

Wojtowicz AM, Oliveira S, Carlson MW, Zawadzka A, Rousseau CF, Baksh D. The importance of both fibroblasts and keratinocytes in a bilayered living cellular construct used in wound healing. Wound Repair Regen. 2014; 22(2): 246-255.

Wraight CJ, Werther GA. Insulin-like growth factor-I and epidermal growth factor regulate insulin-like growth factor binding protein-3 (IGFBP-3) in the human keratinocyte cell line HaCaT. J Invest Dermatol. 1995; 105(4): 602-607.

Xu X, Kawachi Y, Nakamura Y, Sakurai H, Hirota A, Banno T, Takahashi T, Roop DR, Otsuka F. Yin-yang 1 negatively regulates the differentiation-specific transcription of mouse loricrin gene in undifferentiated keratinocytes. J Invest Dermatol. 2004; 123(6): 1120-1126.

Yamaguchi Y, Itami S, Tarutani M, Hosokawa K, Miura H, Yoshikawa K. Regulation of keratin 9 in nonpalmoplantar keratinocytes by palmoplantar fibroblasts through epithelial-mesenchymal interactions. J Invest Dermatol. 1999; 112(4): 483-488.

Yano C, Saeki H, Komine M, Kagami S, Tsunemi Y, Ohtsuki M, Nakagawa H. Mechanism of Macrophage-Derived Chemokine/CCL22 Production by HaCaT Keratinocytes. Ann Dermatol. 2015; 27(2): 152-156.

Yokoyama A, Makishima M, Choi M, Cho Y, Nishida S, Hashimoto Y, Terui T. Induction of SREBP-1c mRNA by differentiation and LXR ligand in human keratinocytes. J Invest Dermatol. 2009; 129(6): 1395-1401.

Yoneda K, Nakagawa T, Lawrence OT, Huard J, Demitsu T, Kubota Y, Presland RB. Interaction of the profilaggrin N-terminal domain with loricrin in human cultured keratinocytes and epidermis. J Invest Dermatol. 2012; 132(4): 1206-1214.

Yoshida H, Kobayashi D, Ohkubo S, Nakahata N. ATP stimulates interleukin-6 production via P2Y receptors in human HaCaT keratinocytes. Eur J Pharmacol. 2006; 540(1-3): 1-9.

Zbytek B, Pfeffer LM, Slominski AT. Corticotropin-releasing hormone inhibits nuclear factor-kappaB pathway in human HaCaT keratinocytes. J Invest Dermatol. 2003; 121(6): 1496-1499.

Zhang JY, Tao S, Kimmel R, Khavari PA. CDK4 regulation by TNFR1 and JNK is required for NF-kappaB-mediated epidermal growth control. J Cell Biol. 2005; 168(4): 561-566.

Zhang Y, Bai X, Wang Y, Li N, Li X, Han F, Su L, Hu D. Role for heat shock protein 90α in the proliferation and migration of HaCaT cells and in the deep second-degree burn wound healing in mice. PLoS One. 2014; 9(8): e103723.

Zhong SP, Zhang YZ, Lim CT. Tissue scaffolds for skin wound healing and dermal reconstruction. Wiley Interdiscip Rev Nanomed Nanobiotechnol. 2010; 2(5): 510-525.

Ziegler A, Jonason AS, Leffell DJ, Simon JA, Sharma HW, Kimmelman J, Remington L, Jacks T, Brash DE. Sunburn and p53 in the onset of skin cancer. Nature. 1994; 372(6508): 773-776.

Ziegler A, Leffell DJ, Kunala S, Sharma HW, Gailani M, Simon JA, Halperin AJ, Baden HP, Shapiro PE, Bale AE, Brash DE. Mutation hotspots due to sunlight in the p53 gene of nonmelanoma skin cancers. Proc Natl Acad Sci U S A. 1993; 90(9): 4216-4220.

Zinn M, Aumailley M, Krieg T, Smola H. Expression of laminin 5 by parental and c-Ha-ras-transformed HaCaT keratinocytes in organotypic cultures. Eur J Cell Biol. 2006; 85(5): 333-343.

SUPPLEMENTAL MATERIAL

1. Statistical Supplemental Material

This supplement shows the statistical way followed through the study. All analyses were made using Excel v.10 and SPSS v.20. Three PDT/CPA assays were carried out. In general, five wells were tested to each day and proved condition (n=5). In spite of the cultured cell growth has been describes as a normal phenomenon (Kubitschek; 1962), the normality test was accomplished. We obtain the same conclusion by the use of both the Kolmogorov-Smirnov Test (K-S) with Lilliefors significance correction and the Shapiro-Wilk (S-W) test.

1.1. Population Doubling Time (PDT) Assay

As first step, a dilution assay was done to generate a linear equation relating the cell number and its associated metabolic activity as function of optical density (OD) produced by formazan in a MTT assay (see Materials and Methods). This procedure was carried out for each of the three assays in the same way that is shows below for the first assay (passage 36). Each cell number had 5 replicates (n=5), thus the reported OD is the average of each one of the readings.

OD	CELL NUMBER
2,435	150000
1,983	75000
1,185	37500
0,567	18750
0,272	9375
0,131	4688
0,053	2344
0,041	1172
0,006	586

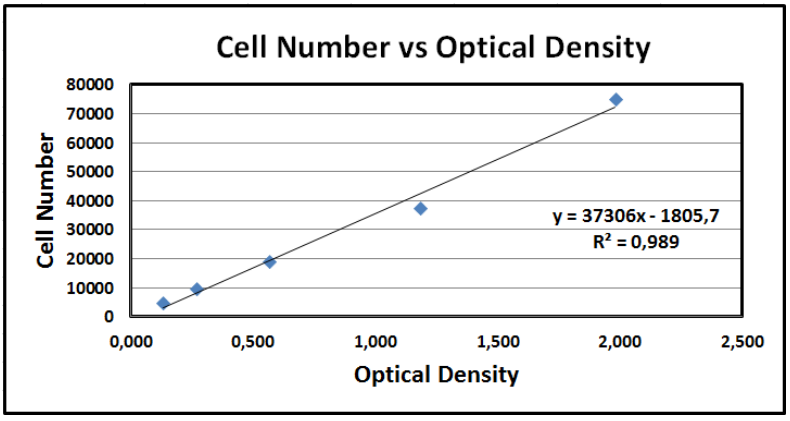

At the end of each evaluated day in the PDTs assays, the cell number (*y* in the equation) was calculated by replace the *x* at the generated equation with the optical density average of wells (n=5). In order to determine the best points to calculate the PDT, the R^2 was determined to linear function of eight first points of each graphic. Cell number showed a good correlation with time in days (all R^2 > 0.85). Days 2 and 4 were selected to calculate PDTs. We used the reported formula by ATCC guidelines: $DT = T \times (ln2/ln(X_e/X_b))$; where *T* is the incubation time in any units (here is 48 h), X_b is the cell number at the beginning of the incubation time, X_e is the cell number at the end of the incubation time.

HaCaT Population Doubling Time(PDT) assay results. SD, Standard Deviation.

	Assay 1 (Passage 36)		Assay 2 (Passage 37)		Assay 3 (Passage38)	
Day	Cell Number	SD	Cell Number	SD	Cell Number	SD
1	30	2	74	18	2129	182
2	2790	163	1298	97	3750	183
3	7252	431	2731	169	5104	257
4	20265	1018	9729	789	25230	2214

5	31926	2930	26980	1307	29198	825
6	37575	767	27763	1939	28387	1326
7	45595	844	39298	2649	28926	1020
8	67046	2035	47192	3375	46041	3159
9	62487	3828	47849	2627	45134	1368
10	48110	1673	44983	2442	27068	1432
PDT	$48h\frac{ln2}{ln\left(\frac{20265}{2790}\right)} \approx 16.78\ h$		$48h\frac{ln2}{ln\left(\frac{9729}{1298}\right)} = 16.52\ h$		$48h\frac{ln2}{ln\left(\frac{25230}{3750}\right)} = 17.45h$	

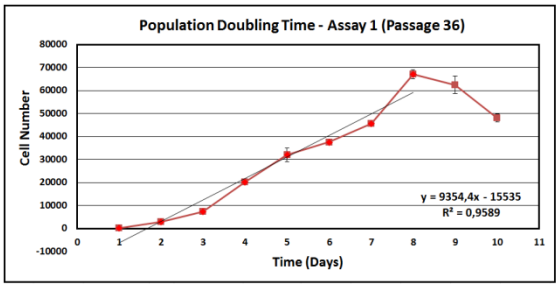

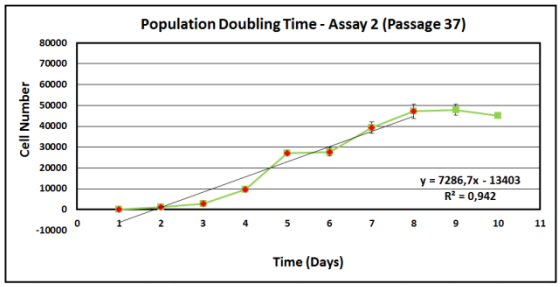

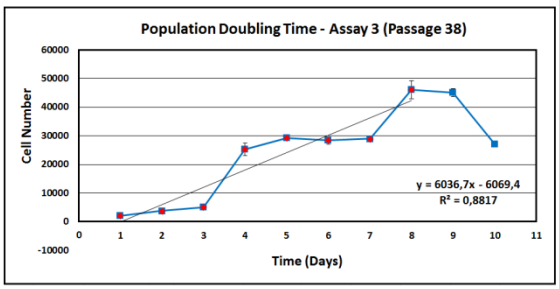

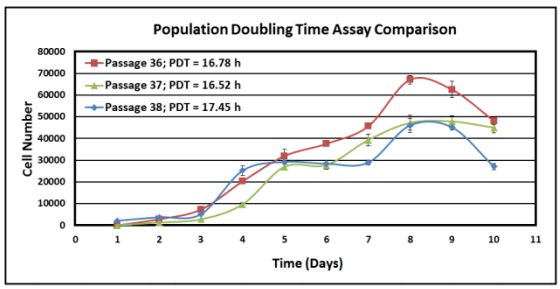

To investigate if there were differences between assays, all conservative statistics tests were applied. First, the Gaussian behavior was determined.

Tests of Normality

		Kolmogorov-Smirnov[a]			Shapiro-Wilk		
		Statistic	df	Sig.	Statistic	df	Sig.
Day 1	Assay 1	0,337	5	0,065	0,800	5	0,081
	Assay 2	0,244	5	0,200*	0,895	5	0,382
	Assay 3	0,356	5	0,038	0,755	5	0,033
Day 2	Assay 1	0,377	5	0,019	0,748	5	0,028
	Assay 2	0,214	5	0,200*	0,915	5	0,497
	Assay 3	0,291	5	0,194	0,893	5	0,372
Day 3	Assay 1	0,310	5	0,130	0,820	5	0,117
	Assay 2	0,132	5	0,200*	0,997	5	0,997
	Assay 3	0,196	5	0,200*	0,921	5	0,538
Day 4	Assay 1	0,222	5	0,200*	0,961	5	0,812
	Assay 2	0,198	5	0,200*	0,932	5	0,608
	Assay 3	0,395	5	0,011	0,677	5	0,005
Day 5	Assay 1	0,193	5	0,200*	0,921	5	0,538
	Assay 2	0,230	5	0,200*	0,947	5	0,716

	Assay 3	0,154	5	0,200*	0,971	5	0,881
Day 6	Assay 1	0,285	5	0,200*	0,932	5	0,607
	Assay 2	0,225	5	0,200*	0,938	5	0,649
	Assay 3	0,218	5	0,200*	0,910	5	0,465
Day 7	Assay 1	0,171	5	0,200*	0,957	5	0,785
	Assay 2	0,412	5	0,006	0,674	5	0,005
	Assay 3	0,350	5	0,045	0,847	5	0,185
Day 8	Assay 1	0,220	5	0,200*	0,898	5	0,397
	Assay 2	0,222	5	0,200*	0,958	5	0,792
	Assay 3	0,200	5	0,200*	0,944	5	0,698
Day 9	Assay 1	0,325	5	0,091	0,692	5	0,008
	Assay 2	0,353	5	0,041	0,783	5	0,058
	Assay 3	0,186	5	0,200*	0,978	5	0,924
Day 10	Assay 1	0,256	5	0,200*	0,894	5	0,376
	Assay 2	0,383	5	0,016	0,721	5	0,016
	Assay 3	0,262	5	0,200*	0,870	5	0,265

*. This is a lower bound of the true significance.

a. Lilliefors Significance Correction.

df, degrees freedom; Sig., significance.

Each day of each assay was considered as an independent assay. As is showed, the p value (i.e. Sig.) is greater than defined error (i.e. α=0,01) in the most of cases to both K-S and S-W test. So, null hypothesis (H_0) is accepted. It is recalled that these statistics define as null hypothesis that the probability distributions of the tested samples are Gaussian or Normal. To check the homoscedasticity of each group of data, a test of homogeneity of variance was accomplished through calculating the Levene´s statistic (LS).

Test of Homogeneity of Variances

	Levene Statistic	df1	df2	Sig.
Day 1	3,610	2	12	0,059
Day 2	0,010	2	12	0,990
Day 3	4,308	2	12	0,039
Day 4	1,337	2	12	0,299
Day 5	2,409	2	12	0,132
Day 6	1,991	2	12	0,179
Day 7	2,320	2	12	0,141
Day 8	0,474	2	12	0,633
Day 9	1,569	2	12	0,248
Day 10	0,544	2	12	0,594

df, degrees freedom; Sig., significance.

LS significance suggests that variances of all tested days in each one of assays are equals (i.e. p value or Sig. > assumed error, α=0.05). Thus, a parametric analysis is ideal to compare its means in order to looking for statistically significant differences. A one factor ANOVA (α=0,01) was done.

ANOVA

		Sum of Squares	df	Mean Square	F	Sig.
Day 1	Between Groups	52214469,421	2	26107234,711	64,045	0,000
	Within Groups	4891634,455	12	407636,205		
	Total	57106103,876	14			
Day 2	Between Groups	60434143,146	2	30217071,573	529,873	0,000
	Within Groups	684324,086	12	57027,007		
	Total	61118467,232	14			
Day 3	Between Groups	70437041,377	2	35218520,688	234,141	0,000
	Within Groups	1804988,274	12	150415,689		
	Total	72242029,650	14			
Day 4	Between Groups	805386731,386	2	402693365,693	166,814	0,000
	Within Groups	28968272,388	12	2414022,699		
	Total	834355003,774	14			
Day 5	Between Groups	75824642,259	2	37912321,129	9,294	0,004
	Within Groups	48950151,313	12	4079179,276		
	Total	124774793,571	14			
Day 6	Between Groups	253081012,196	2	126540506,098	56,301	0,000
	Within Groups	26970853,198	12	2247571,100		
	Total	280051865,394	14			
Day 7	Between Groups	514981647,900	2	257490823,950	81,052	0,000
	Within Groups	38122444,759	12	3176870,397		
	Total	553104092,659	14			
Day 8	Between Groups	1239352149,732	2	619676074,866	69,140	0,000
	Within Groups	107550791,436	12	8962565,953		
	Total	1346902941,168	14			
Day 9	Between Groups	732468575,078	2	366234287,539	44,186	0,000
	Within Groups	99461219,542	12	8288434,962		
	Total	831929794,620	14			
Day 10	Between Groups	1002237230,806	2	501118615,403	129,546	0,000
	Within Groups	46419295,446	12	3868274,621		
	Total	1048656526,253	14			

df, degrees freedom; F, Fisher statistic; Sig., significance.

The ANOVA test shows that no exists statistically significant differences between made PDTs assays. It is conclude based in the fact that p value (i.e. Sig.) is minor than assumed error (i.e. α=0.05). So, the three calculated values were taken. A 95% confidence interval to final mean PDT was carried out using T-student formula.

$$\bar{x} \pm t_{(1-\alpha/2)} \frac{S}{\sqrt{n}}$$

$$\left(\frac{16.78 + 16.52 + 17.45}{3}\right) \pm \left(4.3027 \times \frac{0.3333}{\sqrt{2}}\right)$$

$$16.92\ h \pm 2.03\ h$$

Where $t_{(1-0.05/2)} = 4{,}3027, n\ (freedom\ degrees) = 3 - 1$. In this study is possible to assume that the PDT for HaCaT at the passages 30-40, under tested conditions (see Material and Methods), is 16.92±2,03 h.

1.2. Cell Proliferation Assay (CPA)

To investigate which of used media (see material and methods) induce the maximum cell proliferation on HaCaT cell line, CPA was accomplished in three independents assay (passage 36-38) with five replicates by proven condition. The incubations periods were fixed based in calculated PDT to HaCaT. Obtained result of the first assay is showed below.

	48 HOURS		72 HOURS	
Medium	**CELL NUMBER**	**SD**	**CELL NUMBER**	**SD**
QN	22365	1562	33518	2013
QC	25637	907	42590	1745
EM	15321	1604	26314	859
MM	19854	2000	36298	991
CM	17023	502	30014	2058

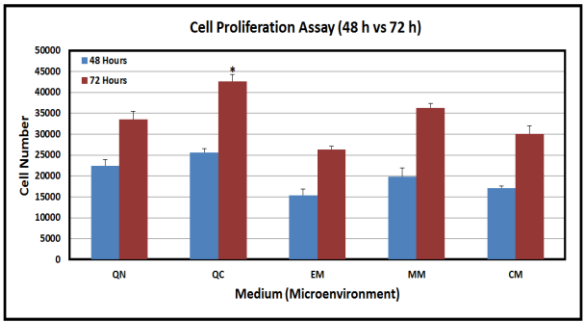

Reported data are the different average of replicates (n=5) done by condition. As in PDT assay, the normality test was carried out through both way the Kolmogorov-Smirnov Test (K-S) with Lilliefors significance correction and the Shapiro-Wilk (S-W). A third approach, the normal Q-Q plot, was made.

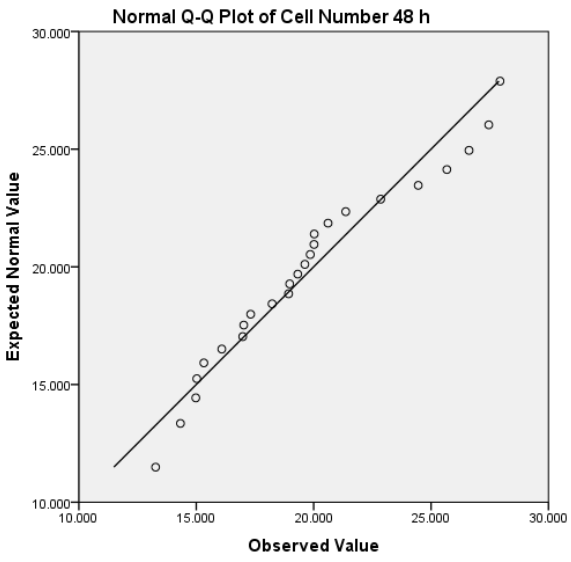

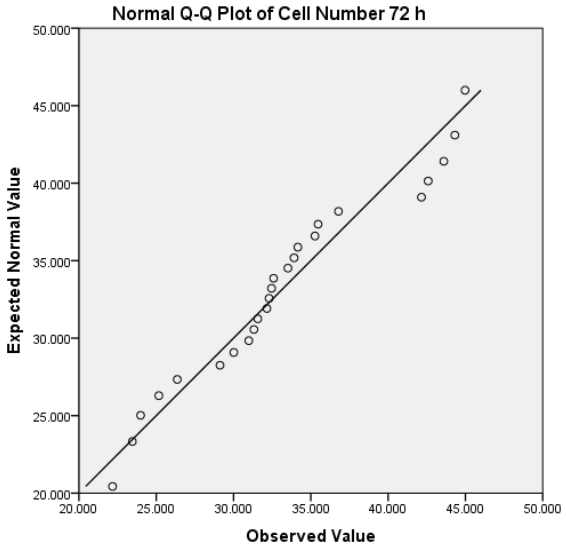

Tests of Normality

	Kolmogorov-Smirnov[a]			Shapiro-Wilk		
	Statistic	df	Sig.	Statistic	df	Sig.
Cell Number 48 h	0,148	25	0,162	0,942	25	0,164
Cell Number 72 h	0,125	25	0,200*	0,943	25	0,172

*. This is a lower bound of the true significance.
a. Lilliefors Significance Correction.
df, degrees freedom; Sig., significance.

As is showed, the p value (i.e. Sig.) is greater than defined error (i.e. α=0,01) to both K-S and S-W tests, so null hypothesis (H_0) is accepted. It is recalled that these statistics define as null hypothesis that the probability distributions of the tested samples are Gaussian. Graphical analysis suggests a similar behavior of observed values respect expected, so is conclude that the cell number have a normal distribution. To check the homoscedasticity of each group of data a test of homogeneity of variance was accomplished by calculating the Levene statistic (LS).

Test of Homogeneity of Variances

	Levene Statistic	df1	df2	Sig.
Cell Number 48 h	2,035	4	20	0,128
Cell Number 72 h	0,412	4	20	0,798

LS significance suggests that variances of all treatments at two evaluated times are equals (i.e. p value or Sig. > assumed error, α=0.05), so a parametric analysis is ideal to compare it. Despite mentioned above, a one factor ANOVA (α=0,01) was done as well as the non-parametric One-way ANOVA on ranks test (i.e. Kruskal–Wallis (K-W) test) to compare the effect of each proven treatments.

ANOVA		Sum of Squares	df	Mean Square	F	Sig.
Cell Number 48 h	Between Groups	393950073,200	4	98487518,300	97,962	0,000
	Within Groups	20107292,800	20	1005364,640		
	Total	414057366,000	24			
Cell Number 72 h	Between Groups	977150846,960	4	244287711,740	125,882	0,000
	Within Groups	38812070,400	20	1940603,520		
	Total	1015962917,360	24			

Kruskal-Wallis Test - Hypothesis Test Summary

	Null Hypothesis	Test	Sig.	Decision
1	The distribution of Cell Number 48 h is the same across categories of Culture Media.	Independent-Samples Kruskal-Wallis Test	0,000	Reject the null hypothesis.
2	The distribution of Cell Number 72 h is the same across categories of Culture Media.	Independent-Samples Kruskal-Wallis Test	0,000	Reject the null hypothesis.

Asymptotic significances are displayed. The significance level is 0,01.

Note that both one factor ANOVA and K-W test leads to conclude that exist at least one treatment that is different respect the other. To explore the differences between treatments and keeping in mind that Levene test was not significant, the parametric Bonferroni Post Hoc test was applied.

Multiple Comparisons by Bonferroni Test. Dependent Variable: Cell Number 48 h.

(I) Culture Media	(J) Culture Media	Mean Difference (I-J)	Std. Error	Sig.	95% Confidence Interval	
					Lower Bound	Upper Bound
QN	QC	-5592,400*	652,129	0,000	-7648,82	-3535,98
	EM	6251,400*	652,129	0,000	4194,98	8307,82
	CM	1354,600	652,129	0,509	-701,82	3411,02
	MM	3708,400*	652,129	0,000	1651,98	5764,82
QC	QN	5592,400*	652,129	0,000	3535,98	7648,82
	EM	11843,800*	652,129	0,000	9787,38	13900,22
	CM	6947,000*	652,129	0,000	4890,58	9003,42
	MM	9300,800*	652,129	0,000	7244,38	11357,22
EM	QN	-6251,400*	652,129	0,000	-8307,82	-4194,98
	QC	-11843,800*	652,129	0,000	-13900,22	-9787,38
	CM	-4896,800*	652,129	0,000	-6953,22	-2840,38
	MM	-2543,000*	652,129	0,009	-4599,42	-486,58
CM	QN	-1354,600	652,129	0,509	-3411,02	701,82
	QC	-6947,000*	652,129	0,000	-9003,42	-4890,58
	EM	4896,800*	652,129	0,000	2840,38	6953,22
	MM	2353,800*	652,129	0,017	297,38	4410,22
MM	QN	-3708,400*	652,129	0,000	-5764,82	-1651,98
	QC	-9300,800*	652,129	0,000	-11357,22	-7244,38
	EM	2543,000*	652,129	0,009	486,58	4599,42
	CM	-2353,800*	652,129	0,017	-4410,22	-297,38

*. The mean difference is significant at the 0.05 level.

Multiple Comparisons by Bonferroni Test. Dependent Variable: Cell Number 72 h.

(I) Culture Media	(J) Culture Media	Mean Difference (I-J)	Std. Error	Sig.	95% Confidence Interval	
					Lower Bound	Upper Bound
QN	QC	-10800,000*	881,046	0,000	-13578,29	-8021,71
	EM	8498,200*	881,046	0,000	5719,91	11276,49
	CM	-2041,000	881,046	0,313	-4819,29	737,29
	MM	1897,600	881,046	0,436	-880,69	4675,89
QC	QN	10800,000*	881,046	0,000	8021,71	13578,29
	EM	19298,200*	881,046	0,000	16519,91	22076,49
	CM	8759,000*	881,046	0,000	5980,71	11537,29
	MM	12697,600*	881,046	0,000	9919,31	15475,89
EM	QN	-8498,200*	881,046	0,000	-11276,49	-5719,91
	QC	-19298,200*	881,046	0,000	-22076,49	-16519,91
	CM	-10539,200*	881,046	0,000	-13317,49	-7760,91
	MM	-6600,600*	881,046	0,000	-9378,89	-3822,31
CM	QN	2041,000	881,046	0,313	-737,29	4819,29
	QC	-8759,000*	881,046	0,000	-11537,29	-5980,71
	EM	10539,200*	881,046	0,000	7760,91	13317,49
	MM	3938,600*	881,046	0,002	1160,31	6716,89
MM	QN	-1897,600	881,046	0,436	-4675,89	880,69
	QC	-12697,600*	881,046	0,000	-15475,89	-9919,31
	EM	6600,600*	881,046	0,000	3822,31	9378,89
	CM	-3938,600*	881,046	0,002	-6716,89	-1160,31

*. The mean difference is significant at the 0.05 level.

Bonferroni test suggest that, with a confidence of 99,99%, the unique treatments which behavior is not significantly different compared with each other are QN, CM, and MM (i.e. p value > α). Then, is

possible to conclude that three mentioned media induce more potent mitogenic effect on HaCaT cells (at passage 30-40) that EM but lesser than QC. These results are in accordance with FBS and EGF concentration, inasmuch as QC is the medium with the highest concentration of them. Moreover, the other parametric tests as Tukey and Student-Newman-Keuls (S-N-K) as well as the non-parametric Tamhane test, thrown the same conclusions. Finally, using the graphical boxplot to observe the dispersion of data and differences,

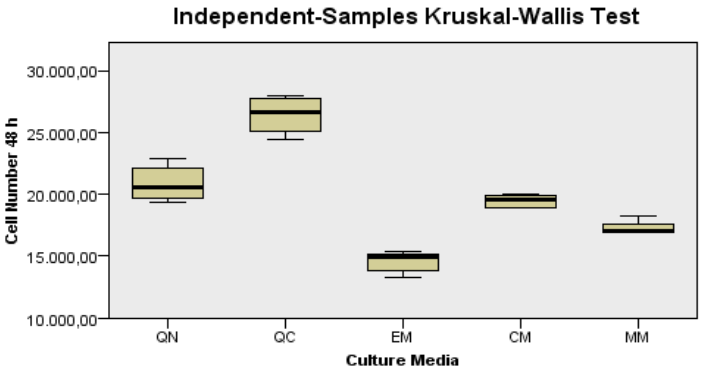

Total N	25
Test Statistic	22,590
Degrees of Freedom	4
Asymptotic Sig. (2-sided test)	,000

1. The test statistic is adjusted for ties.

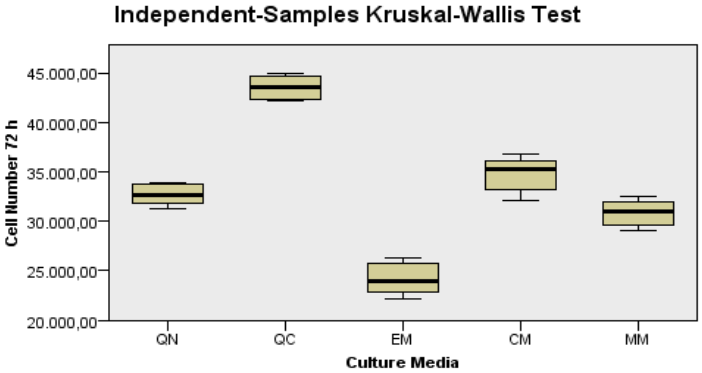

Total N	25
Test Statistic	21,570
Degrees of Freedom	4
Asymptotic Sig. (2-sided test)	,000

1. The test statistic is adjusted for ties.

The showed data corresponds to the first assay (passage 36). Three independent assay was done with similar results.

2. Lucifer Yellow Permeability Assay

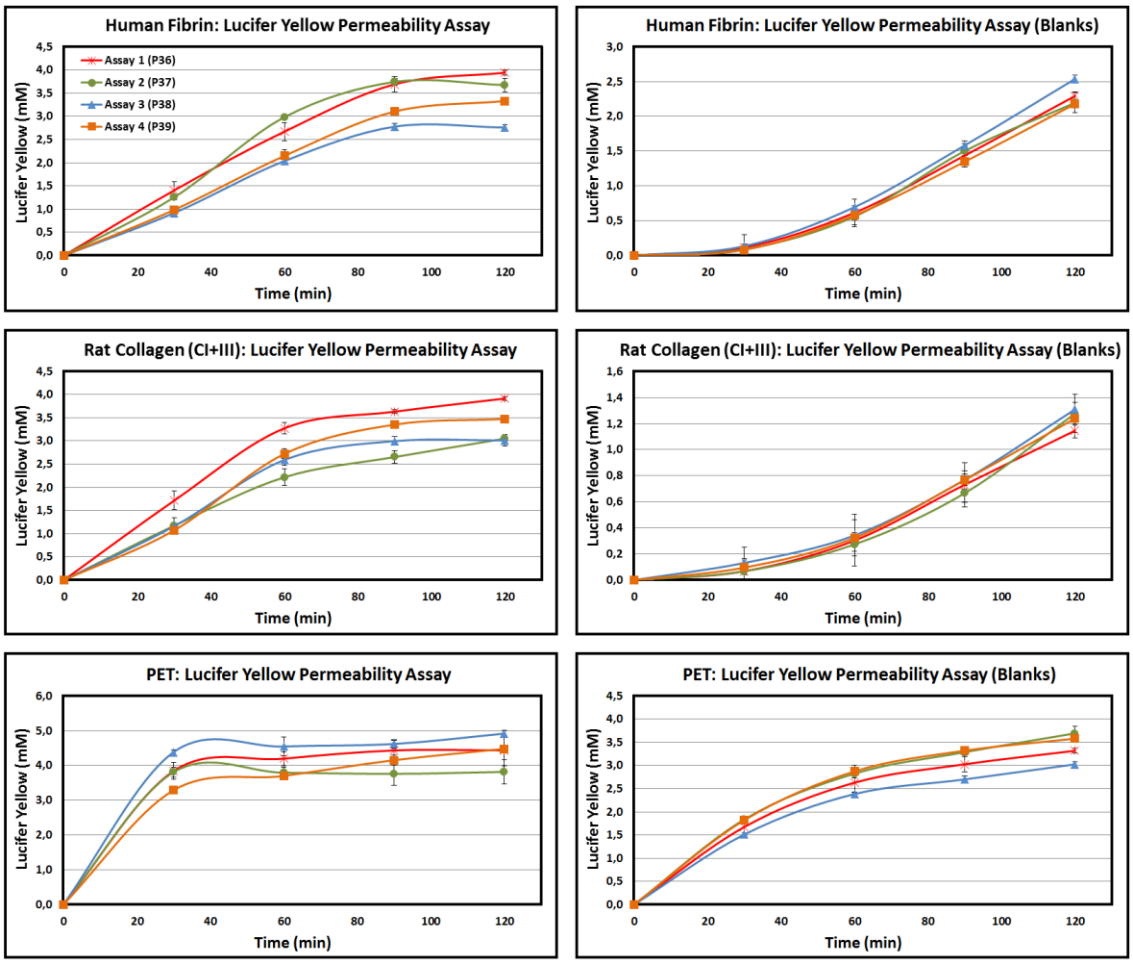

Figure 2S. Lucifer yellow (LY) assay conducted over dermal-epidermal organotypics (DEpOs) after 21 days of culture in the three evaluated matrices: Polyethylen Therephthalat (PET), human fibrin (hF) and rat tail collagen type I and III mixture (CI+III). One factor ANOVA ($p>0.001$) shows significantly differences between LY rate pass through DEpOs and the control (matrices without cells) in all proved matrices. An actively paracellular transporting is suggested. The mild barrier function achieved by obtained epidermis in PET was statistically significantly compared to other two matrices (i.e. hF and CI+III, see manuscript) (Fig. 9D). Each measurement at each day was conducted in four different DEpOs (n=4), in four different independent assays, with similar results (see LY supplemental material). P36, Passage 36; bars represents the standard deviation (SD).

3. Immunohistochemistry Controls

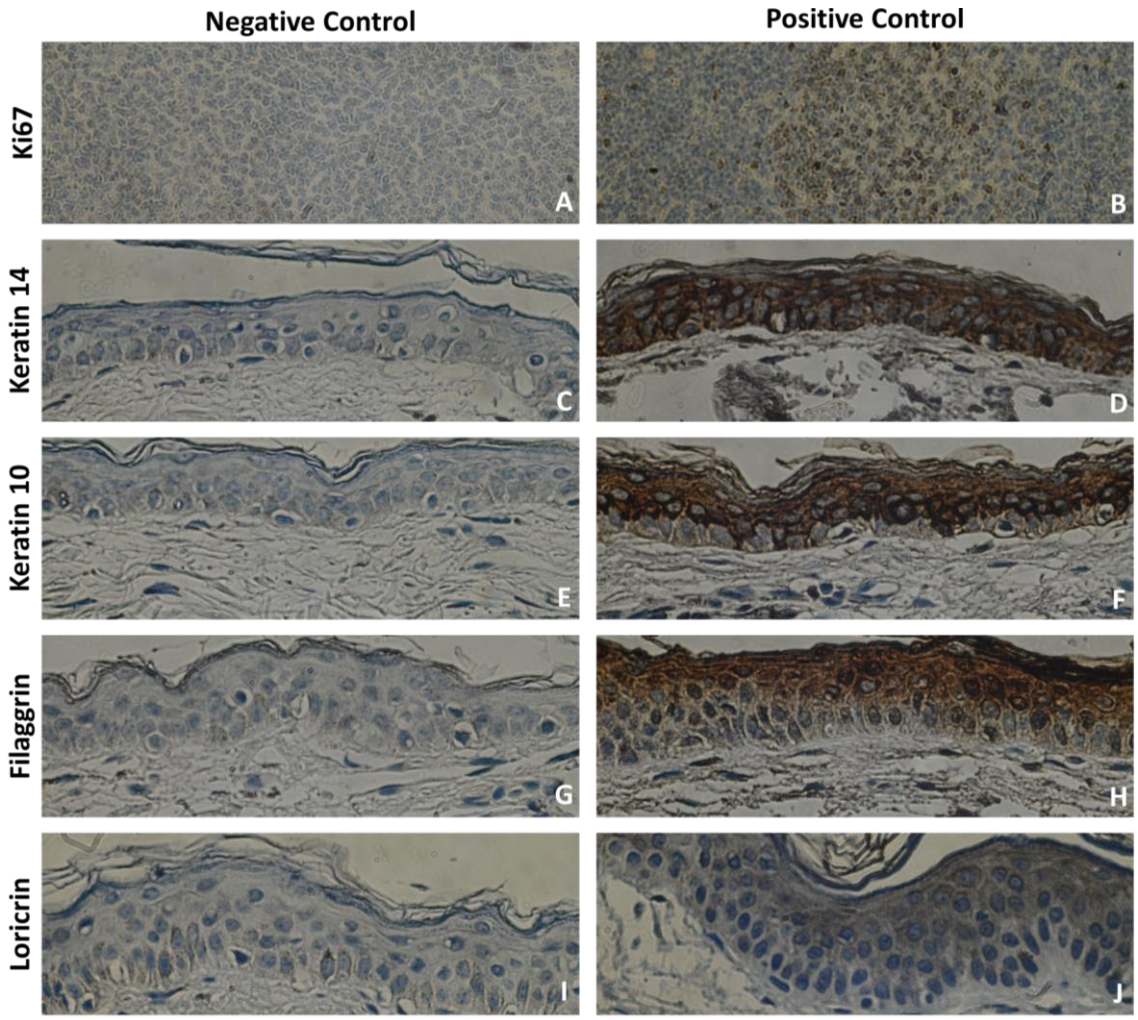

Figure 3S. Immunohistochemistry controls. Formalin-fixed native skin biopsy from retro-auricular area was used to standardize the primary antibody dilution of epidermal evaluated markers (C-J). To standardize Ki-67 proliferation marker, tonsil slide was used (A, B).

4. Calculation of Ki-67 Index

The way to calculate the Ki-67 index followed here has been based on works made by Safferling *et al*. (2013) and Kitagawa *et al.* (2014). The basic difference is that here the procedure is manual compared with digital analysis of them. Of course, a limited number of slides could be analyzed (n=3 per sample) and is highly probably that the counted total basal cells were variably, so the count was done three times per slide. The used criterion to define the basal cells was its direct contact with matrix (PET, fibrin or collagen). Briefly, once the negative and positive cells were counted the following formula was applied:

$$Ki-67\ Index = \frac{Ki-67^{+}\ Basal\ Cells}{Total\ Basal\ Cells} \times 100$$

To exemplify, some counts done in one slide of a collagen based DEpO are showed:

Assay 1	Negatives	Positives
Count 1	159	117
Count 2	145	125
Count 3	154	98
Mean	153	113
Ki-67 Index	$\frac{113}{153+113} \times 100 = 42{,}5$	

A similar analysis was made per triplicate (three independent assays) in each kind of DEpO. The statistical analysis (i.e. one factor ANOVA) carried out to compare each count per slide as well as between independent assay from each used matrix did not shows differences. At the end the reported Ki-67 index were expressed as the mean of three independent experiments ± SD. Finally, one factor ANOVA analysis between Ki-67 index from different kind of DEpOs shown statistical differences with the hierarchy CI+III>Fibrin>PET.